GENETIC ANALYSIS OF AXON GUIDANCE IN *DROSOPHILA MELANOGASTER*

Thesis by

Ashley Palani Wright

In Partial Fulfillment of the Requirements for the

Degree of

Doctor of Philosophy

CALIFORNIA INSTITUTE OF TECHNOLOGY

Pasadena, California

2010

(Defended May 6, 2010)

© 2010

Ashley Palani Wright

All Rights Reserved

ACKNOWLEDGEMENTS

First I need to thank my advisor, Dr. Kai Zinn, for his support, encouragement, and for many wonderful conversations both intellectual and social. Kai's bench is directly across from mine, and we have had many discussions about everything from science to politics to the weather conditions at Mammoth. It is not often an advisor is doing experiments on the next bench over, and it has been a great experience. I would like to thank my thesis committee members, Dr. Paul Sternberg, Dr. Angela Stathopoulos, and Dr. David Prober for very constructive comments on my work and for their time. I would be remiss if I did not thank Dr. Erik Jorgensen for being a great mentor and for allowing me to work in his lab as an undergraduate. The training I received in Dr. Jorgensen's lab under the direction of Dr. Jean-Louis Bessereau laid the groundwork for my success at Caltech, taught me how to think critically, and taught me how to be a good scientist. It was a special experience for a young student.

I want to thank the members of the Zinn lab past and present for making it such a great place to spend my time. Dr. Nina Tang Sherwood and Dr. Rachel Kraut for showing me the ropes. Dr. Kaushiki Menon for many enjoyable scientific conversations and for her friendship. Dr. Nicki Fox for being a fabulous (in every way!) labmate and a truly great friend. I loved our evenings hanging out in the lab and wish you were not so far away. Dr. Karl Johnson, an honorary Zinn lab member, for great conversations and a great collaboration. Violana Nesterova for all of her help over the years. Elena Armand for all she does for the lab. I would especially like to thank Dr. Anna Salazar for her immense knowledge in all things fly and all things

music. For many fun nights out. For so many lunchtime outings and trips to Ernie's. For her sharp wit and her wicked sense of humor. You are an amazing, interesting, and fun person to be around, and my time in the lab has been richer for having known you.

I would like to thank my Caltech family who are too numerous to name. I was lucky enough to come to graduate school with a group of women whom I strive to be more like everyday. Our class formed a tight bond that will remain long after our time at Caltech. Jennifer Green, Adeline Seah, Alice Robie, and Anne Hergarden thank you for emotional support through the years. I want to thank the members of Flyball for many summer evenings spent on the softball field. I want to thank the ladies of room 217 Kerchoff for adopting me as an honorary member of the Sternberg lab. I want to thank the staff at Caltech, Liz Ayala, Gwen Murdock, Janie Malone, Sam Wescott, Andreas Feuerabendt, and Bill Lease for all of their help throughout the years. To all the many friends I have made along the way, thank you for all that you do for me and for making these years some of the best of my life.

I want to thank my family. My parents, Gerry Tucker and Tony Wright, who always told me I could do anything I wanted and be whomever I chose to be. For attending all those softball games, soccer games, plays, and dance recitals. For opening our home to all my friends. For giving me every opportunity to succeed at everything I tackled. No one could have asked for better parents. My mother has taught me so much about courage, persistence, optimism, and strength throughout my life but especially in the last few years. She always keeps a smile on her face even when things are really tough. It is a skill I have tried to put to work at Caltech. I

consider her to be one of my best friends and my biggest fan. My father taught me that you do whatever you can at all times for your kids. He sacrificed so much for me. He supported me through college so I would not have to work full-time and I am convinced that is one of the main reasons I am standing here today. He taught me everything I know about sports and turned me into a lifelong fan. I love you both with all my heart. I would also like to thank my step-parents. Duane Tucker for much important advice, love and for loving and taking care of my Mama. Laurie Wright for all the words of encouragement and love and for making my Dad so happy!

I would like to thank my brothers, Ryan and Dustin Wright, for their love, support, and endless teasing as a kid. I am stronger for having had two big, strong, strapping brothers around. It is a good feeling to know someone is always watching out for you. Every girl needs big brothers. I would like to thank my sisters-in-law, Wendy Wright and Stephanie Wright, for being who they are and loving my brothers. I want to thank my grandparents, Thelma Wright, Frank Wright (who I never knew but feel has always been a part of my life), Carma Preece, and Ralph Preece for so many hugs and kisses and lessons in life. My Grandfather Preece is the reason I am here today. He taught me the value of an education and he gave me the money to pursue that education. This degree is as much his as it is mine.

I would like to thank my in-laws, Paul and Julie Staheli, for so many things. For bringing my husband Josh into the world and giving me another family who are just as supportive and wonderful as my own. I am really lucky to have such an amazing relationship with Paul and Julie. They welcomed me from the very beginning and have given me so much. I like to think that I have three sets of parents, and I am

grateful for having them in my life. I would like to thank my sister-in-law Jessica Staheli. Actually I would like to thank my sister Jessica Staheli. I did not grow up with any sisters and I now I have one. You are the most loyal, loving, caring, and generous person and you mean so much to me. I do not think this dissertation would have been written without many phone calls and text messages of encouragement. I will return the favor here shortly while you are writing your dissertation.

I have found the most incredible group of friends I have ever had during my time in Los Angeles. I am constantly in awe of this group of people. Thank you Tony and Tina Coen and Hershey Entin for always keeping me well fed. I want to thank my "girls," Jessica, Cheryl, Jennie, Amy, and Ashley. What a group of women! So witty, silly, fun, and crazy and always there for me in every way. I would like to thank Jonathan Fletcher for bear hugs; Cameron Brown and Amy Lee for being smart and fun and for all the hot tub parties in our future; Jennie O'Keefe for being kind and sweet; Ashley Baker for her wit and humor. A very special thank you goes out to Cheryl Van Buskirk and David Bond not only for all the fantastic intellectual conversations, but for being so much fun to be around. For lazy Sundays and days spent by the pool. For being the best friends I have ever known. I love you guys!

And most importantly, I thank my husband Joshua Staheli. It has been 13 amazing years and we are happier now than ever. You have been a constant source of love, support, and encouragement. You are the best husband a woman could ask for. I do not know what I would do without you. You are my best friend and my favorite person. You keep me going forward when things are tough and celebrate every triumph with me. You are by my side forever and always. I love you.

Music plays a very big role in my life so one final thank you must go out to Christopher Lawrence and KCRW. They have been the soundtrack to this thesis and my life for the last 10 years.

ABSTRACT

Due to its genetic manipulability and relatively short reproductive cycle, genetic screens are often carried out in the fruit fly, *Drosophila melanogaster.* Deficiency "kits" that cover the *Drosophila* genome with a minimum number of lines have been established by other groups to facilitate gene mapping. These kits cannot be systematically analyzed for many phenotypes, however, because embryos homozygous for many deficiencies fail to develop due to the loss of key gene products. To create new kits that can be screened for more phenotypes, we have examined the development of the nervous system in embryos homozygous for more than 700 distinct deficiency mutations. A kit of ~400 deficiency lines for which homozygotes have a recognizable nervous system and intact body walls encompasses >80% of the genome. Here we show examples of screens of this kit for orphan receptor ligands and neuronal antigen expression. Screens of this kit can also be used to find genes involved in expression, patterning, and subcellular localization of any protein that can be visualized by antibody staining. A subset kit of 233 deficiency lines, for which homozygotes develop relatively normally to late stage 16 (thus allowing for central nervous system development), covers ~50% of the genome. We have screened this smaller kit for motor axon guidance phenotypes, and we present examples of new axon guidance phenotypes in the central nervous system and neuromuscular system. Through screening of these kits, we also found deficiencies that fail to stain with monoclonal antibody BP102, which recognizes an unknown epitope on the proximal segments of central nervous system axons. In addition, we have found a deficiency

that exhibits ectopic BP102 staining on peripheral sensory neurons. By defining the single genes under these deficiencies, we have obtained evidence that BP102 may recognize a chondroitin sulfate proteoglycan and that BP102 epitope expression is regulated by *matrix metalloproteinase 1*. Thus, in addition to this screen providing information about motor axon guidance in the embryo, we have also been able to further characterize an antibody that is frequently used by the *Drosophila* community.

TABLE OF CONTENTS

LIST OF FIGURES

Chapter 1

Page

Introduction

Motor neurons are polarized cells consisting of a cell body that resides within the central nervous system, dendrites that receive information from upstream cells, and axons which transmit information to their downstream muscle targets. Motor neurons are the only means the brain has to control muscle contractions that are essential for life, and these neurons are lost in many diseases such as amyotrophic lateral sclerosis (ALS) and spinal muscular atrophy (SMA) (KANNING *et al.* 2010). These are only two of a group of diseases classified by the National Institute of Neurological Disorders and Stroke as motor neuron diseases (MNDs). These diseases result from the progressive loss of motor neurons. Symptoms include muscle weakening, loss of motor control, twitching, advancing to the inability to swallow or breathe, and eventual death. In order to design therapies for motor neuron disease or spinal cord injury, it is important to understand the basic mechanisms of how axons migrate and innervate targets.

Axons must migrate over long distances through complex environments in order to reach their targets. The motile structure, the growth cone, must integrate both repulsive and attractive cues as it navigates through an environment rich with guidance molecules and extracellular matrix. That neurons make stereotyped connections when confronted with such an environment is remarkable. Our understanding of axon guidance has been aided by the use of antibodies specific for structures within the nervous system and the use of those reagents in genetics screens in model organisms such as the fruit fly, *Drosophila melanogaster*.

In *Drosophila*, the ventral nerve cord is composed of longitudinal tracts on either side of the midline connected by two commissural axon tracts per segment, the anterior and posterior commissures. Neuronal cell bodies reside within the ventral nerve cord. Most motor neuron axons in *Drosophila* cross the midline, extend for a short distance along the longitudinal tract, and leave the CNS in one of two nerve roots. In each abdominal hemisegment of a fruit fly, 36 motor neurons innervate 30 body wall muscles in a stereotyped manner. Guidance across the midline is controlled by myriad factors including attractive cues required for axons to cross and repulsive cues required to keep axons from crossing or re-crossing the midline.

Axons are attracted to the midline through the chemoattractive guidance molecule Netrin. There are two netrins in *Drosophila*: *netrin A* (netA) and *netrin B* (*netB*). Both are expressed at the midline and when both netrin molecules are removed, the commissures do not develop in a normal manner (HARRIS *et al.* 1996; MITCHELL *et al.* 1996). A netrin receptor, Frazzled (Fra), is expressed on commissural and longitudinal axons as they are extending and loss of *fra* results in a thinning of commissural axon bundles and occasional breaks in the longitudinal tracts (KOLODZIEJ *et al.* 1996). Loss of this receptor therefore results in similar phenotypes as those observed when the netrins are deleted and suggests that without this chemoattractant axons cannot effectively cross the midline.

In order to keep axons from recrossing the midline once they have crossed, a secreted chemorepellant, Slit, is also expressed at the midline. In the absence of Slit, the longitudinal fascicles collapse at the midline. The receptors for Slit are Ig domain

superfamily proteins known as Roundabouts (Robos) (KIDD *et al.* 1999; KIDD *et al.* 1998). There are three *robo* family members in *Drosophila*, *robo*, *robo2*, and *robo3*. The most important in regard to midline crossing is *robo*. Robo protein is localized to the cell surface of axons. However, segments of axons crossing the midline do not have cell-surface Robo as it is downregulated by a protein known as *commissureless* (*comm*)(KELEMAN *et al.* 2002). Comm accumulates in the axons at the midline and targets Robo protein for degradation. Once an axon has crossed the midline, Robo is found on the cell surface. The axons can now sense Slit and are repelled from crossing the midline again (ARAUJO and TEAR 2003).

Once axons have crossed the midline they then exit the CNS through one of two nerve roots: the intersegmental nerve root (ISN) and segmental nerve root (SN). The nerve roots further separate to form 5 major pathways: the intersegmental nerve (ISN), intersegmental nerve b (ISNb), and intersegmental nerve d (ISNd) from the ISN nerve root, and segmental nerve a (SNa), and segmental nerve c (SNc) from the SN nerve root.

As motor axons are moving through the environment, they must fasciculate and defasciculate from substrates in order to make their way to the correct target muscle. These events are regulated by adhesive and anti-adhesive factors. A key regulator of axon adhesion and guidance in the periphery is the glycoprotein Fasciclin II (FasII). *FasII* encodes a neural cell adhesion molecule in the Ig domain superfamily that is expressed exclusively on motor axons (GRENNINGLOH *et al.* 1991). Mutation of *FasII* produces subtle fasciculation defects in the nervous system. When levels of

FasII are increased, axon guidance errors occur that are consistent with increased adhesion (LIN and GOODMAN 1994). It has therefore been proposed that FasII acts as an adhesive factor and when the levels of FasII are increased, axons can no longer defasciculate from one another to enter the correct muscle field.

Defasciculation is regulated by *beaten path* (*beat*). *beat* was initially thought to encode a neuronally secreted protein that when mutated causes axons to fail to defasciculate from the nerve fibers at the proper locations. ISNb and ISNd stay fasciculated with the ISN, and SNc remains fasciculated with SNa (FAMBROUGH and GOODMAN 1996). It was proposed that beat functions as an anti-adhesive protein. *FasII* has been shown to suppress the *beat* phenotype in double mutant combinations suggesting that the levels of adhesion between axons or axons and other substrates is critical for proper axon guidance in *Drosophila*. *beat* (now known as *beatIa*) is a member of a large gene family of Ig domain superfamily proteins that are expressed throughout the nervous system. Some members of the *beat* family have been shown to be pro-adhesive and others anti-adhesive (PIPES *et al.* 2001) but the other members of the family have no phenotype or weak phenotypes when mutated. This is likely due to functional redundancy.

Drosophila sidestep encodes an Ig domain superfamily member that is expressed on target muscles and acts as a chemoattractant. In the absence of Side protein, axons stay fasciculated with one another and do enter the muscle fields. In the many hemisegments, only the ISN and SN branches remain with none of the axons reaching their final targets (SINK *et al.* 2001). Loss of FasII cannot rescue the defects

found in side mutants which suggests that loss of adhesion within the neurons cannot overcome the requirement for a target-derived attractant.

It was recently reported that *beat* and *side* interact to guide motor axons into the periphery (SIEBERT *et al.* 2009; ZINN 2009). *beat* was found to encode a transmembrane protein that genetically and physically interacts with *side*. Side protein is expressed on intermediate target tissues as axons are migrating into the periphery. Axons are attracted to Side labeled substrates through the *beat* receptor expressed on the surface of the growth cone. When a growth cone makes contact with the Side expressing tissue, Beat signaling leads to a downregulation of Side. Side is then expressed on the next intermediate target tissue. In late embryos, Side is expressed on muscles, where it guides axons to their final targets. Therefore, Beat and Side define a ligand-receptor system required for proper guidance of motor axons to target muscles.

Defasciculation and target selection are also regulated by attractive and repulsive cues in the muscle field. Semaphorins are transmembrane or secreted glycoproteins which contain a large domain known as a sema domain. Sema I is expressed within the nervous system and mutation of *sema I* leads to axon guidance defects. In *sema I* null mutants, ISNb stalls or fails to defasciculate from the ISN. Guidance of SNa was also found to be defective resulting in stalls. When Sema I is overexpressed on muscles, axons avoid the muscle field (YU *et al.* 1998). These data suggest that the function of Sema I in the nervous system is as a repulsive cue that drives defasciculation at key choice points.

Beat, Side, and Sema are general factors involved in the guidance of all motor neurons. Specific pathfinding choices are regulated by many proteins. One class of proteins shown to be involved in guidance of particular axons are the receptor tyrosine phosphatases (RPTPs). There are 5 RPTPs expressed in neurons in *Drosophila*. They are PTP10D, PTP69D, PTP99A, PTP52F, and Lar and they display a complex series of genetic interactions that regulate axon guidance at choice points in the periphery. Lar, PTP69D, and PTP99A are all involved in the guidance of ISNb. ISNb fails to defasciculate from the ISN resulting in ISNb bypassing the correct muscle targets in PTP69D and Lar mutants (DESAI *et al.* 1996; KRUEGER *et al.* 1996). Mutation of PTP99A has no effect on ISNb guidance, but enhances the PTP69D phenotype (DESAI *et al.* 1996). In contrast, mutation of PTP99A can rescue the bypass phenotype in a Lar mutant suggesting that Lar antagonizes or downregulates PTP99A function at this choice point (DESAI *et al.* 1997). PTP52F has been shown to be involved in guidance of the axons of the SNa (SCHINDELHOLZ *et al.* 2001). While the downstream targets of these phosphatases are not known, these data suggest that cycles of phosphorylation and dephosphorylation have important effects on the ability of axons to navigate through their environments.

Glycosylation

One thing all these various axon guidance pathways have in common is that they involve proteins that are glycosylated. Glycosylation is thought to be the one of the most common posttranslational modification in eukaryotic organisms. Upwards of 90% of proteins that progress through the secretory pathway are glycosylated in

some manner. Glycosylation takes place mostly in the endoplasmic reticulum (ER) and Golgi through a series of enzymatic reactions. While glycosylation does occur in prokaryotes, a large increase in the complexity of glycosylation has occurred in eukaryotes as the evolution of the secretory pathway requires proteins to be trafficked and sorted into many different compartments (LAUC *et al.* 2009; WEERAPANA and IMPERIALI 2006). In multicellular organisms, cells are required to communicate with each other, and this occurs through interactions mediated by extracellular proteins and the extracellular matrix. Most extracellular proteins are modified by some type of glycosylation and often more than one type. There are many different types of glycosylation in eukaryotes including N-linked, O-linked, and proteoglycans (PGs).

N-Linked Glycosylation

Eukaryotic N-linked glycosylation occurs in the ER where a branched chain of 14 sugars is added to one or more Asparagine (Asn) residues en bloc cotranslationally. These chains are then modified extensively in the ER and Golgi through a series of enzymatic steps. N-linked glycosylation is the most common form of glycosylation and is essential for life (LAUC *et al.* 2009). It had been shown in Chinese hamster ovary cells by mutation of a gene involved in N-linked glycosylation that loss of this type of glycosylation is not cell lethal. If the same gene is mutated in mice however, the resultant embryos die embryonically and appear to be underdeveloped as compared to littermates. These data suggest that the primary role of glycosylation is in cell-cell interactions in an intact organism but that it may not be

required for viability of individual cells (IOFFE and STANLEY 1994; STANLEY and IOFFE 1995).

N-linked glycosylation is known to play a key role in protein folding (WEERAPANA and IMPERIALI 2006). When glycosylation is blocked, proteins do not undergo proper folding, do not move through the ER quality control mechanism, and are eventually degraded. The mechanism of this quality-control is quite interesting. Once the sugar tree is added to the protein being translated, two terminal glucose residues are immediately removed from the "A" branch. This leaves one exposed glucose on that branch. This glucose is recognized by one of two lectins in the ER, calnexin or calreticulin, which act as molecular chaperones. Once this remaining glucose is removed, the protein is released from the chaperone and leaves the ER unless it is recognized by a protein that acts as a folding sensor. This folding sensor may recognize unfolded proteins by exposed hydrophobic patches. If a protein fails to fold, it is eventually sent back to the cytosol where it is degraded by the proteasome. It is important that a protein be given enough time to fold properly and the amount of time a protein has been in the ER seems to be imparted by the number of mannose residues left on the "B" branch of the saccharide chain. A membrane bound ER enzyme removes the terminal mannose residue from the "B" branch slowly over time. Mutation or overexpression of this enzyme can dramatically affect the rate of protein degradation (HELENIUS and AEBI 2004). If the unfolded protein contains this mannose residue, it is selectively reglucosylated on the "A" branch and folding is attempted

again. If the mannose residue has been removed from the chains, the protein is sent to the cytosol for degradation.

This role of N-linked glycosylation in protein folding has also been described in *Drosophila*. *wollknauel* (*wol*) encodes the *Drosophila* UDP-glucose:dolichyl-phosphate glucosyltransferase, an enzyme required for N-linked glycosylation, and mutations in *wol* result in an unfolded protein response (UPR) in the ER. The UPR leads to a reduction in translation in the ER and mutations in *wol* lead to defects in embryonic patterning by a reduction in the levels of critical transcription factors (HAECKER *et al.* 2008).

O-Linked Glycosylation

There are a variety of types of O-linked glycosylation that occur at two major sites within the cell. One site is the Golgi where any amino acid with a hydroxyl group (Serine (Ser), Threonine (Thr), Tyrosine (Tyr), Hydroxyproline (Hyp), Hydroxylysine (Hyl)) can be modified by addition of many types of sugars including, N-acetyl-galactosamine (GalNAc), mannose (Man), fucose (Fuc), glucose (Glc), and galactose (Gal) (SPIRO 2002). O-linked mannose type modifications have been shown to have roles in muscular development in humans and flies (TEN HAGEN *et al.* 2009). Mucin type modifications are important for formation of apical and luminal surfaces including trachea in *Drosophila* and vasculature and kidney tube formation in mice. Fucose and glucose O-linked glycosylation have roles in Notch signaling across species (TEN HAGEN *et al.* 2009).

The second site of O-linked glycosylation is the cytoplasm and nucleus where components of the nuclear pore, transcription factors, and RNA polymerase II, as well as many other proteins are modified by the often reversible addition of O-linked N-acetyl-α-D-glucosamine (GlcNAc) on Ser or Thr residues. There is some evidence that this type of carbohydrate modification may act as a nuclear transport signal (HANOVER 2001). There is a relationship between phosphorylation and glycosylation at these sites in many proteins. For RNA Polymerase II (RNA Pol II), phosphorylation is required for elongation to proceed. O-GlcNAc modification of the same site could therefore be responsible for a reduction in the activity of RNA pol II (WELLS and HART 2003). O-linked GlcNAc can be thought of as more similar to phosphorylation than to other types of glycosylation and may be involved in many cell-signaling cascades. Cytosolic proteins are also modified by O-GlcNAc including proteins that interact with actin and tubulin and the plasma membrane (HANOVER 2001). There is evidence that O-GlcNAc modification may be involved in many diseases such as cancer, neurodegeneration, and diabetes.

Proteoglycans

Proteoglycans (PGs) are synthesized in the Golgi and consist of large unbranched side chains known as glycosaminoglycans (GAGs) added one saccharide at a time to a core protein at specific sites. There are two major families of proteoglycans, the heparin/heparan sulfate proteoglycans (HSPGs) which also include the keratan sulfate (KS) family, and the chondroitin/chondroitin sulfate proteoglycans (CSPGs) which contain the dermatan sulfate (DS) family. These two

families are sometimes referred to as the HS/KS and CS/DS proteoglycan families. Both families share a common four-sugar precursor where these sugars are added one at a time to a serine reside starting with a xylose. This xylose (Xyl) is followed by two galactose (Gal) and a glucuronic acid (GlcA). The two pathways then diverge (PRYDZ and DALEN 2000; TEN HAGEN *et al.* 2009).

HSPGs consist of multimers of a disaccharide containing GlcA and GlcNAc. These side chains can be modified by N-deacetylation-N-sulphation, 2-O, 6-O, and 3-O sulfation and epimerization (HACKER *et al.* 2005). There are two major classes of HSPGs, the glypicans and the syndecans. Glypicans are linked to the cell membrane by a glycosylphosphatidylinositiol (GPI) anchor. Syndecans are transmembrane proteins and can carry HS as well as CS and DS side chains. HSPGs are known to be involved in morphogen gradient formation in many organisms including cell culture and animal models. They play a role in Wingless (Wg), TGFB/Bone Morphogenetic protein (BMP), Hedgehog (Hh), and Fibroblast Growth Factor (FGF) signaling pathways, possibly by changing the diffusion of these morphogens within the extracellular matrix (HACKER *et al.* 2005).

CSPGs are multimers of GlcA and GalNAc. In *C. elegans*, mutations exist for some components of the biosynthetic pathway. Mutations in enzymes common to both the HSPG and chondroitin pathways exhibit a squashed vulval phenotype where defects in invagination lead to a partial collapse of the vulva (HERMAN *et al.* 1999; HERMAN and HORVITZ 1999). It was later shown by analysis of *squashed vulva*-5 (*sqv-5*) that the defects in this class of mutants are due to loss of chondroitin but not HS

modifications (HWANG *et al.* 2003). Embryos from homozygous mothers arrest very early due to a defect in cytokinesis and RNAi of *sqv-5* results in the same phenotype (HWANG *et al.* 2003; MIZUGUCHI *et al.* 2003). It is not clear if chondroitin has a structural or signaling role in these two processes.

Developmentally CSPGs are involved in cell migration events including axon guidance and migration of neural crest cells (CARULLI *et al.* 2005) as well as in the guidance of retinal axons into the optic tectum (WALZ *et al.* 2002). CSPGs are also known to play roles in neuronal plasticity by restricting axonal growth and sprouting in the adult brain (BUSCH and SILVER 2007; PIZZI and CROWE 2007; SHERMAN and BACK 2008). One of the most well studied roles of CSPGs in the brain is in the field of regeneration. Adult CNS lesions result in the formation of a glial scar at the site of the lesion. Astrocytes in these "scars" upregulate CSPG synthesis. When either transplanted or newly sprouted axons encounter these scars they retract and cannot cross the region. If the lesion site is treated with chondroitinase, an enzyme that cleaves CS side chains, axons can then extend across the lesion site (BUSCH and SILVER 2007; CARULLI *et al.* 2005; PIZZI and CROWE 2007). It is believed that CSPGs are upregulated on stable structures within the CNS and act to restrict sprouting and growth and that they then form a barrier to growth after injury. They may also be involved in sealing off the blood-brain barrier after trauma occurs (BUSCH and SILVER 2007). It has recently been shown that a transmembrane protein tyrosine phosphatase, PTP-sigma, can act as a receptor for CSPGs on neurons attempting to migrate after injury. Loss of PTP-sigma activity results in neurons being able to cross

the injury site (FRY *et al.* 2009; SHEN *et al.* 2009) thus providing the first evidence for the existence of specific neuronal receptors for CSPGs that mediate the inhibitory effect of this class of molecules.

Introduction References

ARAUJO, S. J., and G. TEAR, 2003 Axon guidance mechanisms and molecules: lessons from invertebrates. Nat Rev Neurosci **4:** 910-922.

BUSCH, S. A., and J. SILVER, 2007 The role of extracellular matrix in CNS regeneration. Curr Opin Neurobiol **17:** 120-127.

CARULLI, D., T. LAABS, H. M. GELLER and J. W. FAWCETT, 2005 Chondroitin sulfate proteoglycans in neural development and regeneration. Curr Opin Neurobiol **15:** 116-120.

DESAI, C. J., J. G. GINDHART, JR., L. S. GOLDSTEIN and K. ZINN, 1996 Receptor tyrosine phosphatases are required for motor axon guidance in the Drosophila embryo. Cell **84:** 599-609.

DESAI, C. J., N. X. KRUEGER, H. SAITO and K. ZINN, 1997 Competition and cooperation among receptor tyrosine phosphatases control motoneuron growth cone guidance in Drosophila. Development **124:** 1941-1952.

FAMBROUGH, D., and C. S. GOODMAN, 1996 The Drosophila beaten path gene encodes a novel secreted protein that regulates defasciculation at motor axon choice points. Cell **87:** 1049-1058.

FRY, E. J., M. J. CHAGNON, R. LOPEZ-VALES, M. L. TREMBLAY and S. DAVID, 2009 Corticospinal tract regeneration after spinal cord injury in receptor protein tyrosine phosphatase sigma deficient mice. Glia **58:** 423-433.

GRENNINGLOH, G., E. J. REHM and C. S. GOODMAN, 1991 Genetic analysis of growth cone guidance in Drosophila: fasciclin II functions as a neuronal recognition molecule. Cell **67:** 45-57.

HACKER, U., K. NYBAKKEN and N. PERRIMON, 2005 Heparan sulphate proteoglycans: the sweet side of development. Nat Rev Mol Cell Biol **6:** 530-541.

HAECKER, A., M. BERGMAN, C. NEUPERT, B. MOUSSIAN, S. LUSCHNIG *et al.*, 2008 Wollknauel is required for embryo patterning and encodes the Drosophila ALG5 UDP-glucose:dolichyl-phosphate glucosyltransferase. Development **135:** 1745-1749.

HANOVER, J. A., 2001 Glycan-dependent signaling: O-linked N-acetylglucosamine. FASEB J **15:** 1865-1876.

HARRIS, R., L. M. SABATELLI and M. A. SEEGER, 1996 Guidance cues at the Drosophila CNS midline: identification and characterization of two Drosophila Netrin/UNC-6 homologs. Neuron **17:** 217-228.

HELENIUS, A., and M. AEBI, 2004 Roles of N-linked glycans in the endoplasmic reticulum. Annu Rev Biochem **73:** 1019-1049.

HERMAN, T., E. HARTWIEG and H. R. HORVITZ, 1999 sqv mutants of Caenorhabditis elegans are defective in vulval epithelial invagination. Proc Natl Acad Sci U S A **96:** 968-973.

HERMAN, T., and H. R. HORVITZ, 1999 Three proteins involved in Caenorhabditis elegans vulval invagination are similar to components of a glycosylation pathway. Proc Natl Acad Sci U S A **96:** 974-979.

HWANG, H. Y., S. K. OLSON, J. D. ESKO and H. R. HORVITZ, 2003 Caenorhabditis elegans early embryogenesis and vulval morphogenesis require chondroitin biosynthesis. Nature **423:** 439-443.

IOFFE, E., and P. STANLEY, 1994 Mice lacking N-acetylglucosaminyltransferase I activity die at mid-gestation, revealing an essential role for complex or hybrid N-linked carbohydrates. Proc Natl Acad Sci U S A **91:** 728-732.

KANNING, K. C., A. KAPLAN and C. E. HENDERSON, 2010 Motor Neuron Diversity in Development and Disease. Annu Rev Neurosci.

KELEMAN, K., S. RAJAGOPALAN, D. CLEPPIEN, D. TEIS, K. PAIHA *et al.*, 2002 Comm sorts robo to control axon guidance at the Drosophila midline. Cell **110:** 415-427.

KIDD, T., K. S. BLAND and C. S. GOODMAN, 1999 Slit is the midline repellent for the robo receptor in Drosophila. Cell **96:** 785-794.

KIDD, T., K. BROSE, K. J. MITCHELL, R. D. FETTER, M. TESSIER-LAVIGNE *et al.*, 1998 Roundabout controls axon crossing of the CNS midline and defines a novel subfamily of evolutionarily conserved guidance receptors. Cell **92:** 205-215.

KOLODZIEJ, P. A., L. C. TIMPE, K. J. MITCHELL, S. R. FRIED, C. S. GOODMAN *et al.*, 1996 frazzled encodes a Drosophila member of the DCC immunoglobulin subfamily and is required for CNS and motor axon guidance. Cell **87:** 197-204.

KRUEGER, N. X., D. VAN VACTOR, H. I. WAN, W. M. GELBART, C. S. GOODMAN *et al.*, 1996 The transmembrane tyrosine phosphatase LAR controls motor axon guidance in Drosophila. Cell **84:** 611-622.

LAUC, G., I. RUDAN, H. CAMPBELL and P. M. RUDD, 2009 Complex genetic regulation of protein glycosylation. Mol Biosyst **6:** 329-335.

LIN, D. M., and C. S. GOODMAN, 1994 Ectopic and increased expression of Fasciclin II alters motoneuron growth cone guidance. Neuron **13:** 507-523.

MITCHELL, K. J., J. L. DOYLE, T. SERAFINI, T. E. KENNEDY, M. TESSIER-LAVIGNE *et al.*, 1996 Genetic analysis of Netrin genes in Drosophila: Netrins guide CNS commissural axons and peripheral motor axons. Neuron **17:** 203-215.

MIZUGUCHI, S., T. UYAMA, H. KITAGAWA, K. H. NOMURA, K. DEJIMA *et al.*, 2003 Chondroitin proteoglycans are involved in cell division of Caenorhabditis elegans. Nature **423:** 443-448.

PIPES, G. C., Q. LIN, S. E. RILEY and C. S. GOODMAN, 2001 The Beat generation: a multigene family encoding IgSF proteins related to the Beat axon guidance molecule in Drosophila. Development **128:** 4545-4552.

PIZZI, M. A., and M. J. CROWE, 2007 Matrix metalloproteinases and proteoglycans in axonal regeneration. Exp Neurol **204:** 496-511.

PRYDZ, K., and K. T. DALEN, 2000 Synthesis and sorting of proteoglycans. J Cell Sci **113 Pt 2:** 193-205.

SCHINDELHOLZ, B., M. KNIRR, R. WARRIOR and K. ZINN, 2001 Regulation of CNS and motor axon guidance in Drosophila by the receptor tyrosine phosphatase DPTP52F. Development **128:** 4371-4382.

SHEN, Y., A. P. TENNEY, S. A. BUSCH, K. P. HORN, F. X. CUASCUT *et al.*, 2009 PTPsigma is a receptor for chondroitin sulfate proteoglycan, an inhibitor of neural regeneration. Science **326:** 592-596.

SHERMAN, L. S., and S. A. BACK, 2008 A 'GAG' reflex prevents repair of the damaged CNS. Trends Neurosci **31:** 44-52.

SINK, H., E. J. REHM, L. RICHSTONE, Y. M. BULLS and C. S. GOODMAN, 2001 sidestep encodes a target-derived attractant essential for motor axon guidance in Drosophila. Cell **105:** 57-67.

SPIRO, R. G., 2002 Protein glycosylation: nature, distribution, enzymatic formation, and disease implications of glycopeptide bonds. Glycobiology **12:** 43R-56R.

STANLEY, P., and E. IOFFE, 1995 Glycosyltransferase mutants: key to new insights in glycobiology. FASEB J **9:** 1436-1444.

TEN HAGEN, K. G., L. ZHANG, E. TIAN and Y. ZHANG, 2009 Glycobiology on the fly: developmental and mechanistic insights from Drosophila. Glycobiology **19:** 102-111.

WALZ, A., R. B. ANDERSON, A. IRIE, C. B. CHIEN and C. E. HOLT, 2002 Chondroitin sulfate disrupts axon pathfinding in the optic tract and alters growth cone dynamics. J Neurobiol **53:** 330-342.

WEERAPANA, E., and B. IMPERIALI, 2006 Asparagine-linked protein glycosylation: from eukaryotic to prokaryotic systems. Glycobiology **16:** 91R-101R.

WELLS, L., and G. W. HART, 2003 O-GlcNAc turns twenty: functional implications for post-translational modification of nuclear and cytosolic proteins with a sugar. FEBS Lett **546:** 154-158.

YU, H. H., H. H. ARAJ, S. A. RALLS and A. L. KOLODKIN, 1998 The transmembrane Semaphorin Sema I is required in Drosophila for embryonic motor and CNS axon guidance. Neuron **20:** 207-220.

CHAPTER 1

Systematic Screening of *Drosophila* Deficiency Mutations for Embryonic Phenotypes and Orphan Receptor Ligands

Ashley P. Wright, A. Nicole Fox, Karl G. Johnson, and Kai Zinn

CHAPTER 1 Introduction

Most of the major findings that have emerged from research on *Drosophila* were driven by the identification of mutations producing a chosen phenotype via unbiased forward genetic screens. The pioneering anatomical screen of Nusslein-Vollhard and Wieschaus examined cuticle patterns of unhatched embryos bearing lethal mutations induced by the chemical mutagen ethyl methanesulfonate (EMS) (Nusslein-Volhard and Wieschaus 1980). The characterization of the genes found in this screen defined many of the fundamental mechanisms that control development in both insects and vertebrates.

Many other groups have since performed anatomical EMS screens of embryos. In the 1990s, Corey Goodman's group used antibody staining of whole-mount embryos to identify genes required for central nervous system (CNS) and motor axon guidance (SEEGER *et al.* 1993; VAN VACTOR *et al.* 1993). These screens identified many interesting genes, including *roundabout* (*robo*) and *slit*, which control axon guidance across the CNS midline (KIDD *et al.* 1999; KIDD *et al.* 1998). However, the necessity to screen thousands of point-mutant lines meant that axonal phenotypes had to be detected by examination of embryos at low magnification under a dissecting microscope. Subtle phenotypes could not be found in this manner. It can also be difficult to identify the gene responsible for a phenotype discovered in an EMS screen. P element insertion screens allow easier identification of mutated genes, but P element mutations are usually not nulls, and on average have weaker embryonic phenotypes than EMS mutations in the same genes.

Screens of deletion mutations, called deficiencies (Dfs), each of which removes multiple genes, have also been used to find genes required for embryonic development. Because many gene products are maternally expressed and deposited in the egg, where they can contribute to early development, embryos homozygous for Dfs can sometimes develop to fairly late stages. *single-minded* (*sim*), a gene required for midline glial fate determination, was identified through a Df screen (CREWS *et al.* 1988; THOMAS *et al.* 1988). Embryos were stained with an antibody that labeled axons, and one Df was identified for which homozygotes had a CNS that consisted of a single line of axons running the length of the embryo. This phenotype was found to be due to the absence of a single gene, *sim*.

Df screening has also been employed to identify closely linked genes that have redundant functions. *reaper* (*rpr*), *hid*, and *grim* are regulators of cell death in *Drosophila* that are encoded by linked genes. A deletion that removed *rpr*, *hid*, and *grim* was found to eliminate all cell death in the embryo, but single mutations affecting the individual genes do not produce this phenotype. Thus, these cell death genes could only have been discovered by examination of Df phenotypes (WHITE *et al.* 1994). Similarly, the closely linked *pyramus* and *thisbe* genes, which encode partially redundant fibroblast growth factor-related ligands, were found by identifying a region whose deletion causes a failure of mesoderm spreading (GRYZIK and MULLER 2004; STATHOPOULOS *et al.* 2004).

Our group had devised methods to screen Df collections for genes required for expression of orphan receptor ligands (FOX and ZINN 2005; LEE *et al.* 2009). We

realized that the Bloomington stock center Df "kit" that existed in 2002, when we began these experiments, was of limited utility for screens requiring dissection and analysis of embryos. We thus began a project to define new kits of publicly available Dfs that could be used for ligand and antigen expression screens, as well as for phenotypic screening. Here we describe these kits, and present the results of screens that we have conducted for genes involved in nervous system development. We have found a variety of central nervous system (CNS) and motor axon guidance phenotypes, some of which represent new phenotypic classes. The kits should accelerate the work of investigators examining development of other embryonic organs, because they will allow high-resolution anatomical screens to be conducted much more rapidly than has been possible in the past.

Results

Development of a Deficiency Kit to Screen for Orphan Receptor Ligand Genes

We initially used Df screening to search for ligands for the receptor tyrosine phosphatase (RPTP) Lar. We fused the extracellular (XC) domain of Lar to human placental alkaline phosphatase (AP), which is a dimeric protein, and expressed the resulting fusion protein (Lar-AP) using a baculovirus vector. Lar-AP-containing cell supernatants were incubated with live-dissected late stage 16 *Drosophila* embryos, and binding was detected with secondary and tertiary antibodies. Lar-AP stains a complex pattern, including CNS axons, midline glia, and muscle attachment sites. To identify genes required for Lar ligand expression, we crossed green fluorescent protein (GFP) balancer chromosomes into the 270 lines in the Bloomington Df kit as it existed in 2002. We dissected GFP-minus late stage 16 embryos and stained them with Lar-AP. We found a Df that lacked Lar-AP muscle attachment site staining, and used overlapping Dfs and insertion mutations to identify the heparan sulfate proteoglycan (HSPG) Syndecan as the Lar ligand encoded within this Df (Fox and Zinn 2005).

In the course of this work, we dissected, stained, and analyzed embryos homozygous for every Df in the Bloomington kit. We found that homozygotes for many of the Dfs failed to develop to late stage 16, and thus could not be screened for ligand expression. Failure to develop is often due to the loss of zygotic expression of a single key gene under the Df. It is thus possible to reduce the sizes of these "unscreenable" regions using other publicly available overlapping Dfs, examining

homozygotes for each Df and finding those that develop well enough to be screened. We also tried to replace Bloomington kit Dfs that were only mapped to cytological resolution with molecularly mapped Dfs. After completing many iterations of this process, involving the dissection and staining of embryos from more than 700 Df lines, we were able to define a new kit of 423 lines, which allows screening of 80-90% of the genome for Lar-AP staining, or staining with other reagents that recognize CNS axons.

In creating this kit, we had two goals that had to be balanced against each other. The first was to assemble a set of lines that would have the highest possible percentage of Dfs for which homozygotes developed relatively normally. The second was to cover the maximum possible percentage of the genome with a minimum number of Dfs. The present kit is a compromise, as it still has a substantial number of Dfs that cause major developmental defects. However, we have tried to reduce the regions that are only covered by Dfs of this kind to the minimum size possible, by iterative screening of Dfs covering smaller and smaller portions of the "problem regions" (see notes in Supplementary Table 1). In some cases, we have reached the limit of our ability to reduce the size of the problem regions using existing Dfs. In other cases, it might be possible to subdivide the Dfs further to obtain greater coverage by Dfs that confer more normal development. However, this would mean that the resulting kit would contain more lines and would consequently be more time-consuming to screen.

We classified phenotypes for late stage 16 embryos homozygous for Dfs in the kit as “mild,” “moderate,” “severe,”or “very severe.” Homozygotes for 394 Dfs, corresponding to 82% of the genome (mild + moderate + severe) have a recognizable pattern of CNS axons and exhibit clear Lar-AP staining, as well as staining with the CNS axon marker monoclonal antibody (mAb) BP102. The 25 very severe Dfs that remain in the kit, representing another ~10% of the genome, are marginally screenable with Lar-AP and BP102 (Supplementary Table 1). We expect that the mild, moderate, and severe Df lines should also be readily screenable for ligands expressed outside the CNS, although development of the desired tissue will need to be evaluated for each Df by double staining with an appropriate antibody, as we did with BP102 in our screen.

We have now completed the screening of this new kit with four different RPTP-AP fusion proteins, corresponding to the XC domains of Lar, Ptp10D, Ptp69D, and Ptp99A. Here we show results from the Ptp99A ligand screening as an example of the method. In wildtype late stage 16 embryos, 99A-AP (visualized with Alexa 488-coupled anti-rabbit IgG) stains CNS axons, the tracheae, and the salivary glands (Figures 1A, G). CNS axons were simultaneously visualized by staining with BP102, followed by Alexa 568-conjugated anti-mouse IgG. BP102 stains most or all CNS axons, but only within the boundaries of the CNS. Motor axons lose BP102 staining after they leave the CNS. The BP102 pattern thus resembles a ladder, with two commissural tracts (anterior and posterior) crossing the midline in each segment, and two longitudinal tracts extending the length of the embryo (Figures 1B, H).

We found three Dfs for which homozygotes have reduced 99A-AP staining on CNS axons, but retain normal staining of the tracheae. Df(2L)Exel7042 and Df(3R)Cha7 both eliminate staining (Figures 1D, I, K). Df(3R)Exel6176 embryos have reduced axonal staining, and cell bodies within the CNS show more staining than in wildtype(Figure 1M). The lack of CNS axon staining in these Df homozygotes is not due to the absence of CNS axons, since BP102 staining reveals that axons are still present (Figures 1E, J, L, N). The decrease in 99A-AP axon staining is a robust phenotype that allows gene mapping, and we have used overlapping Dfs and insertion mutations to identify single genes under each of these three Dfs whose loss accounts for the reduction in staining (data not shown).

A Deficiency Kit for Screening for Axon Guidance Phenotypes

In the course of our screen for genes required for RPTP ligand expression, we noted that homozygotes for 233 of the Dfs in our kit, corresponding to ~50% of the genome, developed a normal or almost normal pattern of CNS axons as visualized by BP102, and also had relatively normal overall embryonic morphologies. 217 of these Dfs can be maintained over GFP balancers, so that homozygous embryos can be easily identified. We reasoned that these lines (classified as "mild") could define a kit that would allow systematic screening for any embryonic phenotype that can be visualized by staining live-dissected embryos with antibodies (Supplementary Table 2). We decided to search for motor axon guidance phenotypes by staining homozygotes for mild Dfs with mAb 1D4, which recognizes the cytoplasmic domain of the transmembrane form of Fasciclin II (FasII) (VAN VACTOR *et al.* 1993). In late stage 16

embryos, 1D4 stains all motor axons and three longitudinal axon bundles on each side of the CNS. We also stained a subset of the Dfs with moderate phenotypes with 1D4 in order to find new CNS phenotypes.

Each abdominal hemisegment (A2-A7) of a Drosophila embryo contains about 36 motor neurons, which innervate 30 body wall muscle fibers in a stereotyped pattern. Motor axons leave the CNS within two nerve roots: the segmental nerve (SN) root and the intersegmental nerve (ISN) root. These nerve roots further divide into five major pathways, known as segmental nerve a (SNa), segmental nerve c (SNc), intersegmental nerve (ISN), intersegmental nerve b (ISNb) (also known as SNb), and intersegmental nerve d (ISNd) (KESHISHIAN *et al.* 1996). Two axons leave the CNS separately from the ISN and SN, and these connect to the axon of the peripheral lateral bipolar dendrite (LBD) neuron to form the transverse nerve (TN).

In the 1990s, 1D4 was employed for a large EMS screen of the autosomes (SINK *et al.* 2001; VAN VACTOR *et al.* 1993) for genes conferring embryonic motor axon guidance phenotypes. Because a point-mutant screen requires the analysis of thousands of lines, these phenotypes had to be discovered through examination of whole-mount embryos at low power under a dissecting microscope. This allowed the identification of mutations conferring relatively severe ISN and ISNb phenotypes, because these phenotypes could be seen at low magnification. However, mutations affecting the other pathways, such as SNa and SNc, or mutations conferring more subtle ISN and ISNb phenotypes, could not be identified in this screen.

In our screen, we dissected live late stage 16 embryos homozygous for most of the balanceable mild Dfs (190 in total), then stained them with 1D4, followed by Alexa 488 anti-mouse secondary and rhodamine-phalloidin to visualize muscle structure and the CNS axon ladder. We examined these embryos under a compound microscope, using a 40X multi-immersion lens. In this way, we could perform a detailed analysis of all of the motor pathways, and simultaneously visualize muscle structure.

To screen for motor axon guidance phenotypes, we typically examined five dissected late stage 16 embryos, or approximately 50 hemisegments. A Df was scored as phenotypically abnormal if multiple hemisegments in each embryo exhibited defects (>20% penetrance). 82 of the mild Dfs had no phenotypes with penetrances above this threshold. The remainder displayed axonal or muscle phenotypes, or both (Supplementary Table 3).

Examples of CNS Phenotypes

In late stage 16 wildtype embryos, 1D4 stains three parallel axon bundles on each side of the midline (Figure 2A). At this stage, FasII is not seen on the commissures. Since most longitudinal axons cross the midline at some point in their trajectory, this means that FasII is restricted to the longitudinal portions of a subset of CNS axons. At earlier stages in development, FasII also labels some commissural pathways.

We found a variety of CNS phenotypes in our screens. Here we show some interesting examples of *robo*-like phenotypes, analyzed by 1D4 staining. *robo* encodes

an immunoglobulin (Ig) domain superfamily member that is a neuronal receptor for the midline glial ligand Slit, which functions as a repellent in this context (KIDD *et al.* 1999; KIDD *et al.* 1998). In the absence of Robo, 1D4-positive axons have reduced sensitivity to the repulsive Slit signal. As a consequence, they cross the midline repeatedly, forming trajectories with a circular appearance (Figure 2B). We found several regions of the genome whose deletion results in phenotypes resembling that of *robo*, although all of the Df phenotypes are more severe than those of *robo* single mutants.

Df(3R)Exel7310, Df(1)BSC627, and Df(2L)Exel8041 embryos all have midline guidance defects in which FasII-positive axons appear to form circles around the midline (Figures 2C, E, F). Each Df has its own characteristic phenotype. Df(3R)Exel7310 deletes a candidate gene, *shadow* (*sad*) that has a published *robo*-like phenotype (GIESEN *et al.* 2003). To determine whether the phenotype of this Df is due to loss of *sad*, we crossed the sad^{1} point mutation to the Df. The resulting transheterozygous embryos also have *robo*-like phenotypes, although they are much weaker than those of Df/Df embryos (Figure 2D). Perhaps sad^{1} is not a null mutation, or other genes under the Df contribute to the phenotype. The other two Dfs appear to define new genes whose absence causes axons to circle around the midline. We have used overlapping Dfs to map these genes to smaller regions within Df(1)BSC627 and Df(2L)8041.

Figures 2G and H show Dfs for which 1D4-positive axons abnormally cross the midline without circling. In Df(3L)HD1 embryos (Figure 2G), axons in the inner 1D4

longitudinal pathway cross the midline. Several other Dfs also have this kind of phenotype. Df(3R)Exel6162 produces an interesting phenotype in which the CNS has a normal organization, but one of the commissural pathways is now 1D4-positive (Figure 2H). This phenotype could arise from abnormal guidance of a small subset of longitudinal 1D4 axons across the midline, or from ectopic expression of FasII on a commissural axon bundle.

SNa Guidance Phenotypes

The SNa exits the CNS in the SN nerve root. SNa has a characteristic bifurcated morphology in wildtype late stage embryos, with a dorsal (or anterior) branch and a lateral (or posterior) branch. The SNa bifurcation point is at the dorsal edge of muscle 12. The dorsal branch of the SNa innervates muscles 21-24, while the lateral branch innervates muscles 5 and 8 (Figures 3A, E). Each mild Df was screened for the presence of a bifurcated SNa pathway. Of the 190 lines screened, 20 had SNa bifurcation defects (Table 1).

The SNa pathway develops later than the other motor axon pathways, and is also fainter than the ISN or ISNb in 1D4-stained preparations. We could not be sure that SNa defects seen in the fluorescent live dissections were not due to developmental delays. Accordingly, we did not attempt to quantitatively score SNa bifurcation failures in live-dissected embryos. Instead, we generated fixed early stage 17 whole-mount embryos stained with 1D4, using horseradish peroxidase (HRP) immunohistochemistry for detection, for a subset of the Dfs that had strong SNa defects. These were then dissected and visualized with differential interference

contrast (DIC) optics. Fixed-dissected embryos can be analyzed at later stages than live-dissected embryos, because live-dissected embryos that have developed cuticle do not stick to glass slides.

Previously reported SNa phenotypes (e.g., *Ptp52F* (SCHINDELHOLZ *et al.* 2001)) usually involve the loss of either the dorsal or lateral branch with an approximately equal probability. Df(3R)BSC42 causes a typical SNa bifurcation defect in which the dorsal, lateral, or both branches are missing with nearly the same penetrances (3%, 3%, and 4% respectively in HRP-stained preparations; Figure 3I). However, Df(2R)BSC19 produces a unique phenotype in which only the dorsal branch of SNa is absent (Figures 3B, G, and I). When we examined this line using fixed-embryo dissections, we found that the dorsal branch of SNa was completely missing in 25% of hemisegments (n=155) while the lateral branch is almost always present. Both SNa branches are present in >98% of hemisegments in wildtype embryos at the same stage (n=135) (Figure 3I).

We examined whether the loss of the dorsal SNa branch in Df(2R)BSC19 embryos might be due to absence or malformation of its target muscles. Using phalloidin staining in live-dissected embryos, we determined that in 25% of abdominal hemisegments (n=88) one or more of the dorsal branch target muscles (21-24) is not present, and this could account for the absence of the branch in these hemisegments. In live-dissected preparations, the SNa phenotype appears to be much stronger, so that 87% of hemisegments have a missing dorsal branch. In most of

these (71% of total hemisegments), we find that the target muscles are in the proper place, yet SNa still fails to bifurcate (Figures 3G, H).

The difference in the apparent strength of SNa phenotypes between live-dissected embryos stained fluorescently and fixed-dissected embryos stained by HRP immunhistochemistry likely results from the greater age of the fixed-dissected embryos, and from differences in the way that scoring is performed. SNa phenotypes appeared to be stronger in live-dissected preparations for other Dfs, including Df(3R)BSC42, as well as for Df(2R)BSC19 (note that the penetrance of the Df(3R)BSC42 phenotype shown in Figure 3I is below the 20% threshold used for Df selection, but this is because quantification was performed on HRP-stained early stage 17 embryos). It is possible that dorsal branch axons extend later in Df(2R)BSC19 embryos than in wildtype. In addition, we scored the fixed-dissected embryos as lacking the dorsal branch only if no branch was visible at all in a given hemisegment. In many hemisegments of these embryos, a single axon is observed following the pathway of the dorsal branch, and these would have been scored as "dorsal branch present" (Figure 3D). This single axon may be too faint to see at all (or had not yet extended) in fluorescent live-dissected embryos, and such SNas would thus have appeared to be completely unbranched.

In many of the hemisegments in Df(2R)BSC19 embryos where the dorsal branch is missing or contains only one axon, there may be too many axons in the lateral branch, as this branch is abnormally thick (Figures 3B, D). We also find that in some hemisegments SNa is bifurcated at the appropriate location, but the axons in the

dorsal branch stall just beyond the bifurcation point (Figure 3C). In summary, the phenotype of Df(2R)BSC19 is likely to be a complex mixture of defects in axon guidance, defects in differentiation of lateral muscles, and developmental delays. We have narrowed down the responsible region of this Df to ~6 genes. Whether all phenotypes are caused by the absence of a single gene remains to be determined.

ISNb Guidance Phenotypes

The ISNb contains the axons of the RP1, RP3, RP4, and RP5 neurons, among others. These axons cross the midline and exit the CNS in the ISN nerve root. They must defasciculate from the common ISN pathway at the "exit junction" in order to enter the ventrolateral muscle (VLM) field. Once there, they innervate muscles 6, 7, 12, 13, 14, and 30 (Figures 4A, C). Of the 190 lines screened, 9 were found to have strong ISNb defects. These ISNb phenotypes include "bypass," in which ISNb axons fail to separate from the ISN and grow past the VLMs, and "stall," in which axons enter the VLM field but fail to reach the normal ISNb termination point at the ventral edge of muscle 12 (Figure 4A). We also found some structural abnormalities in the ISNb that could not be grouped into one of these classes.

Df(3L)Exel6087 produces a highly penetrant stall of the ISNb at the dorsal edge of muscle 6, which corresponds to the ventral edge of muscle 13. We quantified this phenotype in fixed-dissected embryos stained by HRP immunohistochemistry, and found that in 63% of hemisegments (n=144) the ISNb fails to extend across muscle 13 (Figures 4B, D). Muscles 12 and 13 are present and appear normal both by phalloidin staining and DIC optics. Df(2L)Exel7080 causes a bypass phenotype in

which 14% of hemisegments (n=168) have no ISNb axons that grow into the VLM field (Figures 4B, E, F). We have identified the single gene under this Df whose loss is responsible for the bypass phenotype (A. Cording, unpublished results). Df(2L)ED1317 has an interesting structural phenotype in which ISNb axons form loops on muscles 6 and 7 (Figure 4H). When we examined fixed-dissected Df(2L)ED1317 embryos stained by HRP immunohistochemistry, we could not see this phenotype. It is likely that fine axonal branches such as those in the loops can be more readily seen in fluorescent preparations. Also, the aspect of the phenotype in which the axons failed to grow across muscle 13, which should have appeared as a stall in preparations stained by HRP immunohistochemistry, may have corrected itself later in development, so that it was no longer evident in the older embryos that were analyzed as fixed dissections. These results, together with observations we have made on other Df phenotypes, suggest that phenotypes can be detected by examining live dissections that cannot be seen in fixed dissections, even if they are both examined under a compound microscope.

Requirement of the *glial cells missing* Genes for ISNb Guidance

Df(2L)Exel7042 has an ISNb phenotype that is a mixture of stall, bypass, and absence, in which there is no ISNb at all (12%, 8%, and 17% of hemisegments, respectively; n=118) (Figure 4B). The CNS has a wavy 1D4 pattern with occasional breaks in the longitudinal tracts (Figure 5B). When we assessed the genes that are deleted by this molecularly mapped Df, two obvious candidates were found: *glial cells missing* (*gcm*) and *glial cells missing 2* (*gcm2*). *gcm* and *gcm*2 are transcription factors

that are expressed in all glia except for midline glia and are required for glial cell fate determination (HOSOYA *et al.* 1995; JONES *et al.* 1995; VINCENT *et al.* 1996). In the absence of Gcm protein, some presumptive glial cells become neurons. When Gcm or Gcm2 is ectopically expressed in neurons, some of them become glia (ALFONSO and JONES 2002; HOSOYA *et al.* 1995; JONES *et al.* 1995; KAMMERER and GIANGRANDE 2001). *gcm* therefore acts as a molecular switch between the neuronal and glial cell fates. *gcm* and *gcm2* have largely overlapping expression patterns, with *gcm* being expressed at much higher levels than *gcm2*. In *gcm* mutants, a few glial cells remain, usually those in which *gcm2* expression is strongest. In the absence of both Gcm proteins, no glial cells are found (ALFONSO and JONES 2002; KAMMERER and GIANGRANDE 2001).

CNS axon guidance phenotypes have been previously observed in *gcm* mutants, including breaks in the longitudinal fascicles and abnormal trajectories of the pioneer axons of both the ISN and SN nerve roots (HIDALGO and BOOTH 2000; HOSOYA *et al.* 1995; JONES *et al.* 1995; SEPP *et al.* 2001; VINCENT *et al.* 1996). Motor axon pathways usually develop normally in *gcm* mutants, although a published image of a *gcm* embryo has a missing ISNb in one hemisegment (SEPP *et al.* 2001). When we stained *gcm* null alleles with 1D4, we found that ISNb is affected, but with a much lower penetrance than in Df(2L)Exel7042 embryos, and the missing ISNb phenotype is almost never observed (data not shown). Thus, the deletion of both *gcm* and *gcm2* by Df(2L)Exel7042 could account for the severity of its ISNb phenotype. We also examined homozygotes for another Df which deletes both *gcm* and *gcm2*, Df(2L)200,

as well as Df(2L)Exel7042/Df(2L)200 transheterozygotes. Homozygotes for a very small Df, Df(2L)ED684, which deletes only 7 genes, including *gcm* and *gcm2*, were also tested. In all of these cases, we saw the same ISNb defects as in Df(2L)Exel7042, with similar penetrances (data not shown).

To examine how the absence of glia affects the ISNb, we stained Df(2L)Exel7042 embryos with an antibody to Fasciclin III (FasIII), which is a marker for the cell bodies and proximal axons of the ISNb neurons RP1, RP3, RP4 and RP5 (PATEL *et al.* 1987). In wildtype embryos, FasIII staining reveals a regular pattern in which RP axons cross the midline and then extend posteriorly for a short distance before entering the ISN root (Figure 5D). In Df(2L)Exel7042 embryos, a variety of defects were seen that could account for the different classes of guidance errors we see in ISNb (Figure 5E). We found that in many segments of the embryos extra cells express FasIII. This is likely due to the fate switches from glial to neuronal that occur in the absence of *gcm* and *gcm2* function. We also observe that in some segments neurons of the RP cluster fail to extend axons. In other segments they extend axons that enter the longitudinal tracts, but then exit the CNS in the wrong place or never exit at all. In some cases the axons grow anteriorly rather than posteriorly along the longitudinal tracts. All of these phenotypes could result in the loss of the ISNb in the periphery, as well as contributing to the observed breaks in the longitudinal tracts. Are the defects we see in Df(2L)Exel7042 due to a lack of glial cells, or to loss of some other function of *gcm* and *gcm2*? In order to test whether glia are required for ISNb axon guidance we examined *reversed polarity* (*repo*) mutants. *repo* encodes a

transcription factor that is downstream of *gcm* and is also required for glial cell fate (CAMPBELL *et al.* 1994; HALTER *et al.* 1995; HOSOYA *et al.* 1995; XIONG *et al.* 1994) . In the absence of Repo, few glial cells differentiate. We stained embryos homozygous for a null allele of *repo* with 1D4. We found that the longitudinal axon tracts in *repo* embryos are wavy and have breaks (Figure 5C). There are extra midline cells expressing FasIII in some segments. We also observed guidance errors with anti-FasIII in which RP axons turn anteriorly along the longitudinal pathway. However, these defects are not as penetrant as when *gcm* and *gcm2* are both deleted (Figure 5F). In the periphery, the ISNb is usually normal in *repo* embryos, although there are rare stall phenotypes (Figure 5I). This result might be explained by the fact that although *repo* is required for normal glial cell fate, in the absence of *repo* glia still begin to differentiate and express some glial antigens (CAMPBELL *et al.* 1994; HALTER *et al.* 1995; XIONG *et al.* 1994).

In summary, we hypothesize that the unique phenotype produced by Df(2L)Exel7042 occurs because no glial development whatsoever takes place when both *gcm* and *gcm2* are absent. As a consequence, development of the RP cell bodies and axon tracts is abnormal in most segments, resulting in the absence of the ISNb in those segments in which no axons leave the CNS. The ISNb stall phenotypes could result from a partial loss of ISNb axons. If the axons which normally innervate muscles 12 and 13 failed to extend, the ISNb would be expected to terminate proximal to those muscles. ISNb bypass phenotypes could be due to the absence of glial cells near the exit junction. These glia might be required for normal separation of the ISNb

and ISN axons. These ISNb phenotypes were not found before because embryos lacking both Gcm proteins had never been examined for motor axon defects.

Dfs Causing Changes in Antigen Expression

Another potential use of Df screening would be to find genes required for normal cellular or subcellular expression of proteins that can be visualized by antibody staining. In the course of our examination of Df homozygotes by 1D4 staining, we found two Dfs for which homozygotes (or hemizygotes) lack 1D4 antigen. One of these, Df(1)C128, is shown here (Figure 6D). Df(1)C128 embryos clearly contain CNS axons, as shown by rhodamine-phalloidin staining (Figure 6E), and they also stain with BP102 (data not shown). Df(1)C128 does not delete the FasII gene, and we confirmed that the line does not harbor a *FasII* mutation by complementation testing. The most likely explanation for the loss of FasII expression is perhaps that Df(1)C128 deletes a gene encoding a transcription factor necessary for production of *FasII* mRNA. We also found Dfs that eliminate BP102 staining, while preserving 1D4 staining (data not shown).

Embryos homozygous for Df(3R)Exel7310 display 1D4 staining on cells in the periphery that normally do not exhibit staining. These are large, flat cells just anterior to the LBD neuron (Figures 6I, J). We do not know the identities of these cells. They appear to be internal to the epithelial layer, and they do not have morphologies like those of muscles or sensory neurons. Two possible explanations for this the presence of this ectopic 1D4 staining are: (1) the Df deletes a gene encoding a repressor that prevents the FasII gene from being transcribed in these cells; (2) it removes a gene

whose product normally cleaves FasII off the surfaces of these cells. Other models are also possible. We have also found Dfs that cause BP102 to be ectopically expressed in the periphery, while leaving 1D4 staining unaltered (data not shown).

Discussion

Here we show that deficiency (Df) screening can provide a way to systematically screen the *Drosophila* genome for any phenotype or expression pattern that can be visualized in embryos. Df screens are much less time-consuming than point-mutant screens, since only a few hundred Dfs, rather than thousands of point-mutant lines, need to be examined in order to survey most of the genes. In this chapter, we define new kits of publicly available Dfs that can be used to screen for orphan receptor ligands, antigen expression and localization, and embryonic phenotypes. A set of ~400 Dfs for which homozygotes develop well enough to have a recognizable CNS and body walls encompasses 82% of polytene chromosome bands (Supplementary Table 1). Figure 1 illustrates the use of this Df kit to find genes required for expression of ligand(s) for Ptp99A. Homozygotes for three Dfs lack staining of CNS axons by a Ptp99A XC domain fusion protein. We also found Dfs that eliminate expression of the axonal cell surface protein FasII, or which cause FasII to be ectopically expressed (Figure 6).

Subsets of this Df collection that have relatively normal embryonic development can be used to screen for regions of the genome whose deletion confers specific embryonic phenotypes. Figure 2 shows CNS phenotypes in which axons have defects in guidance across the midline. To facilitate systematic examination of

embryonic phenotypes for multiple tissues, we defined a kit of 233 lines with "mild" phenotypes, for which body walls have a wildtype morphology and the CNS has a normal ladder-like structure (Supplementary Table 2). This kit covers ~50% of polytene chromosome bands. We screened it for motor axon guidance defects, and have identified many new regions containing genes necessary for establishment of motor axon pathways. Here we show examples of SNa phenotypes (Figure 3) and ISNb phenotypes (Figures 4, 5). The analysis of these Df phenotypes, which are described in detail in results, provides new information on cell biological mechanisms involved in motor axon guidance.

Development, Characterization, and Use of the "Complete" Df kit

The "complete" kit contains the 233 X, 2nd chromosome, and 3rd chromosome Dfs with mild phenotypes, 83 Dfs with moderate phenotypes, and 78 Dfs with severe phenotypes (Supplementary Table 1). An additional 25 Dfs, covering ~10% of polytene chromosome bands, are classified as very severe. Homozygotes for very severe Dfs, although they all have some CNS axons and were screened by Lar-AP and BP102 staining, fail to develop many embryonic structures. The remaining ~8% of the genome cannot be examined at present using Df screening, because embryos homozygous for Dfs in these regions fail to develop any recognizable late embryonic structures and cannot be dissected.

For identification of homozygote embryos, Dfs are placed over GFP balancer chromosomes, so that Df/Df embryos can be recognized prior to dissection. 29 Dfs on

the X, 2nd, and 3rd chromosomes cannot be maintained over these balancers and must be screened blind. There are also 9 4th chromosome Dfs that lack GFP balancers. To screen the kit for ligand or antigen expression, one collects embryos from groups of up to 10 lines at a time, sorts them for GFP expression, lines up GFP-minus embryos in rows on a glass slide, and dissects 4 or 5 embryos for each line. If the Dfs are being screened for antigen expression or phenotype, they are immediately fixed and stained with the appropriate antibody. If a ligand screen is being conducted, the embryos are first incubated live with receptor fusion proteins, followed by fixation and detection of fusion protein binding with secondary and tertiary antibodies (Fox and Zinn 2005). To facilitate screening, we have published a detailed video protocol for sorting, live dissection, and staining of embryos (LEE *et al.* 2009).

A single person can screen up to 10 lines per day using these methods, so a genome-wide screen can be completed within three or four months of part-time work. This is obviously much faster than any point-mutant screen, but does not identify single genes. These must be found by examination of overlapping Dfs and insertion mutants. However, since thousands of Dfs are available in public collections, and about half of *Drosophila* genes have at least one insertion, it is usually possible to find single genes responsible for Df phenotypes within a relatively short time period. Using these methods, we identified the HSPG Syndecan as a ligand for the Lar RPTP by screening the Bloomington Df kit as it existed in 2002 (Fox and Zinn 2005). This kit contained a large number of Dfs for which homozygotes failed to develop. Also, most of the Dfs were only defined at cytological resolution, making it difficult to localize

individual genes. This provided the impetus for a project in which we analyzed hundreds of additional Dfs for phenotype and ligand staining, so as to define the smallest possible collection of Dfs that would allow genome-wide ligand and phenotype screening, as well as rapid localization of genes within an identified region. In 2009, Kevin Cook and his colleagues at the Bloomington stock center replaced the old Bloomington kit with a new kit of 467 molecularly defined deletions (MARYGOLD *et al.* 2007; PARKS *et al.* 2004). This kit covers ~98% of euchromatic DNA. They were not interested in phenotype when they created this kit, but only in maximum coverage by a minimum number of Dfs. Our project was carried out independently of their work, screening new Dfs for phenotype and adding them to our kit as they were generated by the community. Thus, although our kit is almost entirely composed of lines available from Bloomington, only 31% of the lines in our kit are in the new Bloomington Df mapping kit. Also, our kit was developed by replacing Dfs in the old Bloomington kit one at a time over a multiyear period with Dfs that had better embryonic development, and we retained Dfs from the old kit for which homozygote embryos developed well. As a consequence, our kit contains 185 lines for which the Dfs are not molecularly mapped. In the past, this would have made gene localization under the Dfs difficult, since the Df breakpoints would have to be sequenced to define the deleted region at the molecular level. Now, however, because so many molecularly mapped Dfs are available, if one finds a "hit" in a Df mapped only to cytological resolution, overlapping molecularly mapped Dfs can immediately be

obtained and screened. When one of these is demonstrated to have the desired phenotype, this localizes the gene in question to a molecularly defined interval.

Screening for Ligands and Antigens

To screen the genome for orphan receptor ligands, the first step is to generate fusions of the XC domain of the receptor of interest to AP, an obligate dimer. These dimeric fusion proteins are expressed at high levels using the baculovirus system, and unpurified supernatants are used directly for staining. Live-dissected embryos of various ages are incubated with fusion protein supernatants, followed by fixation, rabbit anti-AP secondary antibody, and tertiary anti-rabbit fluorescent antibody. Once robust staining of a potential ligand(s) has been obtained, the Df collection is screened by double-staining with receptor fusion protein and a mouse monoclonal antibody that recognizes the tissue in which the ligand is expressed. This is necessary in order to ensure that the absence of staining in homozygotes for a particular Df is not due to the absence of the relevant tissue. In our case, we observed that the RPTP-AP fusion proteins all stained CNS axons, so we double-stained each Df with BP102, an antibody which recognizes an epitope on CNS axons (Figure 1).

Some advantages of this method over other ways of identifying orphan receptor ligands, such as cDNA expression cloning in mammalian cell systems, include: (1) since it is a search for genes that are necessary for ligand expression, not genes sufficient for expression, it can identify components of multimeric ligands, which could not be found by expression cloning; (2) its success does not depend on the abundance of the mRNA encoding the ligand(s); and (3) the screen identifies not

only the ligand genes themselves, but other genes required for ligand expression or localization. For example, in the screen that identified Syndecan, we also found genes encoding modification enzymes necessary for HSPG synthesis (Fox and Zinn 2005). This same type of screen can also identify genes required for expression or localization of any antigen recognized by a high-quality antibody. In our screen, we found Dfs that eliminated expression of the FasII protein. We also found Dfs that caused FasII to be expressed in different cell types than in wildtype embryos (Figure 6). The responsible genes under these Dfs might encode transcription factors necessary for *FasII* mRNA expression, or proteins required for transport of FasII to the cell surface. We also found Dfs that eliminate BP102 expression, or shift BP102 antigen onto other cell types. For these Dfs, we have localized the single responsible genes, and this has allowed us to define the previously unknown epitope recognized by BP102 (A. Wright, unpublished results).

The kit could be used in a number of additional ways beyond those we have employed. It could facilitate identification of genes required for appropriate subcellular localization of a protein. For example, if one screened with an antibody recognizing an apical protein, one could find genes necessary for its localization to the apical side of the cell. One could also screen for genes necessary for delivery of proteins to axons or dendrites. Kit screening could also be done using fluorescent *in situ* hybridization. This would allow identification of genes required for appropriate expression of a transcript, even if one does not have a good antibody against the protein encoded by the transcript.

Using Subset Kits to Screen for Phenotypes

In the course of our screening for RPTP ligands, we noted that embryos homozygous for many Dfs developed relatively normally, suggesting that they could be screened for specific phenotypes. We examined the Dfs that had mild phenotypes, and a subset of those with moderate phenotypes, by double-staining with 1D4 and rhodamine-phalloidin. 1D4 recognizes the cytoplasmic domain of the transmembrane form of FasII, and is a marker for motor axons and a subset of longitudinal CNS axons in late embryos. Phalloidin, which binds to polymerized actin, allows examination of muscle fibers and CNS axons.

We found many specific CNS axon guidance phenotypes. Here we show some examples of phenotypes in which 1D4-positive longitudinal axons abnormally cross the midline. Three of these have a *robo*-like appearance, in which axons appear to circle around the midline (Figure 2). The phenotype of one of these Dfs is at least partially due to deletion of the known gene *sad*, while the other two appear to define new genes. These phenotypes were discovered through analysis of a subset of "moderate" lines that had fused commissures when analyzed with BP102. It is likely that a complete survey of the moderate and severe lines with 1D4 would uncover many new and interesting CNS axon guidance phenotypes.

We systematically examined the kit of mild Df lines for motor axon phenotypes, and have defined 20 Dfs that cause SNa bifurcation defects, 9 that produce ISNb defects, and others that cause ISN and SNc defects. At least 24 produce muscle phenotypes (Table 1, Supplementary Table 3). The Dfs of most interest to us

were those for which embryos have altered motor axon pathways and normal muscles, as these may define new genes required for navigation of motor axon growth cones.

The 20 Dfs that produce SNa bifurcation defects may represent an overestimate of the number of regions required for SNa guidance, because SNa develops late and these Dfs might cause developmental delays. We did identify Dfs spanning the *Ptp52F* gene. Our group had shown that Ptp52F is required for SNa bifurcation (SCHINDELHOLZ *et al.* 2001). *Ptp52F* mutants were previously shown to display high-penetrance SNa bifurcation defects in early stage 17 embryos, suggesting that the bifurcation defect in these mutants is not caused by delay. We addressed the issue of developmental delay for other Dfs by examining fixed early stage 17 embryos. Here we show data for two Dfs that still produced bifurcation defects at this stage. Df(2R)BSC19 embryos have an unusual phenotype in which only the dorsal SNa branch is missing, and the dorsal axons are probably misdirected into the lateral branch (Figure 3).

We identified 9 regions whose deletion selectively affects ISNb guidance without visibly altering muscle development. Eight of these appear to define genes that have not been previously shown to affect motor axons. One Df produces a highly penetrant phenotype in which the ISNb terminates at the ventral edge of muscle 13. Another Df produces a unique "looped" ISNb phenotype that can only be detected in live-dissected embryos (Figure 4).

We examined the relationships between the Dfs and the locations of previously identified genes affecting the ISNb, to determine why we did not recover more Dfs spanning known ISNb guidance genes. We did find Dfs spanning one known gene, *sidestep* (*side*), but had classified these as affecting multiple pathways, since *side* mutants also have SNa and ISN defects (SINK *et al.* 2001). For other known ISNb axon guidance genes with high-penetrance mutant phenotypes, the Df in our complete kit that spanned the gene was not within the subset of mild Dfs. For example, the *Lar* gene could not have been discovered using the mild Df kit, because the *screw* gene is embedded in one of its introns. Deletion of *screw* causes early developmental failure (ARORA *et al.* 1994). The only Df in our complete kit that removes *Lar* sequences also spans *screw*, and thus has a very severe phenotype.

The identification of 9 regions selectively affecting ISNb guidance within the ~40% of the genome covered by the mild Dfs we screened suggests that there might be a total of ~22 genes with ISNb-specific loss-of-function (LOF) phenotypes in the whole genome. This seems like a surprisingly small number of genes, but it is important to note that single mutations in many axon guidance genes produce only low-penetrance defects. Deletion of such genes might produce no phenotype, or a phenotype whose penetrance would fall below the threshold (~20%) required for us to classify the Df as abnormal. For example, loss of either Ptp69D or Ptp99A produces weak ISNb phenotypes, but a double mutant has strong phenotypes (DESAI *et al.* 1996; DESAI *et al.* 1997). *robo2* (*leak*) mutants have weak CNS phenotypes, but *robo2* mutations strongly enhance the *robo* phenotype, so that the *robo robo2* double

mutant phenotype resembles that of *slit* (SIMPSON *et al.* 2000). Thus, because of genetic redundancy, there are probably many genes involved in axon guidance that cannot be discovered by LOF screens. Such genes must be identified by candidate gene approaches, like those used to find *Ptp69D*, *Ptp99A*, and *robo2*, or by conducting enhancer/suppressor screens.

We note that the problem of genetic redundancy can be sometimes be addressed using Dfs, since closely related genes are often located near each other. One of the 9 regions we identified as affecting ISNb guidance contains the *gcm* and *gcm2* genes, which encode transcription factors that contribute to glial cell fate determination. When both *gcm* and *gcm2* are deleted, there are no glia at all, and as a consequence the ISNb motor axons sometimes fail to leave the CNS, producing hemisegments that completely lack an ISNb (Figure 5). This phenotype, discussed in detail in results, is almost never observed when only *gcm* is mutant, perhaps because a few glia are still present due to *gcm2* expression. Thus, it could only have been discovered using Dfs. Similar phenomena might be observed for other clusters of related genes.

The use of the Df kit has allowed us to discover phenotypes that had not been seen previously. These include the looped ISNb phenotype (Figure 4), SNc-specific phenotypes, and new phenotypes affecting multiple motor axon pathways. Since most tissues appear to develop normally in homozygotes for mild Dfs, this kit should provide a valuable resource for other groups that are interested in screening for new phenotypes affecting any embryonic organ. The only requirement for performance of

such a screen is a good antibody that recognizes structures within the tissue in question. Such screens can systematically survey ~50% of the genome for any phenotype that can be visualized at high magnification under a compound or confocal microscope. A single person could conduct such a screen in a period of months, making it a much less daunting project than the execution of an EMS or P element screen.

Acknowledgments

We thank Kevin Cook (Bloomington) for providing extensive information on deletions, and the Bloomington, Szeged, and Kyoto stock centers for stocks. We also thank Peter Lee for helpful discussions, Kaushiki Menon and Angela Stathopoulos for comments on the manuscript, Elena Armand for stock maintenance, and Violana Nesterova for figure preparation. Confocal imaging was performed at the Caltech Biological Imaging Facility. 1D4, BP102, and 7G10 supernatants were obtained from cell lines grown by the Caltech Monoclonal Antibody Facility. RPTP-AP fusion proteins were obtained from baculovirus infected cell supernatants generated by the Caltech Protein Expression Center. A. N. F. was supported by an NRSA postdoctoral fellowship. This work was supported by NIH RO1 grants NS028182 and NS062821 to K. Z. and NSF grant IOS-0841551 to K. J.

Materials and Methods

Genetics

Most Df strains and mutants were obtained from the Bloomington Stock Center. A few Df lines were obtained from the Szeged and Kyoto Stock Centers. Deficiency kit lines were balanced over FM7c, P(Gal4-Kr.C)DC1, P(UAS-GFP.S65T)DC5, sn-, CyOarmGFP, TM3armGFP, CyO-Wingless-LacZ, or Tm6B-Ubx-LacZ (Bloomington).

Immunohistochemistry

Homozygous deficiency embryos were identified by the absence of GFP fluorescence from the GFP gene on the balancer chromosome using an Olympus GFP dissecting microscope. See (Fox and Zinn 2005; Lee *et al.* 2009) for dissection and fusion protein staining protocols. Briefly, for 1D4 fluorescent staining, embryos are dissected live on glass slides, fixed and washed in PBS. Embryos are then washed in PBS + 0.5% Triton (PBT), blocked with PBT + 5% heat-inactivated normal goat serum (NGS) and incubated overnight in a dilution of 1:3 1D4 in PBT + 5% NGS. After washing in PBT embryos are incubated at 4 ^{0}C overnight in AlexaFluor anti-mouse 488 secondary antibody and rhodamine-phalloidin (Invitrogen). For fusion protein staining, embryos are incubated in fusion protein for 2 hours after dissection in the absence of detergent. Samples are fixed, washed, and incubated in rabbit-anti-AP and BP102 overnight at 4 ^{0}C and then processed with appropriate secondary antibodies. Samples are mounted in 70% glycerol in PBS.

Fixed embryo immunohistochemistry was performed as previously described (VAN VACTOR *et al.* 1993). Briefly, after fixation embryos are extensively washed in PBS + 0.5% Triton (PBT), incubated overnight at 4C in PBT + 5% heat-inactivated goat serum (HIGS) with a 1:5 dilution of 1D4 antibody plus 1:5000 dilution of rabbit-anti-beta-galactosidase antibody (MP Biomedicals) to label embryos carrying the balancer chromosomes. Embryos are extensively washed in PBT and then incuabated overnight at 4 ^{0}C in PBT + 5% HIGS with 1:500 dilutions of horseradish peroxidase-conjugated goat anti-mouse and goat anti-rabbit (Jackson Immunoresearch). After extensive washing in PBT, the peroxidase reaction was carried out using a DAB peroxidase substrate kit (Vector Laboratories), and the embryos were mounted in 70% glycerol and dissected.

Embryos were scored for fusion protein staining, motor axon defects, CNS defects, and muscle defects on a Zeiss Axioplan microscope with a 40X multi-immersion objective. Screening for CNS, motor axon, and muscle defects was conducted by scoring 5 homozygous deficiency embryos per stock. Abdominal hemisegments A2-A7 were scored. Quantitative data was obtained by analyzing 1D4 HRP immunoreactivity. Homozygous deficiency embryos were scored blind for axon guidance defects in abdominal hemisegments A3-A7.

The following antibodies were used rabbit anti-AP (Serotec) 1:600, mAb bp102 1:30, mAb 1D4 1:3, mAb7G10 1:5 (Caltech Monoclonal Antibody Facility), AlexaFluor anti-mouse 488, Alexa Fluor anti-mouse 568, and AlexaFluor anti-rabbit

488 (Invitrogen) 1:1000. Rhodamine-phalloidin (Invitrogen) was used at 1:2000 to detect muscle structure.

Confocal imaging was performed using a Zeiss LSM inverted microscope using 20X, 40X, and 63X Zeiss oil-immersion objectives. Stacks were projected using Image J software maximum intensity projections.

Figure Legends

Figure 1. Deficiencies that reduce 99A-AP fusion protein staining of CNS axons. Confocal maximum intensity projections of late stage 16 live-dissected *Drosophila* embryos visualized by immunofluorescence (20X objective). Anterior is up. Panels A-F show the ventral nerve cord and one half of the body wall. Panels G-N show a portion of the ventral nerve cord. In Panels A-F scale bar equals 20 μm. In Panels G-N scale bar equals 10 μm. (A) 99A-AP fusion protein staining pattern in a wildtype embryo. The arrow indicates 99A-AP fusion protein binding to axons in the ventral nerve cord while the arrowhead indicates binding to tracheae. (B) mAb BP102 staining labels commissures and longitudinal connectives of the ventral nerve cord (arrow) in the same embryo. (C) Wildtype merged image (99A-AP, green; BP102, magenta). (D) 99A-AP fusion protein staining is absent from the ventral nerve cord in a Df(2L)Exel7042 embryo, while tracheal staining remains unaltered (arrowhead). (E) mAb BP102 staining in Df(2L)Exel7042 reveals that axons are still present in the ventral nerve cord (arrow). (F) Df(2L)Exel7042 merged image. (G and H) wildtype embryo stained with 99A-AP fusion protein and mAb BP102. (I and J) Df(2L)Exel7042 embryo stained with 99A-AP fusion protein and mAb BP102. (K and L) Df(3R)Cha7 embryo lacks 99A-AP fusion protein staining of CNS axons, but has axons as evidenced by BP102 staining (L). (M and N) Df(3R)Exel6176 embryo has reduced 99A-AP fusion protein binding to CNS axons, but has axons as evidenced by BP102 staining (N). Note that there appears to be more staining of cell bodies in the CNS than in (I) and (K).

Figure 2. Examples of CNS phenotypes in deficiency homozygotes.

(A-H) are confocal maximum intensity projections of mAb 1D4 immunofluorescence in live-dissected stage 16 embryos (20X objective). Anterior is up. Scale bar equals 10 μm. (A) wildtype embryonic nerve cord showing three parallel longitudinal bundles on either side of the midline and no FasII positive bundles crossing the midline. (B) Staining of FasII in *robo*^{1} reveals a phenotype where axons repeatedly cross the midline in a circular fashion (arrow). This is a *robo*^{1} phenotype of "average" strength. Most published *robo* images are of unusually strong phenotypes. (C) Df(3R)Exel7310 embryonic nerve cord has a phenotype where axons appear to circle the midline (arrow). (D) *sad*^{1}/Df(3R)Exel7310 has a phenotype in which FasII positive axons cross the midline. It is weaker than the phenotype in (C), however. (E) Df(1)BSC627 and (F) Df(2L)Exel8041 also have phenotypes where axons appear to circle the midline (arrows). Each of the three phenotypes has a unique overall appearance, however. (G) In Df(3L)HD1, FasII positive axons of the inner fascicle cross the midline inappropriately (arrows). (H) Df(3R)Exel6162 has a phenotype in which the nerve cord has a normal geometry, but one commissural bundle per segment is FasII positive (arrow).

Figure 3. SNa defects in Df(2R)BSC19 and Df(3R)BSC42.

(A-D) each show 2 abdominal hemisegments from late stage 16 embryos fixed and stained with mAb 1D4 using horseradish peroxidase immunohistochemistry (63X oil immersion objective and DIC optics). Anterior is to the left and dorsal is up. (A) The wildtype SNa has a characteristic bifurcated morphology where the dorsal branch innervates muscles 21-24 and the lateral branch innervates muscles 5 and 8. The bifurcation point is just dorsal to muscle 12 (labeled) and is indicated by an asterisk. (B) Df(2R)BSC19 abdominal hemisegments lack the dorsal branch of the SNa (asterisk) while the lateral branch appears thicker than wildtype (arrowhead). (C) Df(2R)BSC19 abdominal hemisegment where a short dorsal branch has extended but not reached the target muscles (arrow). (D) Df(2R)BSC19 abdominal hemisegments in which only one axon has extended dorsally (arrows). The lateral branch appears thicker in the left hemisegment (arrowhead). (E-H) Maximum intensity confocal projections of stage 16 live-dissected embryos double stained with 1D4 and rhodamine phalloidin (63X oil immersion objective). Anterior is to the left and dorsal is up. Scale bar equals 10 μm. (E-F) wildtype abdominal hemisegments showing a bifurcated SNa (asterisk). The target muscles of the dorsal branch of SNa (muscles 21-24) are indicated by brackets in (F). (G-H) Df(2R)BSC19 abdominal hemisegments showing the absence of the dorsal branch of SNa (asterisks) but the presence of target muscles 21-24 (brackets). (I) Chart showing quantification of various SNa defects in

wildtype, Df(2R)BSC19 and Df(3R)BSC42. The number of abdominal hemisegments A3-A7 scored is as follows: wt = 135, Df(2R)BSC19 = 155 , Df(3R)BSC42 = 126.

Figure 4. Examples of ISNb defects in deficiency homozygotes.

(A) Schematic showing the axons of the of ISNb and their muscle targets in wildtype. Axons of the ISNb (blue) defasciculate from the ISN (red) at the exit junction (EJ) and enter the ventrolateral muscle field (green). The ISNd is in olive green. First panel is a side view with internal to the left. The second panel is a top view with anterior to the left and dorsal up. Two types of ISNb defects are illustrated in the third and fourth panels. The first defect is a stall of the ISNb where it does not project beyond the dorsal edge of muscle 6. The second defect is bypass, in which the axons of the ISNb do not enter the muscle field and grow dorsally past their normal muscle targets. Bypass phenotypes can represent a failure of ISNb axons to defasciculate from the ISN (fusion bypass), or successful defasciculation followed by a failure to enter the muscle field (parallel bypass). (B) Chart showing quantification of deficiencies with various types of ISNb defects. The number of abdominal hemisegments A3-A7 scored is as follows: wt = 139, Df(3L)Exel6087 = 144 , Df(2L)Exel7080 = 168 , Df(2L)Exel7042 = 118. (D-F) each show abdominal hemisegments from late stage 16 embryos fixed and stained with mAb 1D4 using horseradish peroxidase immunohistochemistry (63X oil immersion objective and DIC optics). Anterior is to the left and dorsal is up. (C) ISNb in a wildtype embryo. The projection onto muscles 6 and 7 is indicated by an arrow. The projection onto muscles 12 and 13 is indicated by an arrowhead. The muscles are

labeled with numbers. (D) ISNb in an embryo from Df(3L)Exel6087 showing a stall at the boundary between muscles 6 and 13 (arrow). Arrowhead indicates the normal ISNb termination point at the muscle 12/13 junction. The muscles are present and look wildtype and are labeled with numbers. (E-F) ISNbs in Df(2L)Exel7080 embryos showing bypass phenotypes (arrows). (G-H) are confocal maximum intensity projections from stage 16 live dissected embryos fluorescently stained with mAb 1D4 and rhodamine-phalloidin. Scale bar equals 10 μm. (G) Three hemisegments of a wildtype embryo, showing ISNb (arrows) projecting normally into the muscle field. (H) Three hemisegments of a Df(2L)ED1317 embryo, where ISNb forms looping structures on the target muscles (arrows). This phenotype was not visible when embryos were fixed, dissected, and stained with the same antibody using HRP immunohistochemistry.

Figure 5 CNS and motor axon guidance phenotypes in mutants affecting glial development.

(A-C) are confocal maximum intensity projections of the CNS in stage 16 live-dissected embryos stained with mAb 1D4 by immunofluorescence. Anterior is up. Scale bar in F equals 10 μm. (A) Ventral nerve cord of a wildtype embryo where mAb 1D4 labels 3 longitudinal bundles on either side of the midline. (B) Df(2L)Exel7042 embryo where breaks in the outer fascicle are evident in the longitudinal bundles (arrow). (C) *repo*^{3702} embryo where ventral nerve cord appears disorganized. (D-F) are confocal maximum intensity projections of stage 16 live dissected embryonic CNS

showing FasIII immunofluorescence. Scale bar equals 10 μm. (D) FasIII staining in a wildtype embryo reveals neurons of the RP cluster indicated by an arrow and their proximal projections into the periphery indicated by an asterisk. These axons cross the midline and then project posteriorly before leaving the nerve cord. (E) Df(2L)Exel7042 embryo where FasIII staining shows a very disorganized CNS. Axons sometimes project normally (asterisk), project posteriorly and never leave the CNS (arrowhead), or project anteriorly instead of posteriorly (double arrow). Some neurons never send out axons (brackets). (F) *repo*^{3702} embryo where more cells than normal express FasIII (arrow). Axons occasionally project anteriorly instead of posteriorly, but the projections of most axons are normal (asterisk). (G-I) are confocal maximum intensity projections from live-dissected stage 16 embryos stained fluorescently with mAb 1D4 and rhodamine conjugated phalloidin. Anterior is to the left and dorsal is up. The scale bars are equal to 10 μm. (G) Two hemisegments of a wildtype embryo. Projection of the ISN is labeled with an asterisk. ISNb projections onto target muscles are indicated by an arrow. (H) Two hemisegments of Df(2L)Exel7042 embryo. The ISN projects normally (asterisk), but the ISNb is missing from the left hemisegment. The SN root is at an abnormal position (double arrow). See bar graph in Figure 4 for penetrance of the various ISNb defects in this deficiency line. (I) Two hemisegments from a *repo*^{3702} embryo. In the left hemisegment, the ISNb stalls on muscle 6, and appears to be thinner than usual (arrow). Such phenotypes are rare in *repo* mutants.

Figure 6. Deficiencies causing loss or ectopic expression of 1D4 antigen. Panels A-F are maximum intensity confocal projections of stage 16 live-dissected embryos double-stained with mAb 1D4 and rhodamine-phalloidin (20X objective). Anterior is up. Scale bar equals 10 μm. (A) 1D4 staining in a wildtype embryo. (B) Phalloidin staining in a wildtype embryo. (C) Wildtype merged image (1D4, green; phalloidin, magenta). (D) 1D4 staining in a Df(1)C128 embryo. The image is black because these embryos completely lack 1D4 antigen. (E)Phalloidin staining in a Df(1)C128 embryo, showing than CNS axons are present. (F) Df(1)C128 embryo merged image. Panels G and I are confocal maximum intensity projections of stage 16 live-dissected embryos stained with 1D4 (63X objective). Anterior is to the left and dorsal is up. Scale bar equals 7 μm. Panels H and J are equivalent to the boxed areas in G and I. (G) 1D4 staining in 3 abdominal hemisegments in a wildtype embryo. FasII expression is mostly restricted to neurons, although there is some weak staining of other cell types. The LBD neuron is indicated by an arrow. (H) Detail of boxed area in G. The LBD is indicated by an arrow. (I) 1D4 staining in 3 abdominal hemisegments in a Df(3R)Exel7310 embryo. Bright FasII expression is seen on non-neuronal cells, including flat cells (arrowhead) adjacent to the LBD (arrow). Other 1D4-expressing cells are located more dorsally, just anterior to the ISN (double arrowhead). (J) Detail of boxed area in (I). The LBD is indicated by an arrow. The bracket indicates the group of cells that ectopically express 1D4 antigen.

Supplementary Table 1

Headings for columns A-D are self-evident or are explained in the paper text. For the other columns, "m" (column E) refers to whether a Df is molecularly mapped. "o" (column F) is the suggested order of kit screening, where (1) is the collection of Dfs that are mild, moderate, or severe and are balanceable over GFP, (2) is the collection of Dfs that are balanceable over GFP but may be redundant with (1), (3) are Dfs that cannot be balanced over GFP, and (4) are very severe Dfs that are only marginally screenable. Annotation of lines as DK1, DK2, and DK3 refers to the old (2002) Df kit from the Bloomington Stock Center, not the new molecularly mapped kit. "Notes on lines" (column G) contains useful information about the Dfs and the reasons for their incorporation into the kit; it also contains instructions for screening nonbalanceable Df lines, and notes on regions covered only by Dfs that cannot be screened. "Further notes on mapping" (column H) contains complementation data and overlap information from the old Bloomington kit.

Table 1

Phenotypic Class	Number of Dfs
SNa	20
ISNb	9
ISN	12
SNc	9
Muscle Defects	24
Multiple Pathways	9
Other	23
Total	106

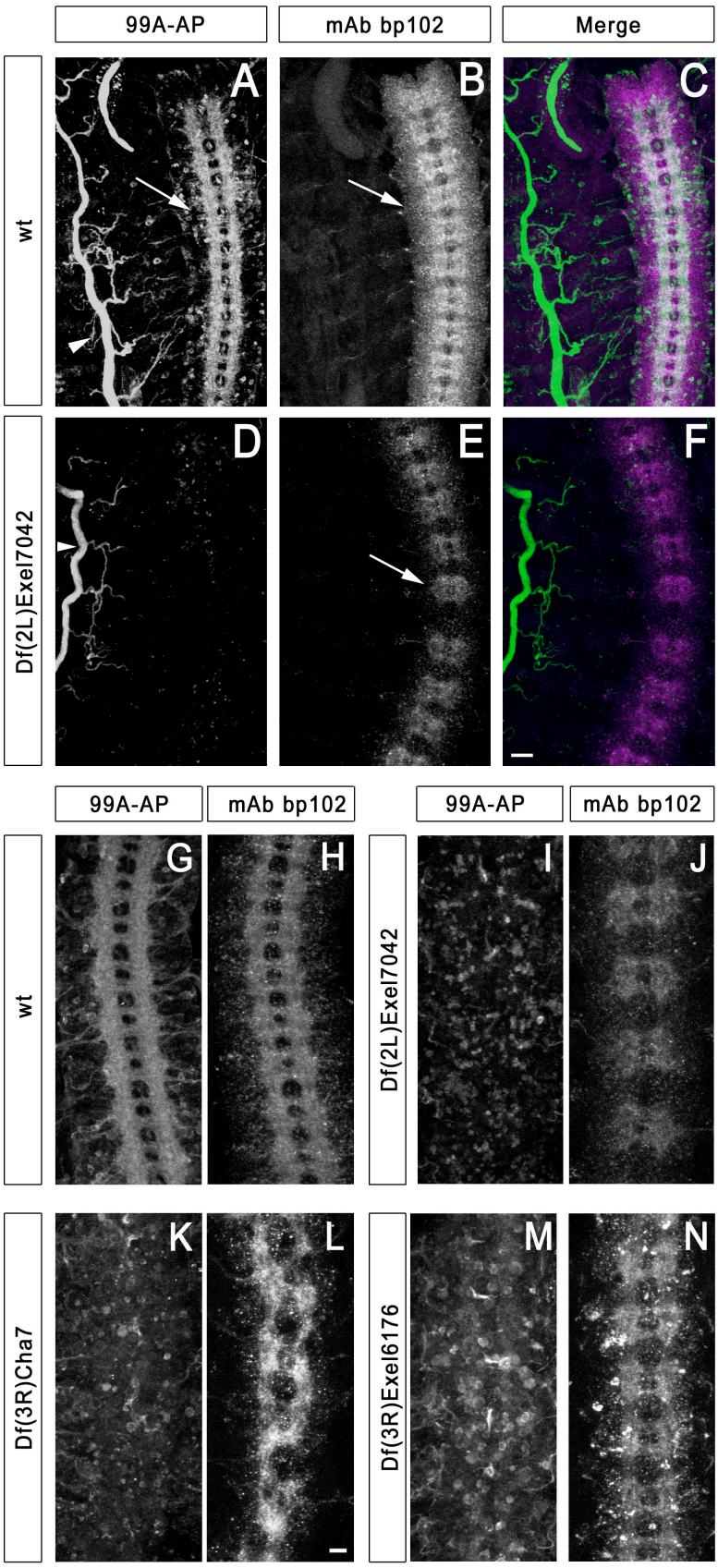
99A-AP
mAb bp102
Merge
wt
Df(2L)Exel7042
A
B
C
D
E
F
99A-AP
mAb bp102
99A-AP
mAb bp102
wt
Df(2L)Exel7042
G
H
I
J
Df(3R)Cha7
Df(3R)Exel6176
K
L
M
N

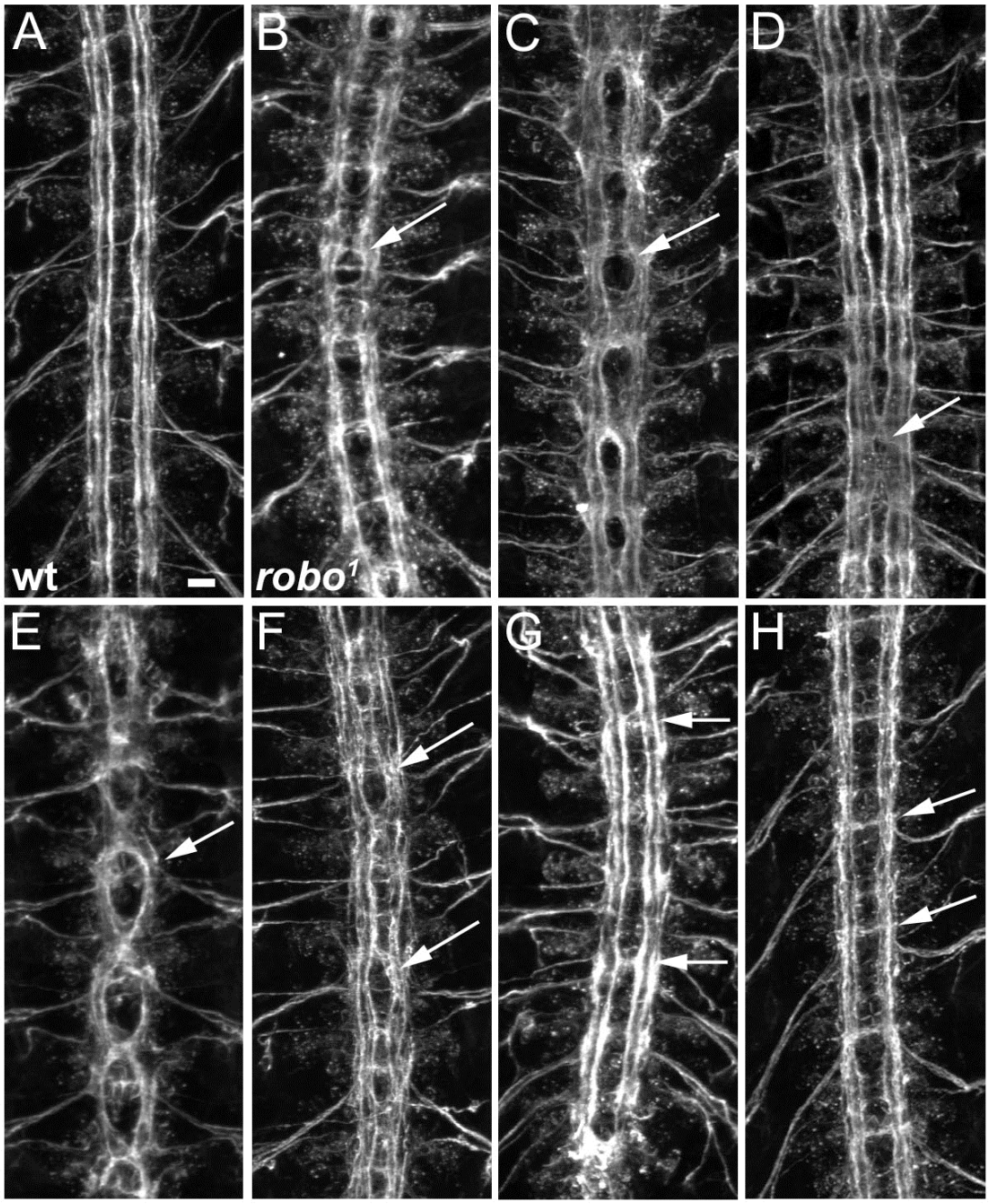
A
B
C
D
wt
robo1
E
F
G
H

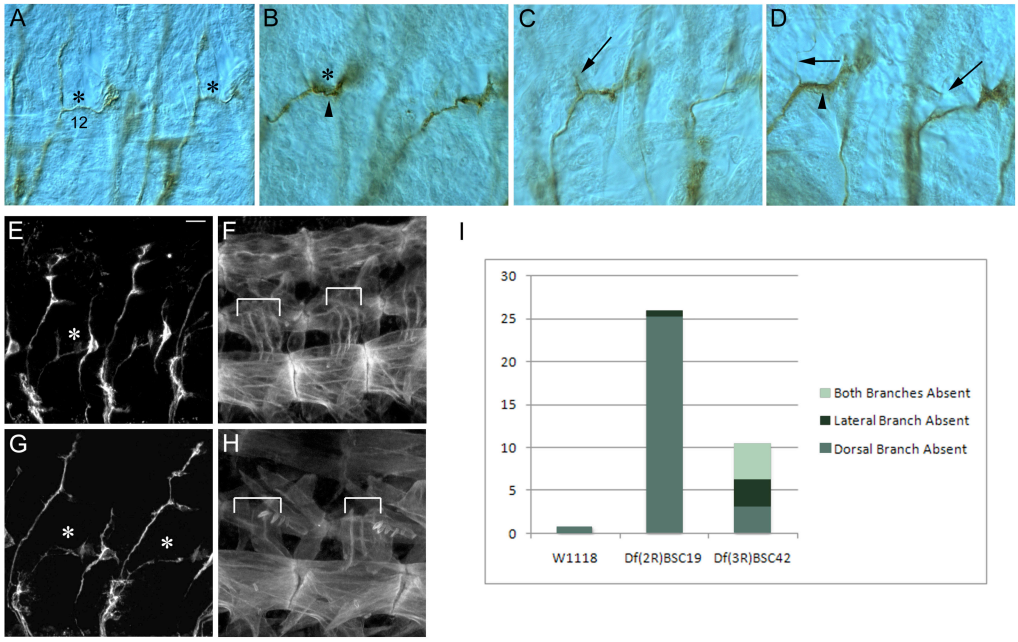
A
B
C
D
12
E
F
G
H
I
30
25
20
15
10
5
0
W1118
Df(2R)BSC19
Df(3R)BSC42
Both Branches Absent
Lateral Branch Absent
Dorsal Branch Absent

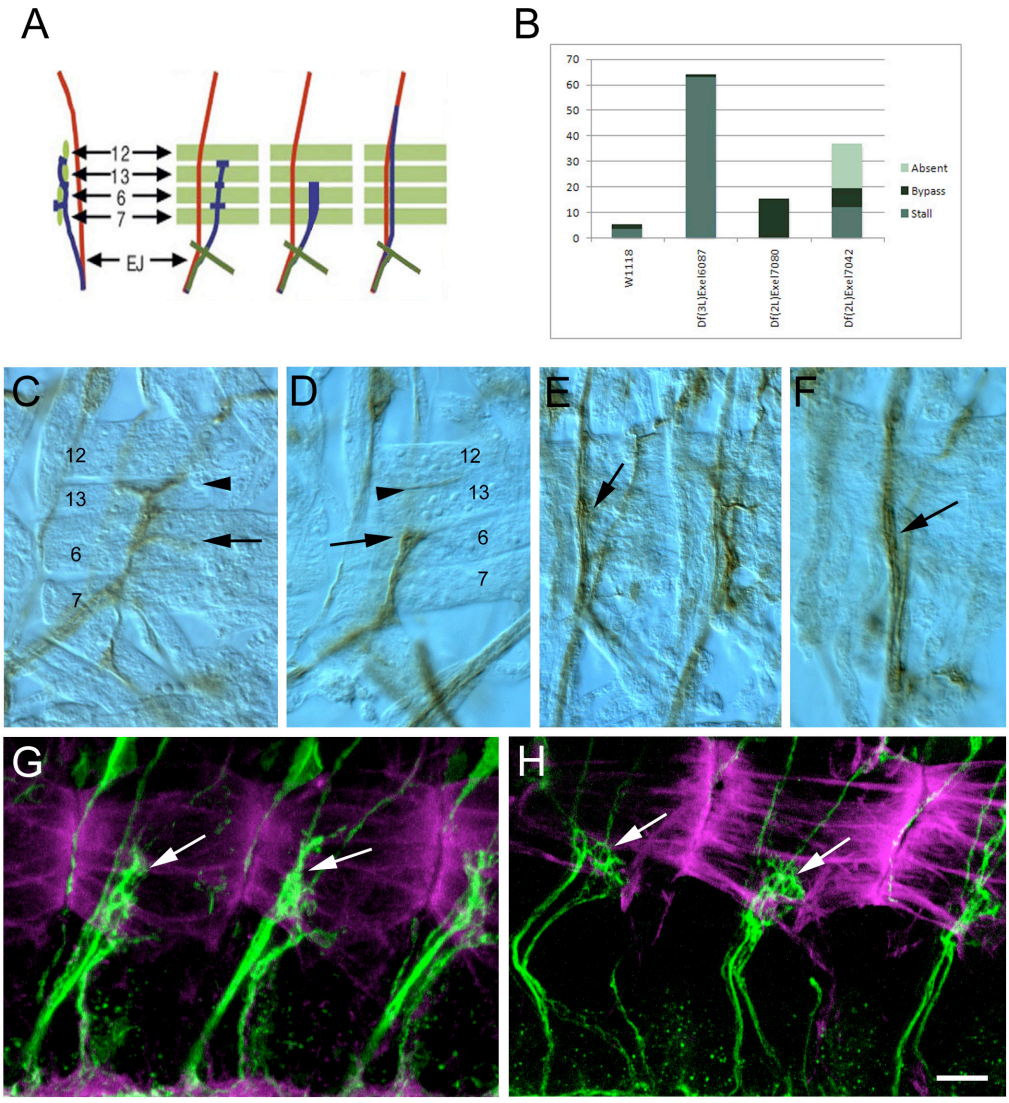
A
12
13
6
7
EJ
B
70
60
50
40
30
20
10
0
W1118
Df(3L)Exel6087
Df(2L)Exel7080
Df(2L)Exel7042
Absent
Bypass
Stall
C
12
13
6
7
D
12
13
6
7
E
F
G
H

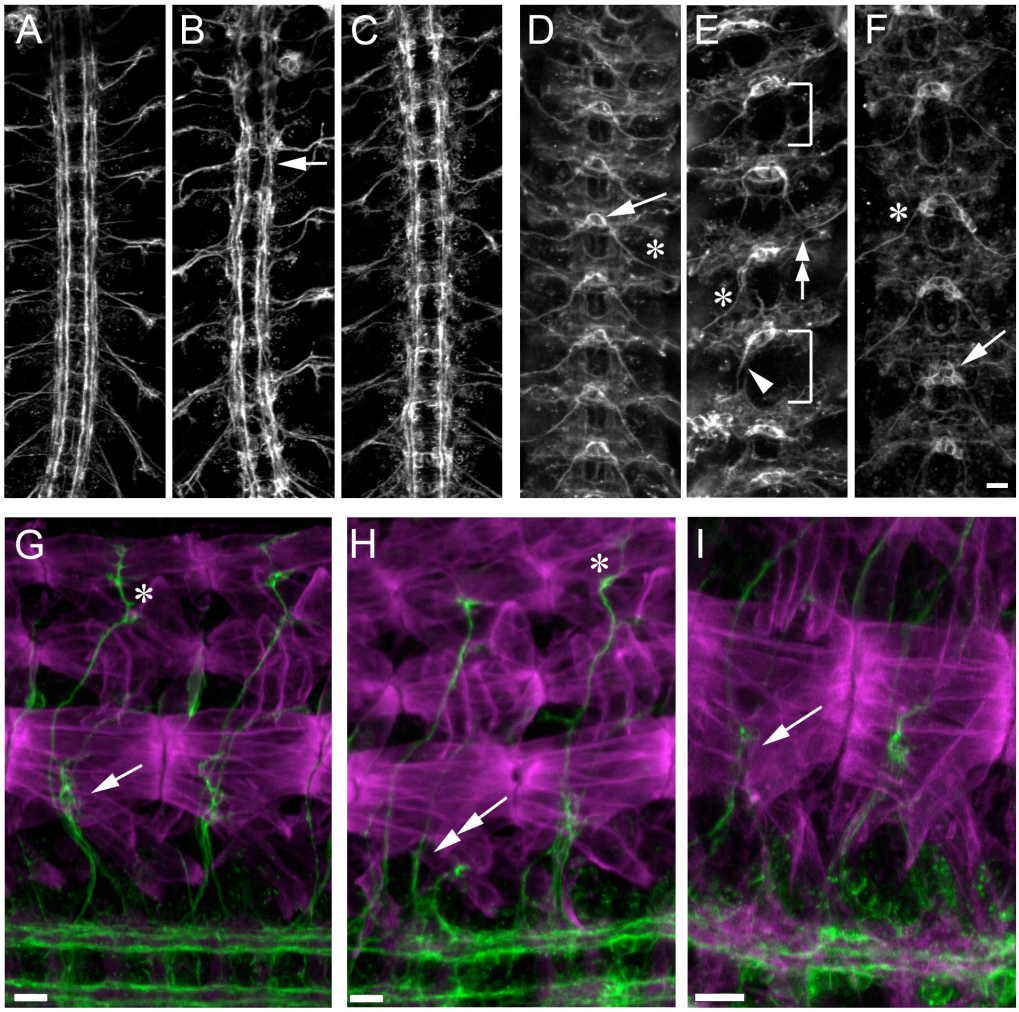
A
B
C
D
E
F
G
H
I

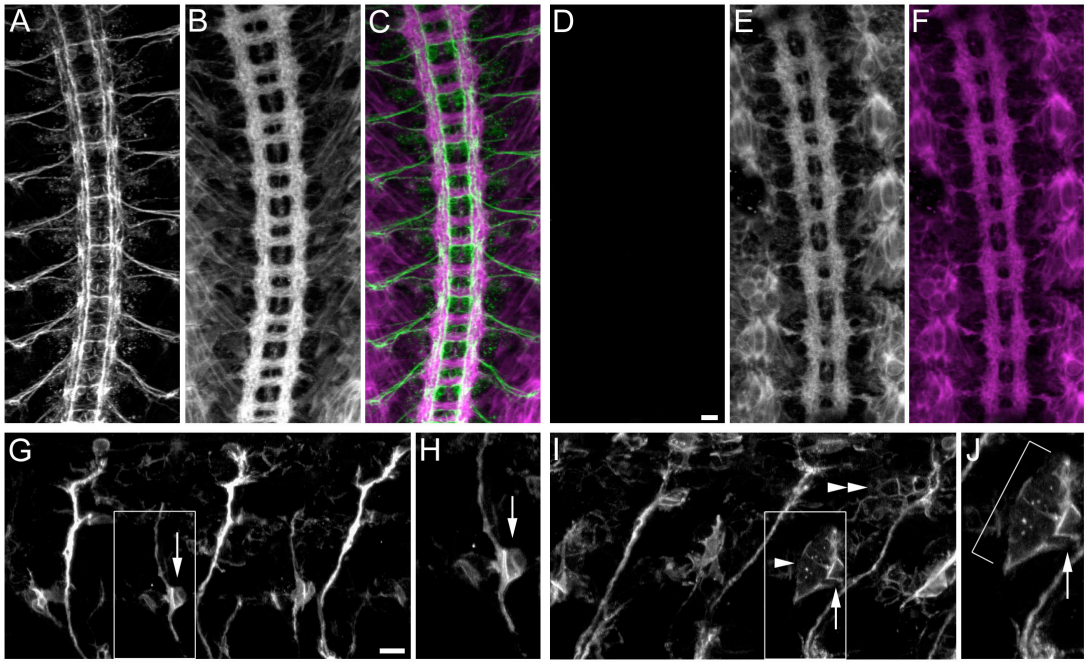
A
B
C
D
E
F
G
H
I
J

Supplementary Table 1

cytology	BL#	name	phenotype	m	o
chromosome 1					
1A1;1B4-6	722	Df(1)260-1	severe	no	1
1B5;1B8	9052	Df(1)ED6396	moderate	yes	1
1B8;1B14					
1B14;1E1	9053	Df(1)ED6443	mild	yes	1
1D2;1E3	8030	Df(1)ED404	mild	yes	1
1E3;2B12	933	Df(1)A94	mild	no	1
2B12;2C2-4					
2C2-4;2E2-3	2986	Df(1)Pgd35	mild	no	1
2E1;3A2	9054	Df(1)ED6574	very severe	yes	4
2F6;3C5	935	Df(1)JC19	moderate	no	1
3C3;3E2	25059	Df(1)BSC531	very severe	yes	4
3C11;3E4	939	Df(1)dm75e19	mild	no	1
3D4-5;3F7-8	1877	Df(1)GA102	severe	no	1
3E8;4F11-12	941	Df(1)HC244	mild	no	1
4C15-16;5A1-2	944	Df(1)JC70	mild	no	1
4F10;5A2	7708	Df(1)Exel6234	mild	yes	2
5A2;5A6	7709	Df(1)Exel6235	mild	yes	1
5A6;5A8-9					
5A8-9;5C5-6	945	Df(1)C149	mild	no	1
5C2;5D5-6	946	Df(1)N73	mild	no	1
5C3-10;6C3-12	5281	Df(1)dx81	severe	no	3
5F3;6D3	9212	Df(1)ED6849	mild	yes	1
6C12;6D8	9625	Df(1)ED6878	mild	yes	1
6D8;6E2					
6E2;7A6	3196	Df(1)Sxl-Bt	severe	no	1
6E4-5;7A6	947	Df(1)HA32	moderate	no	2
7A5-6;7B8-C1	726	Df(1)ct268-42	moderate	no	1
7B2-4;7C3-4	3221	Df(1)ct4b1	mild	no	1
7B7;7E2	6698	Df(1)hl-a	severe	no	3
7D1;7D5-6	949	Df(1)C128	moderate	no	1
7D6;7F1	26514	Df(1)BSC662	very severe	yes	4
7D12-13;7E3-4	1879	Df(1)GE202	severe	no	3
7E11;8A2	25426	Df(1)BSC592	severe	yes	1
7F7;8B4	25702	Df(1)BSC627	severe	yes	1
8B6;8C13	8033	Df(1)ED6957	mild	yes	1
8C10;8E1-2	3689	Df(1)18.1.15	mild	no	1
8E;9C-D	952	Df(1)C52	mild	no	1
9B1-2;10A1-2	954	Df(1)v-L15	moderate	no	1
9F13;10A5	6219	Df(1)v-L1	mild	no	1
10A5;10A7					
10A7;10B17	956	Df(1)RA37	very severe	no	4
10B8;10C10	9154	Df(1)ED7067	moderate	yes	1

10C1-2;11A1-2	959	Df(1)HA85	severe	no	1
11A1;11B14	9217	Df(1)ED7161	moderate	yes	1
11B15;11E8	8898	Df(1)ED7170	mild	yes	1
11D-E;12A1-2	967	Df(1)C246	mild	no	1
12A1-2;12A3-10					
12A3-10;12E9	727	Df(1)g	moderate	no	1
12D2-E1;13A2-5	998	Df(1)RK2	severe	no	1
12F5-6;13A9-B1	1039	Df(1)RK4	mild	no	3
13B1;13C3	8035	Df(1)ED7294	mild	yes	1
13B5-6;13E1-2	7339	In(1)AC2[L]AB[R]	mild	no	1
13E1;13F17	9220	Df(1)ED7344	moderate	yes	1
13F1;14B1	3347	Df(1)sd72b	mild	no	1
14A;15D	2099	Df(1)XR38	mild?	no	3
14B8;14C1	125	Df(1)4b18	mild	no	2
14B13;15A9	3217	Tp(1;2)r[+]75c	mild?	no	3
14C5-6;15B1	5272	Df(1)r-D1	severe?	no	3
15A1;15E3	8954	Df(1)ED7374	mild	yes	1
15D3;16A4-6	4741	Df(1)B25	severe	no	1
16A2;16C7-10	4953	Df(1)BK10	moderate	no	1
16C;16F	6217	Df(1)RR79	moderate	no	1
16C1;16F6	25737	Df(1)BSC647	mild	yes	1
16F7;17A8	24376	Df(1)BSC352	very severe	yes	4
17A3;17D6	26568	Df(1)BSC716	very severe	yes	4
17B1;18B2	25419	Df(1)BSC585	very severe	yes	4
17D1;18C1	9350	Df(1)ED7424	severe	yes	1
18A3;18C2	8951	Df(1)ED7441	mild	yes	1
18B7;18C8	7768	Df(1)Exel7468	mild	yes	1
18C8;18D3	23171	Df(1)BSC275	mild	yes	1
18D10;19A2	9059	Df(1)ED7620	severe	yes	1
18D13;18F2	7721	Df(1)Exel6253	moderate	yes	2
18F2;19D1	25420	Df(1)BSC586	moderate	yes	1
19C4;19E4	25736	Df(1)BSC646	very severe	yes	4
19E1;19F4	25701	Df(1)BSC626	very severe	yes	4
19F3;20A4	25422	Df(1)BSC588	mild	yes	1
20A1;20C1	7723	Df(1)Exel6255	mild	yes	1
20C3;20F1	9346	Df(1)ED14021	severe	yes	1
chromosome 2					
21A1;21B7-8	3638	Df(2L)net-PMF	mild	no	1
21B7-C1;21C2-3	6283	Df(2L)BSC4	mild	no	1
21B8;21C4	8672	Df(2L)BSC106	mild	yes	1
21C3-4;21C6-8	6608	Df(2L)BSC16	mild	no	1
21D1-2;22B2-3	3084	Df(2L)ast2	moderate	no	3
22A2-3;22D5-E1	3133	Df(2L)dp-79b	moderate	no	3
22D2-3;22F1-2	7144	Df(2L)BSC37	mild	no	1
22E4-F2;22F3-23A1	6648	Df(2L)dpp[d14]	mild	no	1

22F3-4;23C3-5	90	Df(2L)C144	mild?	no	3
23C1-2;23E1-2	1567	Df(2L)JS17	mild	no	1
23C5-D1;23E2	6875	Df(2L)BSC28	mild	no	1
23E5;23F4-5	6965	Df(2L)BSC31	mild	no	1
23F3-4;24A1-2	6507	Df(2L)drm-P2	severe	no	1
24A2;24D4	5330	Df(2L)ed1	severe	no	1
24D4;24F3	23680	Df(2L)BSC295	severe	yes	1
24F4;25A7	9270	Df(2L)ED250	mild	yes	1
25A1;25C3	8470	Df(2L)BSC51	moderate	yes	3
25C4;25C8	8674	Df(2L)BSC109	mild	yes	1
25C8;25D5	7497	Df(2L)Exel6011	mild	yes	1
25D5;25E6	7498	Df(2L)Exel6012	moderate	yes	1
25E5;25F3	9560	Df(2L)BSC169	mild	yes	1
25F2;25F5	7499	Df(2L)Exel6013	mild	yes	1
25F5;26B5	9272	Df(2L)ED347	mild	yes	1
26B5;26B11-C1	7501	Df(2L)Exel6015	mild	yes	1
26C2;26C3	7800	Df(2L)Exel9038	mild	yes	1
26C3;26D3-E1					
26D3-E1;26F4-7	6338	Df(2L)BSC7	severe	no	1
26D10-E1;27C1	6374	Df(2L)BSC7	moderate	no	1
27C2-3;27C4-5	5420	Df(2L)Dwee1-W05	mild	no	1
27C4;27D4	7802	Df(2L)Exel7029	mild	yes	1
27D6;27F2	23676	Df(2L)BSC291	very severe	yes	4
27F2;28A3	7804	Df(2L)Exel7031	mild	yes	1
27F4;28C4	9274	Df(2L)ED499	mild	yes	1
28A4-B1;28D3-9	7147	Df(2L)BSC41	moderate	no	1
28C3;28D3	9502	Df(2L)BSC142	moderate	yes	2
28DE;28DE	140	Df(2L)Trf-C6R31	mild	no	1
28E4-7;29B2-C1	179	Df(2L)TE29Aa-11	moderate	no	1
28F5;29B1	8836	Df(2L)BSC111	mild	yes	1
29B1;29C1					
29C4;29D5	7809	Df(2L)Exel7038	mild	yes	1
29D3;29E2	9643	Df(2L)BSC215	mild	yes	1
29D5;29F1	7810	Df(2L)Exel7039	moderate	yes	1
29F1;29F6	7811	Df(2L)Exel7040	moderate	yes	1
29F5;30B12	8906	Df(2L)ED678	severe	yes	1
30B10;30C1	7812	Df(2L)Exel7042	moderate	yes	1
30C1;30C3-5					
30C3-5;30F1	6478	Df(2L)BSC17	mild	no	1
30F1;30F4-5					
30F5;31B1	8469	Df(2L)BSC50	very severe	yes	4
31B1;31D9	9503	Df(2L)BSC143	mild	yes	1
31D9;31E3					
31E3;31F5	7999	Df(2L)Exel7048	mild	yes	1
31F4;32A5	8043	Df(2L)ED746	mild	yes	1

32A1-2;32C5-D1	7142	Df(2L)BSC32	moderate	no	1
32C1;32C5	9505	Df(2L)BSC145	moderate	yes	1
32C5;32D1					
32D1;32D4-E1	7143	Df(2L)BSC36	mild	no	1
32D1;32F1-3	5869	Df(2L)FCK-20	mild	no	1
32F1-3;33F1-2	3079	Df(2L)Prl	severe	no	1
33E9;34A7	7420	Df(2L)ED778	moderate	yes	1
34A3;34B7-9	6999	Df(2L)BSC30	very severe	no	4
34B4;34C4	9594	Df(2L)BSC159	mild	yes	3
34B12-C1;35B10-C1	3138	Df(2L)b87e25	mild	no	1
35B4;35D4	6244	Df(2L)TE35BC-24	mild	no	1
35D1-2;35E2	6085	Df(2L)Sco[rv14]	very severe	no	4
35D6;35E2	7521	Df(2L)Exel6038	mild	yes	1
35E1;35F1	23678	Df(2L)BSC293	mild	yes	1
35F12;36A10	24113	Df(2L)ED1102	mild?	yes	3
36A1;36A12	7833	Df(2L)Exel7066	mild	yes	1
36B1;36C9	7835	Df(2L)Exel8036	mild	yes	1
36C2-4;37B9-C1	420	Df(2L)TW137	severe	no	1
36C8;36E3	9507	Df(2L)BSC148	mild	yes	1
36E3;36F2	23156	Df(2L)BSC256	mild	yes	1
36E5;36F5	7840	Df(2L)Exel8038	severe	yes	1
36F5;36F10	9508	Df(2L)BSC149	severe	yes	1
36F7;37C5	8935	Df(2L)ED1203	severe	yes	1
37C5;37E3	9174	Df(2L)ED1231	moderate	yes	1
37D7;37F2	7849	Df(2L)Exel8041	moderate	yes	1
37F2;38A3	7526	Df(2L)Exel6044	very severe	yes	4
38A3;38A7	7527	Df(2L)Exel6045	mild	yes	1
38A7;38B2	7850	Df(2L)Exel7077	mild	yes	1
38B4;38F5	9269	Df(2L)ED1315	moderate	yes	1
38D1;38F5	9175	Df(2L)ED1317	mild	yes	2
38F3;39A2	7853	Df(2L)Exel7080	mild	yes	1
39A2;39B4	7529	Df(2L)Exel6047	mild	yes	1
39B4;39D1	7530	Df(2L)6048	mild	yes	1
39D1-39E3					
39E3;40A5	9340	Df(2L)ED1466	mild	yes	1
39E7;40D3	7531	Df(2L)Exel6049	mild	yes	1
40A5;40E5	9510	Df(2L)BSC151	mild	no	1
h35;h38L	4959	Df(2L)C'	mild	no	1
h42-h43;42A2-3	749	In(2R)bw[VDe2L]Cy[R]	mild	no	3
h46;41C1-6	8475	Df(2R)Nipped-D	mild	no	1
42A1-2;42E6-F1	1007	Df(2R)nap9	mild	no	1
42E1;43D3	9062	Df(2R)ED1673	moderate	yes	1
42F3;43E12	7858	Df(2R)Exel7092	mild	yes	1
43E4;44B5	8941	Df(2R)ED1725	moderate	yes	1
43F;44D3-8	198	Df(2R)H3C1	severe	no	1
44B8;44E3	9276	Df(2R)ED1742	very severe	yes	4

44E2;45A1	26501	Df(2R)BSC268	mild	yes	1
44F10;45D9-E1	3591	Df(2R)Np5	mild	no	1
45A6-7;45E2-3	4966	Df(2R)w45-30n	mild	no	1
45D3-4;45F2-6	6917	Df(2R)BSC29	mild	no	1
45F5-6;46C4-7	6864	Df(2R)01D099Y-M073	moderate	no	1
45F6;46B12	9410	Df(2R)BSC132	mild	yes	1
46C4-7;46E1					
46E1;46F3	23686	Df(2R)BSC303	mild	yes	1
46F1;47A9	23666	Df(2R)BSC281	mild	yes	1
47A7;47C6	9277	Df(2R)ED2098	very severe	yes	4
47A10;47C1	8909	Df(2R)ED2076	severe?	yes	1
47C6;47F8	9344	Df(2R)ED2155	moderate	yes	1
47D3;48B2	190	Df(2R)en-A	very severe	no	4
47F13;48B6	8911	Df(2R)ED2222	severe	yes	1
48A3-4;48C6-8	1145	Df(2R)en30	mild	no	1
48C5-D1;48D5-E1	7145	Df(2R)BSC39	mild	no	1
48E;49A	4960	Df(2R)CB21	moderate	no	1
48E1-2;48E2-10	7146	Df(2R)BSC40	moderate	no	1
48E12-F4;49A11-B6	5879	Df(2R)BSC3	moderate	no	1
49A4-13;49E7-F1	754	Df(2R)vg-C	moderate	no	1
49E6;49F1	7544	Df(2R)Exel6062	mild	yes	1
49F1-F10					
49F10;50A1	7872	Df(2R)Exel7124	mild	yes	1
49F15-16;50A15-B2	9401	Df(2R)cnn	moderate	no	1
50A15-B2;50C20-23					
50C20-23;50D4-7	8114	Df(2R)50C-38	very severe	no	4
50D4;50E4	7875	Df(2R)Exel7130	mild	yes	1
50E4;50E6	7876	Df(2R)Exel7131	mild	yes	1
50E6-F1;51E2-4	6455	Df(2R)BSC11	moderate	no	3
51E2;51E11	7879	Df(2R)Exel7135	mild	yes	1
51E11;51F13					
51F13;52F8-9	3517	Df(2R)Jp4	very severe	no	4
52A4;52B5	7750	Df(2R)Exel6285	moderate	yes	1
52A13-B3;52F10-11	3519	Df(2R)Jp5	severe	no	1
52F5-9;52F10-53A1	3520	Df(2R)Jp8	mild	no	1
52F6;53C3	7545	Df(2R)Exel6063	mild	yes	1
53A4;53C4	7886	Df(2R)Exel7142	mild	yes	1
53C4;53C11					
53C11;53D11	7546	Df(2R)Exel6064	mild	yes	1
53D11;53F8	9278	Df(2R)ED2747	severe	yes	1
53D14;54A1	24356	Df(2R)BSC331	severe	yes	1
53F8;54B6	7548	Df(2R)Exel6066	moderate	yes	1
54B2;54B17	9596	Df(2R)BSC161	mild	yes	1
54B16;54C3	24379	Df(2R)BSC355	mild	yes	
54C3;54C8-D1					
54C8-D1;54E2-7	7441	Df(2R)BSC45	mild	no	1
54D1-2;54E5-7	6779	Df(2R)14H10Y-53	mild	no	1

54E1;54E9	7891	Df(2R)Exel7150	mild	yes	1
54E8;54F3-4	6778	Df(2R)02B10W-08	mild	no	1
54F3-4;55A1					
55A1;55B7	24987	Df(2R)BSC483	mild	yes	1
55B8;55E3	9413	Df(2R)ED3636	moderate	yes	1
55B9;55C1	7893	Df(2R)Exel7153	mild	yes	2
55C2;56C4	8918	Df(2R)ED3683	severe	yes	1
55D2-E1;56B2	6146	Df(2R)PC66	mild	no	2
56A1;56B5	7550	Df(2R)Exel6068	mild	yes	2
56B5;56C11	7551	Df(2R)Exel6069	severe	yes	1
56C4;56D6-10	6866	Df(2R)BSC26	moderate	no	1
56D7-E3;56F9-12	6647	Df(2R)BSC22	severe	no	1
56F9-17;57D11-12	3467	Df(2R)AA21	moderate	no	1
56F11;56F16	7896	Df(2R)Exel7162	mild	yes	2
56F12-14;57A4	6609	Df(2R)BSC19	mild	no	2
57E1;57F3	7556	Df(2R)Exel6076	severe	yes	1
57F2;58A1	5764	Df(2R)XE-2900	mild	no	1
57F6;57F10	8942	Df(2R)ED3923	mild	yes	1
57F10;58D4	9158	Df(2R)ED3943	moderate	yes	1
58D1-2;59A	282	Df(2R)X58-12	moderate	no	1
59B;59D8-E1	3909	Df(2R)59AD	mild	no	1
59C3;59D2	7906	Df(2R)Exel7177	mild	yes	1
59D5;59D10	7908	Df(2R)Exel7178	mild	yes	1
59E3;59F6	7909	Df(2R)Exel7180	very severe	yes	4
59F5;60B6	9424	Df(2R)BSC156	?	yes	3
60B1-3;60B8					
60B8;60C4	24380	Df(2R)BSC356	mild	yes	1
60B12;60C4	7912	Df(2R)Exel7184	mild	yes	1
60C4;60C7	7561	Df(2R)Exel6082	mild	yes	1
60C5-6;60D9-10	2604	Df(2R)Px2	mild	no	1
60C8;60E8	9069	Df(2R)ED4065	moderate	yes	1
60E2-3;60E11-12	2471	Df(2R)M60E	mild	no	3
60F1;60F5	4961	Df(2R)Kr10	very severe	no	4
chromosome 3					
61A;61D3	2577	Df(3L)emc-E12	mild	no	1
61C5-8;62A8	439	Df(3L)Ar14-8	mild	no	1
62A2;62A7	7566	Df(3L)Exel6087	mild	yes	1
62A7;62A10-B1					
62A10-B1;62D2-5	600	Df(3L)Aprt-1	moderate	no	1
62B4-7;62D5-E5	2400	Df(3L)R-G7	mild	no	1
62E8;63B5-6	6755	Df((3L)BSC23	mild	no	1
62F;63D	3650	Df(3L)M21	moderate	no	3
63C2;63F7	3649	Df(3L)HR119	mild	no	1
63E6-9;64A8-9	463	Df(3L)GN34	moderate	no	1
64A1;64A7	24393	Df(3L)BSC369	moderate	yes	1
64A10;64B1	24394	Df(3L)BSC370	very severe	yes	4

64A12;64B12	8062	Df(3L)ED4342	severe	yes	1
64B5;64B11	7580	Df(3L)Exel6101	mild	yes	2
64B9;64C13	8061	Df(3L)ED210	mild	yes	1
64C;65C	3096	Df(3L)XD198	severe	no	3
65A2;65E1	4393	Df(3L)XD198	mild	no	1
65D4-5;65E4-6	6867	Df(3L)BSC27	mild	no	1
65E4-6;65E10-F1					
65E10-F1;65F2-6	6964	Df(3L)BSC33	mild	no	1
65F7;66A4	7929	Df(3L)Exel8104	mild	yes	1
66A1-12;66B	8619	Df(3L)Hn	severe	no	1
66A17-20;66C1-5	5877	Df(3L)ZP1	moderate	no	1
66B8-9;66C9-10	1541	Df(3L)66C-G28	mild	no	1
66B12-C1;66D2-4	6460	Df(3L)BSC13	mild	no	1
66C12;66D8	24413	Df(3L)BSC389	severe	yes	1
66D10;66E1	25687	Df(3L)BSC612	severe	yes	1
66D12;66E6	8702	Df(3L)ED4414	mild	yes	1
66E1-6;66F1-6	4500	Df(3L)Scf-R6	mild	no	1
66F1-2;67B2-3	7079	Df(3L)BSC35	severe	no	1
67B1;67B5	8970	Df(3L)BSC118	mild	yes	1
67B7;67C5	24415	Df(3L)BSC391	mild	yes	1
67B10;67C5	7593	Df(3L)Exel6144	mild	yes	1
67C2-4;67C8-10	7442	Df(3L)BSC46	mild	no	1
67C7;67D5	23668	Df(3L)BSC283	moderate	yes	1
67C7;67D10	26525	Df(3L)BSC673	mild	yes	1
67D10;67E2					
67E2;68A7	9355	Df(3L)ED4457	moderate	yes	1
67E3-7;68A2-6	6471	Df(3L)BSC14	mild	no	1
68A2-3;69A1-3	2611	Df(3L)vin5	severe	no	1
68C8-11;69B4-5	2612	Df(3L)vin7	severe	no	1
69A4-5;69D4-6	5492	Df(3L)eyg[C1]	mild	no	1
69D4-5;69F5-7	6456	Df(3L)BSC10	moderate	no	1
69F5-7;69F6-70A1					
69F6-70A1;70A1-2	6457	Df(3L)BSC12	mild	no	1
70A1-2;70C3-4	4366	In(3LR)C190[L]Ubx[42TR]	moderate	no	3
70C1-2;70D4-5	3124	Df(3L)fz-GF3b	severe	no	1
70D2-3;71E4-5	3126	Df(3L)fz-M21	severe	no	1
71C2-3;72B1-C1	6551	Df(3L)XG5	severe	no	1
71F1-4;72D1-10	3640	Df(3L)brm11	mild	no	1
72C1-D1;73A3-4	2993	Df(3L)st-f13	moderate	no	1
73A2;73C1	25123	Df(3LBSC561	severe	yes	1
73B5;73E5	8098	Df(3L)ED4674	severe	yes	1
73E1;74C3	24918	Df(3L)BSC414	moderate	yes	1
74B2;74D2	7611	Df(3L)Exel6132	mild	yes	1
74D1;75B11	8100	Df(3L)ED4710	very severe	yes	4
74D3-75A1;75B2-5	6411	Df(3L)BSC8	moderate	no	1
75A6-7;75C1-2	2608	Df(3L)W10	severe	no	3
75B8;75F1	2990	Df(3L)Cat	mild	no	3

75F1;75F2					
75F2;76A1	8082	Df(3L)ED4782	mild	yes	1
75F10-11;76A1-5	6754	Df(3L)fz2	mild	no	3
76A7-B1;76B4-5	6646	Df(3L)BSC20	mild	no	3
76B1-2;76D5	3617	Df(3L)kto2	severe	no	3
76B4;77B	5126	Df(3L)XS533	severe	no	1
77A1;77D1	2052	Df(3L)rdgC-co2	mild	no	1
77B-C;77F-78A	3127	Df(3L)ri-79c	severe	no	1
77E1;77F1	24956	Df(3L)BSC452	very severe	yes	4
77F2;78C2	24953	Df(3L)BSC449	severe	yes	1
78A2;78C2	25116	Df(3L)BSC553	severe	yes	1
78C2;78D8	24923	Df(3L)BSC419	severe	yes	1
78C5-6;78E3-79A1	4430	Df(3L)Pc-2q	mild	no	1
78D5;79A2	8101	Df(3L)ED4978	mild	yes	1
79A3;79B3	9700	Df(3L)BSC223	mild	yes	1
79B2;79D1	23149	Df(3L)BSC249	mild	yes	1
79C1-3;79E3-8	4506	Df(3L)Ten-m-AL29	mild	no	1
79D3-E1;79F3-6	5951	Df(3L)HD1	mild	no	1
79E5-F1;80A2-3	6649	Df(3L)BSC21	mild	no	1
79C2;80A4	8089	Df(3L)ED230	mild	yes	1
80A4;80C2	8102	Df(3L)ED5017	mild	yes	1
80B1;80C1	8090	Df(3L)ED231	moderate	yes	4
80C2;81F3-6					
81F3-6;82F5-7	1518	Df(3R)ME15	mild	no	1
82F3-4;82F10-11	4787	Df(3R)3-4	mild	no	1
82F8-10;83A1-3	5694	Df(3R)e1025-14	mild	no	1
82F8;83A4	8965	Df(3R)ED5156	mild	yes	1
83A4;83A6					
83A6;83B6	7623	Df(3R)Exel6144	moderate	yes	1
83B4;83B6	8103	Df(3R)ED5177	mild	yes	1
83B6;83B7-C1					
83B7-C1;83C6-D1	7443	Df(3R)BSC47	mild	no	1
83C1-2;83D4-5	1990	Df(3R)Tpl10	mild	no	1
83D4-5;84A4-5	2934	Df(3R)Tpl9	severe	no	3
83E1-2;84A5	2393	Df(3R)WIN11	severe	no	1
83E5;83F4	9620	Df(3R)BSC393	mild	yes	1
83F1;84B2	24971	Df(3R)BSC467	very severe	yes	4
84A5;84D9	1842	Df(3R)Antp17	severe	no	1
84C4;84E11	9201	Df(3R)ED5221	mild	yes	1
84E6;85A5	8682	Df(3R)ED5230	mild	yes	1
85A2;85A5	7628	Df(3R)Exel6149	moderate	yes	1
85A5;85B6	7629	Df(3R)Exel6150	severe	yes	1
85B1;85C2	25010	Df(3R)BSC506	severe	yes	1
85C3;85C11	7630	Df(3R)Exel6151	mild	yes	1
85C11;85D2	7631	Df(3R)Exel6152	mild	yes	1
85D1;85D11	9204	Df(3R)ED5339	mild	yes	1
85D8-12;85E7-F1	1931	Df(3R)by10	severe	no	1

85F1-2;86C7-8	7080	Df(3R)BSC38	mild	no	1
86C7;86D7	7957	Df(3R)Exel7306	mild	yes	1
86D5;86D7	7958	Df(3R)Exel8152	mild	yes	1
86D9;86E5	7959	Df(3R)Exel7308	severe	yes	1
86E5;86E11	7963	Df(3R)Exel8153	mild	yes	1
86E11;86E18					
86E18;87A1	7965	Df(3R)Exel7310	moderate	yes	1
86F9;87B2	25018	Df(3R)BSC514	moderate	yes	2
87A1;87B5	7641	Df(3R)Exel6162	mild	yes	1
87B5;87B13	9206	Df(3R)ED5573	moderate	yes	1
87B11-13;87E8-11	3007	Df(3R)ry615	severe	no	1
87C7;87F6	9088	Df(3R)ED5612	severe	yes	1
87E3;87F6	9089	Df(3R)ED5613	mild	yes	2
87E3;88A4	8921	Df(3R)ED5623	severe	yes	1
87F10;88C2	9279	Df(3R)ED5642	severe	yes	1
88B1;88D3-4	3341	Df(3R)red1	moderate	no	1
88D1;88D7	7742	Df(3R)Exel6275	mild	yes	1
88D7;88E1	7652	Df(3R)Exel6173	mild	yes	1
88E2;88E5	24138	Df(3R)ED10566	mild	yes	1
88E5;88E7-13					
88E7-13;89A1	383	Df(3R)ea	severe?	no	3
88F9-89A1;89B9-10	756	Df(3R)sbd105	mild	no	1
89B5;89C2-7	1920	Df(3R)sbd104	severe	no	3
89B7-8;89E7	1467	Df(3R)P115	severe	no	3
89C1-2;89E1-2	3483	Df(3R)P10	moderate	no	1
89E1;89E5	3673	Df(3R)P9	moderate	no	3
89E1-F4;91B1-B2	4431	Df(3R)DG2	severe	no	3
90F1-F4;91F5	3011	Df(3R)Cha7	moderate	no	1
91C5;91F4	8683	Df(3R)ED5911	moderate	yes	2
91F4;91F12					
91F12;92B3	8922	Df(3R)ED5942	mild	yes	1
92A11;92E2	9209	Df(3R)ED6025	severe	yes	1
92B3;92F13	4962	Df(3R)H-B79	mild	no	1
92E2;92F1	7664	Df(3R)Exel6185	mild	yes	2
92F7-93A1;93B3-6	7413	Df(3R)BSC43	mild	no	1
93B;94A3-8	2425	Df(3R)e-N19	moderate	no	1
93B6-7;93D2	3340	Df(3R)e-R1	moderate	no	1
93D1;93F6-8	5805	Df(3R)e-H4	moderate	no	2
94A3-4;94D1-4	2586	Df(3R)23D1	severe	no	1
94D2-10;93E1-6	8491	Df(3R)BSC55	moderate	no	1
94E1-2;94F1-2	8583	Df(3R)BSC56	severe	no	1
94F1;95A4	7673	Df(3R)Exel6194	mild	yes	1
95A1-4;95A8-B1	9497	Df(3R)BSC137	mild	no	1
95A4;95B1	7674	Df(3R)Exel6195	mild	yes	1
95A5-7;95C10-11	4940	Df(3R)mbc-30	severe	no	1

99A5-7;95D6-11	2585	Df(3R)mbc-R1	mild	no	1
95B1;95D1	7992	Df(3R)Exel9014	moderate	yes	1
95C12;95D8	7675	Df(3R)Exel6196	mild	yes	1
95D7-11;95F15	4432	Df(3R)crb-F89-4	mild	no	1
95D8;95E5	7676	Df(3R)Exel6197	mild	yes	2
95E5;95F8	7677	Df(3R)Exel6198	mild	yes	2
95F15;96A2					
96A2;96A13	7948	Df(3R)Exel7357	mild	yes	1
96A2-7;96A21-25	1972	Df(3R)XS	moderate	no	1
96A20;96B4	7679	Df(3R)Exel6200	mild	yes	1
96B2;96B20	24344	Df(3R)BSC318	mild	yes	1
96B15;96C2	24998	Df(3R)BSC494	mild	yes	1
96C2;96C4	7680	Df(3R)Exel6201	mild	yes	1
96C4;96C5	7994	Df(3R)Exel9056	mild	yes	1
96C5;96D1					
96D1;96E2	7681	Df(3R)Exel6202	mild	yes	1
96E2;96E6	7682	Df(3R)Exel6203	mild	yes	1
96E6;96F9					
96F9;97A6	7683	Df(3R)Exel6204	very severe	yes	4
97A1;97B2	25016	Df(3R)BSC512	mild	yes	1
97A6;97D4	25000	Df(3R)BSC496	mild	yes	1
97A;98A1-2	1910	Df(3R)Tl-P	moderate	no	1
97E3;98A5	823	Df(3R)D605	mild	no	1
97F1-2;98A	9529	Df(3R)IR16	moderate	no	1
98A4;98B5	25002	Df(3R)BSC498	mild	yes	1
98B6;98D2	24964	Df(3R)BSC460	mild	yes	1
98C4;98D6	7726	Df(3R)Exel6259	mild	yes	1
98D6;98E1	7687	Df(3R)Exel6209	mild	yes	1
98E1;98F5	7688	Df(3R)Exel6210	mild	yes	1
98F5;98F6	7689	Df(3R)Exel6211	severe	yes	1
98F6;99A1-2					
99A1-2;99B6-11	669	Df(3R)Dr-rv1	moderate	no	1
99B5;99C2	25075	Df(3R)BSC547	moderate	yes	1
99C5;99D3	25695	Df(3R)BSC620	mild	yes	1
99E3;99F6	25007	Df(3R)BSC503	moderate	yes	1
99F4;100A2	25008	Df(3R)BSC504	severe	yes	1
100A2;100A5					
100A5;100B1	24142	Df(3RED6346	severe	yes	1
100B1;100C1	26847	Df(3R)BSC749	mild	yes	1
100B5;100C4	27365	Df(3R)BSC793	mild	yes	1
100B4;100B8	7697	Df(3R)Exel6219	mild	yes	1
100C7;100E3	24143	Df(3R)ED6361	severe	yes	1
100E1;100F5	24516	Df(3R)ED50003	mild	yes	1
4th chromosome					
101E;102B	9433	Df(4)M101-62f	severe?	no	4
101F2-102A1;102A3	1082	Df(4)M101-63a	mild?	no	4
102A3;102B1	8067	Df(4)ED6366	mild?	yes	4

102A3;102B8	9422	Df(4)ED6369	mild?	yes	4
102B6;102C2	9579	Df(4)ED6380	mild?	yes	4
<102C2;102C2-D2>	7082	Df(4)J2	mild?	no	4
102E2;102E10	1197	Df(4)38	mild?	no	4
102E2-7;102E-F2	759	Df(4)G	moderate?	no	4

This table has been modified from the original version due to space constraints

Supplementary Table 2

cytology	BL#	name	phenotype
1B14;1E1	9053	Df(1)ED6443	mild
1D2;1E3	8030	Df(1)ED404	mild
1E3;2B12	933	Df(1)A94	mild
2C2-4;2E2-3	2986	Df(1)Pgd35	mild
3C11;3E4	939	Df(1)dm75e19	mild
3E8;4F11-12	941	Df(1)HC244	mild
4C15-16;5A1-2	944	Df(1)JC70	mild
4F10;5A2	7708	Df(1)Exel6234	mild
5A2;5A6	7709	Df(1)Exel6235	mild
5A8-9;5C5-6	945	Df(1)C149	mild
5C2;5D5-6	946	Df(1)N73	mild
5F3;6D3	9212	Df(1)ED6849	mild
6C12;6D8	9625	Df(1)ED6878	mild
7B2-4;7C3-4	3221	Df(1)ct4b1	mild
8B6;8C13	8033	Df(1)ED6957	mild
8C10;8E1-2	3689	Df(1)18.1.15	mild
8E;9C-D	952	Df(1)C52	mild
9F13;10A5	6219	Df(1)v-L1	mild
11B15;11E8	8898	Df(1)ED7170	mild
11D-E;12A1-2	967	Df(1)C246	mild
12F5-6;13A9-B1	1039	Df(1)RK4	mild
13B1;13C3	8035	Df(1)ED7294	mild
13B5-6;13E1-2	7339	In(1)AC2[L]AB[R]	mild
13F1;14B1	3347	Df(1)sd72b	mild
14A;15D	2099	Df(1)XR38	mild?
14B8;14C1	125	Df(1)4b18	mild
14B13;15A9	3217	Tp(1;2)r[+]75c	mild?
15A1;15E3	8954	Df(1)ED7374	mild
16C1;16F6	25737	Df(1)BSC647	mild
18A2;18A2	7754	Df(1)Exel6253	mild
18A3;18C2	8951	Df(1)ED7441	mild
18B7;18C8	7768	Df(1)Exel7468	mild
18C8;18D3	23171	Df(1)BSC275	mild
19F3;20A4	25422	Df(1)BSC588	mild
20A1;20C1	7723	Df(1)Exel6255	mild
21A1;21B7-8	3638	Df(2L)net-PMF	mild
21B7-C1;21C2-3	6283	Df(2L)BSC4	mild
21B8;21C4	8672	Df(2L)BSC106	mild
21C3-4;21C6-8	6608	Df(2L)BSC16	mild
22D2-3;22F1-2	7144	Df(2L)BSC37	mild
22E4-F2;22F3-23A1	6648	Df(2L)dpp[d14]	mild
22F3-4;23C3-5	90	Df(2L)C144	mild?

23C1-2;23E1-2	1567	Df(2L)JS17	mild
23C5-D1;23E2	6875	Df(2L)BSC28	mild
23E5;23F4-5	6965	Df(2L)BSC31	mild
24F4;25A7	9270	Df(2L)ED250	mild
25C4;25C8	8674	Df(2L)BSC109	mild
25C8;25D5	7497	Df(2L)Exel6011	mild
25E5;25F3	9560	Df(2L)BSC169	mild
25F2;25F5	7499	Df(2L)Exel6013	mild
25F5;26B5	9272	Df(2L)ED347	mild
26B5;26B11-C1	7501	Df(2L)Exel6015	mild
26C2;26C3	7800	Df(2L)Exel9038	mild
27C2-3;27C4-5	5420	Df(2L)Dwee1-W05	mild
27C4;27D4	7802	Df(2L)Exel7029	mild
27F2;28A3	7804	Df(2L)Exel7031	mild
27F4;28C4	9274	Df(2L)ED499	mild
28DE;28DE	140	Df(2L)Trf-C6R31	mild
28F5;29B1	8836	Df(2L)BSC111	mild
29C4;29D5	7809	Df(2L)Exel7038	mild
29D3;29E2	9643	Df(2L)BSC215	mild
30C3-5;30F1	6478	Df(2L)BSC17	mild
31B1;31D9	9503	Df(2L)BSC143	mild
31E3;31F5	7999	Df(2L)Exel7048	mild
31F4;32A5	8043	Df(2L)ED746	mild
32D1;32D4-E1	7143	Df(2L)BSC36	mild
32D1;32F1-3	5869	Df(2L)FCK-20	mild
34B4;34C4	9594	Df(2L)BSC159	mild
34B12-C1;35B10-C1	3138	Df(2L)b87e25	mild
35B4;35D4	6244	Df(2L)TE35BC-24	mild
35D6;35E2	7521	Df(2L)Exel6038	mild
35E1;35F1	23678	Df(2L)BSC293	mild
35F12;36A10	24113	Df(2L)ED1102	mild?
36A1;36A12	7833	Df(2L)Exel7066	mild
36B1;36C9	7835	Df(2L)Exel8036	mild
36C8;36E3	9507	Df(2L)BSC148	mild
36E3;36F2	23156	Df(2L)BSC256	mild
38A3;38A7	7527	Df(2L)Exel6045	mild
38A7;38B2	7850	Df(2L)Exel7077	mild
38D1;38F5	9175	Df(2L)ED1317	mild
38F3;39A2	7853	Df(2L)Exel7080	mild
39A2;39B4	7529	Df(2L)Exel6047	mild
39B4;39D1	7530	Df(2L)6048	mild
39E3;40A5	9340	Df(2L)ED1466	mild
39E7;40D3	7531	Df(2L)Exel6049	mild
40A5;40E5	9510	Df(2L)BSC151	mild
h35;h38L	4959	Df(2L)C'	mild
h42-h43;42A2-3	749	In(2R)bw[VDe2L]Cy[R]	mild
h46;41C1-6	8475	Df(2R)Nipped-D	mild
42A1-2;42E6-F1	1007	Df(2R)nap9	mild

42F3;43E12	7858	Df(2R)Exel7092	mild
44E2;45A1	26501	Df(2R)BSC268	mild
44F10;45D9-E1	3591	Df(2R)Np5	mild
45A6-7;45E2-3	4966	Df(2R)w45-30n	mild
45D3-4;45F2-6	6917	Df(2R)BSC29	mild
45F6;46B12	9410	Df(2R)BSC132	mild
46E1;46F3	23686	Df(2R)BSC303	mild
46F1;47A9	23666	Df(2R)BSC281	mild
48A3-4;48C6-8	1145	Df(2R)en30	mild
48C5-D1;48D5-E1	7145	Df(2R)BSC39	mild
49E6;49F1	7544	Df(2R)Exel6062	mild
49F10;50A1	7872	Df(2R)Exel7124	mild
50D4;50E4	7875	Df(2R)Exel7130	mild
50E4;50E6	7876	Df(2R)Exel7131	mild
51E2;51E11	7879	Df(2R)Exel7135	mild
52F5-9;52F10-53A1	3520	Df(2R)Jp8	mild
52F6;53C3	7545	Df(2R)Exel6063	mild
53A4;53C4	7886	Df(2R)Exel7142	mild
53C11;53D11	7546	Df(2R)Exel6064	mild
54B2;54B17	9596	Df(2R)BSC161	mild
54B16;54C3	24379	Df(2R)BSC355	mild
54C8-D1;54E2-7	7441	Df(2R)BSC45	mild
54D1-2;54E5-7	6779	Df(2R)14H10Y-53	mild
54E1;54E9	7891	Df(2R)Exel7150	mild
54E8;54F3-4	6778	Df(2R)02B10W-08	mild
55A1;55B7	24987	Df(2R)BSC483	mild
55B9;55C1	7893	Df(2R)Exel7153	mild
55D2-E1;56B2	6146	Df(2R)PC66	mild
56A1;56B5	7550	Df(2R)Exel6068	mild
56F11;56F16	7896	Df(2R)Exel7162	mild
56F12-14;57A4	6609	Df(2R)BSC19	mild
57F2;58A1	5764	Df(2R)XE-2900	mild
57F6;57F10	8942	Df(2R)ED3923	mild
59B;59D8-E1	3909	Df(2R)59AD	mild
59C3;59D2	7906	Df(2R)Exel7177	mild
59D5;59D10	7908	Df(2R)Exel7178	mild
60B8;60C4	24380	Df(2R)BSC356	mild
60B12;60C4	7912	Df(2R)Exel7184	mild
60C4;60C7	7561	Df(2R)Exel6082	mild
60C5-6;60D9-10	2604	Df(2R)Px2	mild
60E2-3;60E11-12	2471	Df(2R)M60E	mild
61A;61D3	2577	Df(3L)emc-E12	mild
61C5-8;62A8	439	Df(3L)Ar14-8	mild
62A2;62A7	7566	Df(3L)Exel6087	mild
62B4-7;62D5-E5	2400	Df(3L)R-G7	mild
62E8;63B5-6	6755	Df((3L)BSC23	mild

63C2;63F7	3649	Df(3L)HR119	mild
64B5;64B11	7580	Df(3L)Exel6101	mild
64B9;64C13	8061	Df(3L)ED210	mild
65A2;65E1	4393	Df(3L)XD198	mild
65D4-5;65E4-6	6867	Df(3L)BSC27	mild
65E10-F1;65F2-6	6964	Df(3L)BSC33	mild
65F7;66A4	7929	Df(3L)Exel8104	mild
66B8-9;66C9-10	1541	Df(3L)66C-G28	mild
66B12-C1;66D2-4	6460	Df(3L)BSC13	mild
66D12;66E6	8702	Df(3L)ED4414	mild
66E1-6;66F1-6	4500	Df(3L)Scf-R6	mild
67B1;67B5	8970	Df(3L)BSC118	mild
67B7;67C5	24415	Df(3L)BSC391	mild
67B10;67C5	7593	Df(3L)Exel6144	mild
67C2-4;67C8-10	7442	Df(3L)BSC46	mild
67C7;67D10	26525	Df(3L)BSC673	mild
67E3-7;68A2-6	6471	Df(3L)BSC14	mild
69A4-5;69D4-6	5492	Df(3L)eyg[C1]	mild
69F6-70A1;70A1-2	6457	Df(3L)BSC12	mild
71F1-4;72D1-10	3640	Df(3L)brm11	mild
74B2;74D2	7611	Df(3L)Exel6132	mild
75B8;75F1	2990	Df(3L)Cat	mild
75F2;76A1	8082	Df(3L)ED4782	mild
75F10-11;76A1-5	6754	Df(3L)fz2	mild
76A7-B1;76B4-5	6646	Df(3L)BSC20	mild
77A1;77D1	2052	Df(3L)rdgC-co2	mild
78C5-6;78E3-79A1	4430	Df(3L)Pc-2q	mild
78D5;79A2	8101	Df(3L)ED4978	mild
79A3;79B3	9700	Df(3L)BSC223	mild
79B2;79D1	23149	Df(3L)BSC249	mild
79C1-3;79E3-8	4506	Df(3L)Ten-m-AL29	mild
79D3-E1;79F3-6	5951	Df(3L)HD1	mild
79E5-F1;80A2-3	6649	Df(3L)BSC21	mild
79C2;80A4	8089	Df(3L)ED230	mild
80A4;80C2	8102	Df(3L)ED5017	mild
81F3-6;82F5-7	1518	Df(3R)ME15	mild
82F3-4;82F10-11	4787	Df(3R)3-4	mild
82F8-10;83A1-3	5694	Df(3R)e1025-14	mild
82F8;83A4	8965	Df(3R)ED5156	mild
83B4;83B6	8103	Df(3R)ED5177	mild
83B7-C1;83C6-D1	7443	Df(3R)BSC47	mild
83C1-2;83D4-5	1990	Df(3R)Tpl10	mild
83E5;83F4	9620	Df(3R)BSC393	mild
84C4;84E11	9201	Df(3R)ED5221	mild
84E6;85A5	8682	Df(3R)ED5230	mild
85C3;85C11	7630	Df(3R)Exel6151	mild

85C11;85D2	7631	Df(3R)Exel6152	mild
85D1;85D11	9204	Df(3R)ED5339	mild
85F1-2;86C7-8	7080	Df(3R)BSC38	mild
86C7;86D7	7957	Df(3R)Exel7306	mild
86D5;86D7	7958	Df(3R)Exel8152	mild
86E5;86E11	7963	Df(3R)Exel8153	mild
87A1;87B5	7641	Df(3R)Exel6162	mild
87E3;87F6	9089	Df(3R)ED5613	mild
88D1;88D7	7742	Df(3R)Exel6275	mild
88D7;88E1	7652	Df(3R)Exel6173	mild
88E2;88E5	24138	Df(3R)ED10566	mild
88F9-89A1;89B9-10	756	Df(3R)sbd105	mild
91F12;92B3	8922	Df(3R)ED5942	mild
92B3;92F13	4962	Df(3R)H-B79	mild
92E2;92F1	7664	Df(3R)Exel6185	mild
92F7-93A1;93B3-6	7413	Df(3R)BSC43	mild
94F1;95A4	7673	Df(3R)Exel6194	mild
95A1-4;95A8-B1	9497	Df(3R)BSC137	mild
95A4;95B1	7674	Df(3R)Exel6195	mild
99A5-7;95D6-11	2585	Df(3R)mbc-R1	mild
95C12;95D8	7675	Df(3R)Exel6196	mild
95D7-11;95F15	4432	Df(3R)crb-F89-4	mild
95D8;95E5	7676	Df(3R)Exel6197	mild
95E5;95F8	7677	Df(3R)Exel6198	mild
96A2;96A13	7948	Df(3R)Exel7357	mild
96A20;96B4	7679	Df(3R)Exel6200	mild
96B2;96B20	24344	Df(3R)BSC318	mild
96B15;96C2	24998	Df(3R)BSC494	mild
96C2;96C4	7680	Df(3R)Exel6201	mild
96C4;96C5	7994	Df(3R)Exel9056	mild
96D1;96E2	7681	Df(3R)Exel6202	mild
96E2;96E6	7682	Df(3R)Exel6203	mild
97A1;97B2	25016	Df(3R)BSC512	mild
97A6;97D4	25000	Df(3R)BSC496	mild
97E3;98A5	823	Df(3R)D605	mild
98A4;98B5	25002	Df(3R)BSC498	mild
98B6;98D2	24964	Df(3R)BSC460	mild
98C4;98D6	7726	Df(3R)Exel6259	mild
98D6;98E1	7687	Df(3R)Exel6209	mild
98E1;98F5	7688	Df(3R)Exel6210	mild
99C5;99D3	25695	Df(3R)BSC620	mild
100B1;100C1	26847	Df(3R)BSC749	mild
100B5;100C4	27365	Df(3R)BSC793	mild
100B4;100B8	7697	Df(3R)Exel6219	mild
100E1;100F5	24516	Df(3R)ED50003	mild
101F2-	1082	Df(4)M101-63a	mild?

102A1;102A3			
102A3;102B1	8067	Df(4)ED6366	mild?
102A3;102B8	9422	Df(4)ED6369	mild?
102B6;102C2	9579	Df(4)ED6380	mild?
<102C2;102C2-D2>	7082	Df(4)J2	mild?
102E2;102E10	1197	Df(4)38	mild?

Supplementary Table 3

Stock#	Df Name	Notes
24998	Df(3R)BSC494	Possible Sna
5420	Df(2L)Dwee1-W05	possible Sna
7809	Df(2L)Exel7038	possible SNa and SNc
6146	Df(2R)PC66	possible Sna and SNc
6778	Df(2R)02B10W-08	Possible SNa fuzzy, branchy
939	Df(1)dm75e19	possible SNa phenotype
7414	Df(2R)BSC44	possible SNa phenotype
5680	Df(2R)robl-c	possible SNa phenotype
7891	Df(2R)Exel7150	possible SNa phenotype
8061	Df(3L)ED210	possible SNa phenotype
7593	Df(3L)Exel6144	possible SNa phenotype
7664	Df(3R)Exel6185	possible SNa phenotype
4393	Df(3L)XD198	SNa Phenotype
7413	Df(3R)BSC43	SNa Phenotype
6117	Df(2L)J1	SNa Phenotype
6609	Df(2R)BSC19	SNa Phenotype
3520	Df(2R)Jp8	SNa phenotype, SNc phenotype
6755	Df(3L)BSC23	SNa phenotype, SNc phenotype
4500	Df(3L)Scf-R6	ISNb frequent stalls, possible SNa
2986	Df(1)Pgd35	ISNb stalls, delay, SNa defect
7853	Df(2L)Exel7080	ISNb bypass
7550	Df(2R)Exel6068	ISNb stalls
7145	Df(2R)BSC39	possible ISNb
7886	Df(2R)Exel7142	possible ISNb bypass
9175	Df(2L)ED1317	SNc missing, ISNb loops
7566	Df(3L)Exel6087	ISN delay, ISNb stalls
25737	Df(1)BSC647	ISN stall, ISNb club shaped
1567	Df(2L)JS17	ISN
3638	Df(2L)net-PMF	ISN delay
9340	Df(2L)ED1466	ISN simple
7908	Df(2R)Exel7178	ISN simple, fuzzy
946	Df(1)N73	ISN stall
7412	Df(3R)BSC42	ISN stalls
7730	Df(3R)Exel6263	ISN stalls
7819	Df(2L)Exel7046	ISN stalls
7680	Df(3R)Exel6201	possible ISN phenotype
7521	Df(2L)Exel6038	possible ISN phenotype, defasciculated all over
8835	Df(2L)BSC110	Possible SNc phenotype
6244	Df(2L)TE35BC-24	Possible SNc phenotype

7896	Df(2R)Exel7162	Possible SNc phenotype
6965	Df(2L)BSC31	Possible SNc phenotype, fibers thin
823	Df(3R)D605	No axonal branching; removes sidestep
2400	Df(3L)R-G7	Defects in all pathways
7929	Df(3L)Exel8104	Defects in all pathways
6457	Df(3L)BSC12	Defects in all pathways
3689	Df(1)18.1.15	Defects in all pathways
7443	Df(3R)BSC47	Defects in all pathways
8702	Df(3L)ED4414	Defects in all pathways
8475	Df(2R)Nipped-D	Defects in all pathways
1039	Df(1)RK4	Muscle Defect
1541	Df(3L)66C-G28	Muscle Defect
7948	Df(3R)Exel7357	Muscle Defect
8672	Df(2L)BSC106	Muscle Defect
7531	Df(2L)Exel6049	Muscle Defect
7544	Df(2R)Exel6062	Muscle Defect
5951	Df(3L)HD1	Muscle Defect
8898	Df(1)ED7170	Muscle Defect
6283	Df(2L)BSC4	Muscle Defect
4966	Df(2R)w45-30n	Muscle Defect
4430	Df(3L)Pc-2q	Muscle Defect
9186	Df(2L)ED353	Muscle Defect
9503	Df(2L)BSC143	Muscle Defect
7497	Df(2L)Exel6011	Muscle Defect
7627	Df(3R)Exel6148	Muscle Defect
1007	Df(2R)nap9	Muscle Defect
8033	Df(1)ED6957	Muscle Defect
4741	Df(1)B25	Muscle Defect
933	Df(1)A94	Muscle Defect
7498	Df(2L)Exel6012	Muscle Defect
941	Df(1)HC244	Muscle Defect
3591	Df(2R)Np5	Muscle Defect
6471	Df(3L)BSC14	Muscle Defect
6867	Df(3L)BSC27	Muscle Defect
140	Df(2L)TrfC6R31	Developmental Delay
6478	Df(2L)BSC17	Developmental Delay
7879	Df(2R)Exel7135	Developmental Delay
7441	Df(2R)BSC45	Developmental Delay
945	Df(1)C149	Developmental Delay
6964	Df(3L)BSC33	Developmental Delay
5492	Df(3L)eyg[C1]	Developmental Delay
2052	Df(3L)rdgC-co2	Developmental Delay
6649	Df(3L)BSC21	Developmental Delay
7802	Df(2L)Exel7029	Strange 1D4 pattern

Chapter 1 References

ALFONSO, T. B., and B. W. JONES, 2002 gcm2 promotes glial cell differentiation and is required with glial cells missing for macrophage development in Drosophila. Dev Biol **248:** 369-383.

ARAUJO, S. J., H. ASLAM, G. TEAR and J. CASANOVA, 2005 mummy/cystic encodes an enzyme required for chitin and glycan synthesis, involved in trachea, embryonic cuticle and CNS development--analysis of its role in Drosophila tracheal morphogenesis. Dev Biol **288:** 179-193.

ARAUJO, S. J., and G. TEAR, 2003 Axon guidance mechanisms and molecules: lessons from invertebrates. Nat Rev Neurosci **4:** 910-922.

ARORA, K., M. S. LEVINE and M. B. O'CONNOR, 1994 The screw gene encodes a ubiquitously expressed member of the TGF-beta family required for specification of dorsal cell fates in the Drosophila embryo. Genes Dev **8:** 2588-2601.

BELLAICHE, Y., I. THE and N. PERRIMON, 1998 Tout-velu is a Drosophila homologue of the putative tumour suppressor EXT-1 and is needed for Hh diffusion. Nature **394:** 85-88.

BINARI, R. C., B. E. STAVELEY, W. A. JOHNSON, R. GODAVARTI, R. SASISEKHARAN *et al.*, 1997 Genetic evidence that heparin-like glycosaminoglycans are involved in wingless signaling. Development **124:** 2623-2632.

BUSCH, S. A., and J. SILVER, 2007 The role of extracellular matrix in CNS regeneration. Curr Opin Neurobiol **17:** 120-127.

CAMPBELL, G., H. GORING, T. LIN, E. SPANA, S. ANDERSSON *et al.*, 1994 RK2, a glial-specific homeodomain protein required for embryonic nerve cord condensation and viability in Drosophila. Development **120:** 2957-2966.

CARULLI, D., T. LAABS, H. M. GELLER and J. W. FAWCETT, 2005 Chondroitin sulfate proteoglycans in neural development and regeneration. Curr Opin Neurobiol **15:** 116-120.

CRESPO, D., R. A. ASHER, R. LIN, K. E. RHODES and J. W. FAWCETT, 2007 How does chondroitinase promote functional recovery in the damaged CNS? Exp Neurol **206:** 159-171.

CREWS, S. T., J. B. THOMAS and C. S. GOODMAN, 1988 The Drosophila single-minded gene encodes a nuclear protein with sequence similarity to the per gene product. Cell **52:** 143-151.

DESAI, C. J., J. G. GINDHART, JR., L. S. GOLDSTEIN and K. ZINN, 1996 Receptor tyrosine phosphatases are required for motor axon guidance in the Drosophila embryo. Cell **84:** 599-609.

DESAI, C. J., N. X. KRUEGER, H. SAITO and K. ZINN, 1997 Competition and cooperation among receptor tyrosine phosphatases control motoneuron growth cone guidance in Drosophila. Development **124:** 1941-1952.

DEVINE, W. P., B. LUBARSKY, K. SHAW, S. LUSCHNIG, L. MESSINA *et al.*, 2005 Requirement for chitin biosynthesis in epithelial tube morphogenesis. Proc Natl Acad Sci U S A **102:** 17014-17019.

DIEKMAN, A. B., and E. GOLDBERG, 1994 Characterization of a human antigen with sera from infertile patients. Biol Reprod **50:** 1087-1093.

FAMBROUGH, D., and C. S. GOODMAN, 1996 The Drosophila beaten path gene encodes a novel secreted protein that regulates defasciculation at motor axon choice points. Cell **87:** 1049-1058.

FOX, A. N., and K. ZINN, 2005 The heparan sulfate proteoglycan syndecan is an in vivo ligand for the Drosophila LAR receptor tyrosine phosphatase. Curr Biol **15:** 1701-1711.

FRY, E. J., M. J. CHAGNON, R. LOPEZ-VALES, M. L. TREMBLAY and S. DAVID, 2009 Corticospinal tract regeneration after spinal cord injury in receptor protein tyrosine phosphatase sigma deficient mice. Glia **58:** 423-433.

GIESEN, K., U. LAMMEL, D. LANGEHANS, K. KRUKKERT, I. BUNSE *et al.*, 2003 Regulation of glial cell number and differentiation by ecdysone and Fos signaling. Mech Dev **120:** 401-413.

GOMIS-RUTH, F. X., K. MASKOS, M. BETZ, A. BERGNER, R. HUBER *et al.*, 1997 Mechanism of inhibition of the human matrix metalloproteinase stromelysin-1 by TIMP-1. Nature **389:** 77-81.

GRENNINGLOH, G., E. J. REHM and C. S. GOODMAN, 1991 Genetic analysis of growth cone guidance in Drosophila: fasciclin II functions as a neuronal recognition molecule. Cell **67:** 45-57.

GRYZIK, T., and H. A. MULLER, 2004 FGF8-like1 and FGF8-like2 encode putative ligands of the FGF receptor Htl and are required for mesoderm migration in the Drosophila gastrula. Curr Biol **14:** 659-667.

HACKER, U., X. LIN and N. PERRIMON, 1997 The Drosophila sugarless gene modulates Wingless signaling and encodes an enzyme involved in polysaccharide biosynthesis. Development **124:** 3565-3573.

HACKER, U., K. NYBAKKEN and N. PERRIMON, 2005 Heparan sulphate proteoglycans: the sweet side of development. Nat Rev Mol Cell Biol **6:** 530-541.

HAECKER, A., M. BERGMAN, C. NEUPERT, B. MOUSSIAN, S. LUSCHNIG *et al.*, 2008 Wollknauel is required for embryo patterning and encodes the Drosophila ALG5 UDP-glucose:dolichyl-phosphate glucosyltransferase. Development **135:** 1745-1749.

HAERRY, T. E., T. R. HESLIP, J. L. MARSH and M. B. O'CONNOR, 1997 Defects in glucuronate biosynthesis disrupt Wingless signaling in Drosophila. Development **124:** 3055-3064.

HALTER, D. A., J. URBAN, C. RICKERT, S. S. NER, K. ITO *et al.*, 1995 The homeobox gene repo is required for the differentiation and maintenance of glia function in the embryonic nervous system of Drosophila melanogaster. Development **121:** 317-332.

HAN, C., T. Y. BELENKAYA, M. KHODOUN, M. TAUCHI and X. LIN, 2004 Distinct and collaborative roles of Drosophila EXT family proteins in morphogen signalling and gradient formation. Development **131:** 1563-1575.

HANOVER, J. A., 2001 Glycan-dependent signaling: O-linked N-acetylglucosamine. FASEB J **15:** 1865-1876.

HARRIS, R., L. M. SABATELLI and M. A. SEEGER, 1996 Guidance cues at the Drosophila CNS midline: identification and characterization of two Drosophila Netrin/UNC-6 homologs. Neuron **17:** 217-228.

HELENIUS, A., and M. AEBI, 2004 Roles of N-linked glycans in the endoplasmic reticulum. Annu Rev Biochem **73:** 1019-1049.

HERMAN, T., E. HARTWIEG and H. R. HORVITZ, 1999 sqv mutants of Caenorhabditis elegans are defective in vulval epithelial invagination. Proc Natl Acad Sci U S A **96:** 968-973.

HERMAN, T., and H. R. HORVITZ, 1999 Three proteins involved in Caenorhabditis elegans vulval invagination are similar to components of a glycosylation pathway. Proc Natl Acad Sci U S A **96:** 974-979.

HIDALGO, A., and G. E. BOOTH, 2000 Glia dictate pioneer axon trajectories in the Drosophila embryonic CNS. Development **127:** 393-402.

HOSOYA, T., K. TAKIZAWA, K. NITTA and Y. HOTTA, 1995 glial cells missing: a binary switch between neuronal and glial determination in Drosophila. Cell **82:** 1025-1036.

HWANG, H. Y., S. K. OLSON, J. D. ESKO and H. R. HORVITZ, 2003 Caenorhabditis elegans early embryogenesis and vulval morphogenesis require chondroitin biosynthesis. Nature **423:** 439-443.

IOFFE, E., and P. STANLEY, 1994 Mice lacking N-acetylglucosaminyltransferase I activity die at mid-gestation, revealing an essential role for complex or hybrid N-linked carbohydrates. Proc Natl Acad Sci U S A **91:** 728-732.

JOHNSON, K. G., A. GHOSE, E. EPSTEIN, J. LINCECUM, M. B. O'CONNOR *et al.*, 2004 Axonal heparan sulfate proteoglycans regulate the distribution and efficiency of the repellent slit during midline axon guidance. Curr Biol **14:** 499-504.

JONES, B. W., R. D. FETTER, G. TEAR and C. S. GOODMAN, 1995 glial cells missing: a genetic switch that controls glial versus neuronal fate. Cell **82:** 1013-1023.

KAMMERER, M., and A. GIANGRANDE, 2001 Glide2, a second glial promoting factor in Drosophila melanogaster. EMBO J **20:** 4664-4673.

KANNING, K. C., A. KAPLAN and C. E. HENDERSON, 2010 Motor Neuron Diversity in Development and Disease. Annu Rev Neurosci.

KATSUKI, T., D. AILANI, M. HIRAMOTO and Y. HIROMI, 2009 Intra-axonal patterning: intrinsic compartmentalization of the axonal membrane in Drosophila neurons. Neuron **64:** 188-199.

KATZ, F., W. MOATS and Y. N. JAN, 1988 A carbohydrate epitope expressed uniquely on the cell surface of Drosophila neurons is altered in the mutant nac (neurally altered carbohydrate). EMBO J **7:** 3471-3477.

KELEMAN, K., S. RAJAGOPALAN, D. CLEPPIEN, D. TEIS, K. PAIHA *et al.*, 2002 Comm sorts robo to control axon guidance at the Drosophila midline. Cell **110:** 415-427.

KESHISHIAN, H., K. BROADIE, A. CHIBA and M. BATE, 1996 The drosophila neuromuscular junction: a model system for studying synaptic development and function. Annu Rev Neurosci **19:** 545-575.

KIDD, T., K. S. BLAND and C. S. GOODMAN, 1999 Slit is the midline repellent for the robo receptor in Drosophila. Cell **96:** 785-794.

KIDD, T., K. BROSE, K. J. MITCHELL, R. D. FETTER, M. TESSIER-LAVIGNE *et al.*, 1998 Roundabout controls axon crossing of the CNS midline and defines a novel subfamily of evolutionarily conserved guidance receptors. Cell **92:** 205-215.

KOLES, K., J. M. LIM, K. AOKI, M. PORTERFIELD, M. TIEMEYER *et al.*, 2007 Identification of N-glycosylated proteins from the central nervous system of Drosophila melanogaster. Glycobiology **17:** 1388-1403.

KOLODZIEJ, P. A., L. C. TIMPE, K. J. MITCHELL, S. R. FRIED, C. S. GOODMAN *et al.*, 1996 frazzled encodes a Drosophila member of the DCC immunoglobulin subfamily and is required for CNS and motor axon guidance. Cell **87:** 197-204.

KRUEGER, N. X., D. VAN VACTOR, H. I. WAN, W. M. GELBART, C. S. GOODMAN *et al.*, 1996 The transmembrane tyrosine phosphatase LAR controls motor axon guidance in Drosophila. Cell **84:** 611-622.

LAUC, G., I. RUDAN, H. CAMPBELL and P. M. RUDD, 2009 Complex genetic regulation of protein glycosylation. Mol Biosyst **6:** 329-335.

LEE, H. K., A. P. WRIGHT and K. ZINN, 2009 Live dissection of Drosophila embryos: streamlined methods for screening mutant collections by antibody staining. J Vis Exp.

LIN, D. M., and C. S. GOODMAN, 1994 Ectopic and increased expression of Fasciclin II alters motoneuron growth cone guidance. Neuron **13:** 507-523.

LIN, X., E. M. BUFF, N. PERRIMON and A. M. MICHELSON, 1999 Heparan sulfate proteoglycans are essential for FGF receptor signaling during Drosophila embryonic development. Development **126:** 3715-3723.

LLANO, E., G. ADAM, A. M. PENDAS, V. QUESADA, L. M. SANCHEZ *et al.*, 2002 Structural and enzymatic characterization of Drosophila Dm2-MMP, a membrane-bound matrix metalloproteinase with tissue-specific expression. J Biol Chem **277:** 23321-23329.

LLANO, E., A. M. PENDAS, P. AZA-BLANC, T. B. KORNBERG and C. LOPEZ-OTIN, 2000 Dm1-MMP, a matrix metalloproteinase from Drosophila with a potential role in extracellular matrix remodeling during neural development. J Biol Chem **275:** 35978-35985.

LO, E. H., X. WANG and M. L. CUZNER, 2002 Extracellular proteolysis in brain injury and inflammation: role for plasminogen activators and matrix metalloproteinases. J Neurosci Res **69:** 1-9.

MARYGOLD, S. J., J. ROOTE, G. REUTER, A. LAMBERTSSON, M. ASHBURNER *et al.*, 2007 The ribosomal protein genes and Minute loci of Drosophila melanogaster. Genome Biol **8:** R216.

MILLER, C. M., A. PAGE-MCCAW and H. T. BROIHIER, 2008 Matrix metalloproteinases promote motor axon fasciculation in the Drosophila embryo. Development **135:** 95-109.

MITCHELL, K. J., J. L. DOYLE, T. SERAFINI, T. E. KENNEDY, M. TESSIER-LAVIGNE *et al.*, 1996 Genetic analysis of Netrin genes in Drosophila: Netrins guide CNS commissural axons and peripheral motor axons. Neuron **17:** 203-215.

MIZUGUCHI, S., T. UYAMA, H. KITAGAWA, K. H. NOMURA, K. DEJIMA *et al.*, 2003 Chondroitin proteoglycans are involved in cell division of Caenorhabditis elegans. Nature **423:** 443-448.

NUSSLEIN-VOLHARD, C., and E. WIESCHAUS, 1980 Mutations affecting segment number and polarity in Drosophila. Nature **287:** 795-801.

PAGE-MCCAW, A., 2008 Remodeling the model organism: matrix metalloproteinase functions in invertebrates. Semin Cell Dev Biol **19:** 14-23.

PAGE-MCCAW, A., A. J. EWALD and Z. WERB, 2007 Matrix metalloproteinases and the regulation of tissue remodelling. Nat Rev Mol Cell Biol **8:** 221-233.

PAGE-MCCAW, A., J. SERANO, J. M. SANTE and G. M. RUBIN, 2003 Drosophila matrix metalloproteinases are required for tissue remodeling, but not embryonic development. Dev Cell **4:** 95-106.

PARKS, A. L., K. R. COOK, M. BELVIN, N. A. DOMPE, R. FAWCETT *et al.*, 2004 Systematic generation of high-resolution deletion coverage of the Drosophila melanogaster genome. Nat Genet **36:** 288-292.

PATEL, N. H., 1994 Imaging neuronal subsets and other cell types in whole-mount Drosophila embryos and larvae using antibody probes. Methods Cell Biol **44:** 445-487.

PATEL, N. H., P. M. SNOW and C. S. GOODMAN, 1987 Characterization and cloning of fasciclin III: a glycoprotein expressed on a subset of neurons and axon pathways in Drosophila. Cell **48:** 975-988.

PERRIMON, N., A. LANJUIN, C. ARNOLD and E. NOLL, 1996 Zygotic lethal mutations with maternal effect phenotypes in Drosophila melanogaster. II. Loci on the second and third chromosomes identified by P-element-induced mutations. Genetics **144:** 1681-1692.

PIPES, G. C., Q. LIN, S. E. RILEY and C. S. GOODMAN, 2001 The Beat generation: a multigene family encoding IgSF proteins related to the Beat axon guidance molecule in Drosophila. Development **128:** 4545-4552.

PIZZI, M. A., and M. J. CROWE, 2007 Matrix metalloproteinases and proteoglycans in axonal regeneration. Exp Neurol **204:** 496-511.

PRYDZ, K., and K. T. DALEN, 2000 Synthesis and sorting of proteoglycans. J Cell Sci **113 Pt 2:** 193-205.

SCHIMMELPFENG, K., M. STRUNK, T. STORK and C. KLAMBT, 2006 Mummy encodes an UDP-N-acetylglucosamine-dipohosphorylase and is required during Drosophila dorsal closure and nervous system development. Mech Dev **123:** 487-499.

SCHINDELHOLZ, B., M. KNIRR, R. WARRIOR and K. ZINN, 2001 Regulation of CNS and motor axon guidance in Drosophila by the receptor tyrosine phosphatase DPTP52F. Development **128:** 4371-4382.

SEEGER, M., G. TEAR, D. FERRES-MARCO and C. S. GOODMAN, 1993 Mutations affecting growth cone guidance in Drosophila: genes necessary for guidance toward or away from the midline. Neuron **10:** 409-426.

SELLECK, S. B., 2001 Genetic dissection of proteoglycan function in Drosophila and C. elegans. Semin Cell Dev Biol **12:** 127-134.

SEN, J., J. S. GOLTZ, L. STEVENS and D. STEIN, 1998 Spatially restricted expression of pipe in the Drosophila egg chamber defines embryonic dorsal-ventral polarity. Cell **95:** 471-481.

SEPP, K. J., J. SCHULTE and V. J. AULD, 2001 Peripheral glia direct axon guidance across the CNS/PNS transition zone. Dev Biol **238:** 47-63.

SERGEEV, P., A. STREIT, A. HELLER and M. STEINMANN-ZWICKY, 2001 The Drosophila dorsoventral determinant PIPE contains ten copies of a variable domain homologous to mammalian heparan sulfate 2-sulfotransferase. Dev Dyn **220:** 122-132.

SHEN, Y., A. P. TENNEY, S. A. BUSCH, K. P. HORN, F. X. CUASCUT *et al.*, 2009 PTPsigma is a receptor for chondroitin sulfate proteoglycan, an inhibitor of neural regeneration. Science **326:** 592-596.

SHERMAN, L. S., and S. A. BACK, 2008 A 'GAG' reflex prevents repair of the damaged CNS. Trends Neurosci **31:** 44-52.

SIEBERT, M., D. BANOVIC, B. GOELLNER and H. ABERLE, 2009 Drosophila motor axons recognize and follow a Sidestep-labeled substrate pathway to reach their target fields. Genes Dev **23:** 1052-1062.

SIMPSON, J. H., T. KIDD, K. S. BLAND and C. S. GOODMAN, 2000 Short-range and long-range guidance by slit and its Robo receptors. Robo and Robo2 play distinct roles in midline guidance. Neuron **28:** 753-766.

SINK, H., E. J. REHM, L. RICHSTONE, Y. M. BULLS and C. S. GOODMAN, 2001 sidestep encodes a target-derived attractant essential for motor axon guidance in Drosophila. Cell **105:** 57-67.

SNOW, P. M., N. H. PATEL, A. L. HARRELSON and C. S. GOODMAN, 1987 Neural-specific carbohydrate moiety shared by many surface glycoproteins in Drosophila and grasshopper embryos. J Neurosci **7:** 4137-4144.

SPIRO, R. G., 2002 Protein glycosylation: nature, distribution, enzymatic formation, and disease implications of glycopeptide bonds. Glycobiology **12:** 43R-56R.

SPRING, J., S. E. PAINE-SAUNDERS, R. O. HYNES and M. BERNFIELD, 1994 Drosophila syndecan: conservation of a cell-surface heparan sulfate proteoglycan. Proc Natl Acad Sci U S A **91:** 3334-3338.

STANLEY, P., and E. IOFFE, 1995 Glycosyltransferase mutants: key to new insights in glycobiology. FASEB J **9:** 1436-1444.

STATHOPOULOS, A., B. TAM, M. RONSHAUGEN, M. FRASCH and M. LEVINE, 2004 pyramus and thisbe: FGF genes that pattern the mesoderm of Drosophila embryos. Genes Dev **18:** 687-699.

STEIN, D., S. ROTH, E. VOGELSANG and C. NUSSLEIN-VOLHARD, 1991 The polarity of the dorsoventral axis in the Drosophila embryo is defined by an extracellular signal. Cell **65:** 725-735.

TAKEI, Y., Y. OZAWA, M. SATO, A. WATANABE and T. TABATA, 2004 Three Drosophila EXT genes shape morphogen gradients through synthesis of heparan sulfate proteoglycans. Development **131:** 73-82.

TEN HAGEN, K. G., L. ZHANG, E. TIAN and Y. ZHANG, 2009 Glycobiology on the fly: developmental and mechanistic insights from Drosophila. Glycobiology **19:** 102-111.

THE, I., Y. BELLAICHE and N. PERRIMON, 1999 Hedgehog movement is regulated through tout velu-dependent synthesis of a heparan sulfate proteoglycan. Mol Cell **4:** 633-639.

THOMAS, J. B., S. T. CREWS and C. S. GOODMAN, 1988 Molecular genetics of the single-minded locus: a gene involved in the development of the Drosophila nervous system. Cell **52:** 133-141.

TONNING, A., S. HELMS, H. SCHWARZ, A. E. UV and B. MOUSSIAN, 2006 Hormonal regulation of mummy is needed for apical extracellular matrix formation and epithelial morphogenesis in Drosophila. Development **133:** 331-341.

TOYODA, H., A. KINOSHITA-TOYODA, B. FOX and S. B. SELLECK, 2000 Structural analysis of glycosaminoglycans in animals bearing mutations in sugarless, sulfateless, and tout-velu. Drosophila homologues of vertebrate genes encoding glycosaminoglycan biosynthetic enzymes. J Biol Chem **275:** 21856-21861.

VAN VACTOR, D. V., H. SINK, D. FAMBROUGH, R. TSOO and C. S. GOODMAN, 1993 Genes that control neuromuscular specificity in Drosophila. Cell **73:** 1137-1153.

VINCENT, S., J. L. VONESCH and A. GIANGRANDE, 1996 Glide directs glial fate commitment and cell fate switch between neurones and glia. Development **122:** 131-139.

WALZ, A., R. B. ANDERSON, A. IRIE, C. B. CHIEN and C. E. HOLT, 2002 Chondroitin sulfate disrupts axon pathfinding in the optic tract and alters growth cone dynamics. J Neurobiol **53:** 330-342.

WANG-GILLAM, A., I. PASTUSZAK and A. D. ELBEIN, 1998 A 17-amino acid insert changes UDP-N-acetylhexosamine pyrophosphorylase specificity from UDP-GalNAc to UDP-GlcNAc. J Biol Chem **273:** 27055-27057.

WEERAPANA, E., and B. IMPERIALI, 2006 Asparagine-linked protein glycosylation: from eukaryotic to prokaryotic systems. Glycobiology **16:** 91R-101R.

WELLS, L., and G. W. HART, 2003 O-GlcNAc turns twenty: functional implications for post-translational modification of nuclear and cytosolic proteins with a sugar. FEBS Lett **546:** 154-158.

WHITE, K., M. E. GRETHER, J. M. ABRAMS, L. YOUNG, K. FARRELL *et al.*, 1994 Genetic control of programmed cell death in Drosophila. Science **264:** 677-683.

XIONG, W. C., H. OKANO, N. H. PATEL, J. A. BLENDY and C. MONTELL, 1994 repo encodes a glial-specific homeo domain protein required in the Drosophila nervous system. Genes Dev **8:** 981-994.

YONG, V. W., 2005 Metalloproteinases: mediators of pathology and regeneration in the CNS. Nat Rev Neurosci **6:** 931-944.

YU, H. H., H. H. ARAJ, S. A. RALLS and A. L. KOLODKIN, 1998 The transmembrane Semaphorin Sema I is required in Drosophila for embryonic motor and CNS axon guidance. Neuron **20:** 207-220.

ZHU, X., J. SEN, L. STEVENS, J. S. GOLTZ and D. STEIN, 2005 Drosophila pipe protein activity in the ovary and the embryonic salivary gland does not require heparan sulfate glycosaminoglycans. Development **132:** 3813-3822.

ZINN, K., 2009 Choosing the road less traveled by: a ligand-receptor system that controls target recognition by Drosophila motor axons. Genes Dev **23:** 1042-1045.

ZUO, J., T. A. FERGUSON, Y. J. HERNANDEZ, W. G. STETLER-STEVENSON and D. MUIR, 1998 Neuronal matrix metalloproteinase-2 degrades and inactivates a neurite-inhibiting chondroitin sulfate proteoglycan. J Neurosci **18:** 5203-5211.

Chapter 2

The Epitope of Monoclonal Antibody BP102 is a Proteoglycan That is Regulated by *matrix metalloproteinase 1*

Chapter 2 Introduction

N-linked glycosylation and proteoglycan synthesis and function have been studied in *Drosophila*. A survey of N-glycosylated proteins found in the *Drosophila* central nervous system (CNS) found that many different types of proteins are modified in this way including proteins involved in carbohydrate metabolism, proteolysis, cell adhesion, cell surface receptors, extracellular matrix components and many other processes. In total, 205 proteins were found to be N-glycosylated at 307 sites (KOLES *et al.* 2007). This number is almost certainly an underestimate as low abundance proteins would not have been identified, and the thresholds set would likely result in valid glycoproteins being discarded. There are greater than 1200 proteins in Drosophila that contain signal sequences and most of these would be expected to be N-glycosylated.

The components of the biosynthetic pathway for HSPG and CSPG synthesis are known in *Drosophila* and mutations exist in many genes in these pathways. The initial step in the synthesis of PGs is carried out by the enzyme UDP-glucose dehydrogenase (known as *sugarless* (*sgl*) in *Drosophila*). Sgl produces UDP-glucuronic acid (GlcA) that is then imported into the ER and Golgi where it is converted by the action of other enzymes into UDP-xylose (Xyl). Xyl is the first sugar attached to Serine residues during GAG synthesis and loss of Sgl inhibits both HSPG and CSPG formation. Mutations in *sgl* were first identified in genetic screens looking for enhancers of Wingless (Wg) signaling (HAERRY *et al.* 1997) and in screens for cuticle defects resembling *wg* or *hedgehog* (*hh*) mutants in maternal effect lethal lines (BINARI *et al.*

1997; HACKER *et al.* 1997; PERRIMON *et al.* 1996). Wg and Hh are secreted morphogens required for proper patterning in early Drosophila embryos. Sgl has also been shown to be involved in Decapentaplegic (Dpp) (HAERRY *et al.* 1997), and Fibroblast Growth Factor (FGF) signaling (LIN *et al.* 1999).

The enzyme responsible for HS GAG chain initiation is encoded by *brother of tout-velu* (*botv*) in *Drosophila*. The chains are then elongated through the action of *botv* as well as a complex formed by *tout-velu* (*ttv*) and *sister of tout-velu* (*sotv*). Mutation of any one of these three proteins leads to dramatic reduction in HSPG synthesis and Wg, Hh, and Dpp signaling are affected in the wing disc (BELLAICHE *et al.* 1998; HAN *et al.* 2004; TAKEI *et al.* 2004). Zygotic nulls in these enzymes results in segment polarity defects. *ttv* has also been shown to have a role in Hh movement in embryonic tissue (THE *et al.* 1999). It has therefore been proposed that the defects found in maternal null *sgl* mutants are due to loss of HSPG synthesis not CSPG synthesis.

Once side chains have been added to the protein core they can be further modified by 2-O, 3-O, or 6-O sulfation. *sulfateless* (*sfl*), encodes a heparan sulfate N-deacetylase/N-sulfotransferase (NDST) and is specifically required for GAG modification in the HS pathway. *sfl* was isolated in one of the same genetic screens as *sgl* and also has a segment polarity cuticle defect similar to *wg* mutants (PERRIMON *et al.* 1996). Loss of Sfl also leads to defects in FGF signaling (LIN *et al.* 1999). Sfl function is required for sulfation of heparin side chains to occur.

The enzymes responsible for 2-O, 3-O, and 6-O sulfation have been identified but have not yet been characterized. Pipe, a sulfotransferase required for dorsal-ventral polarity in Drosophila oocytes, was thought to be the *HS 2-sulfotransferase* (Hs2st) by sequence similarity to mouse Hs2st (SEN *et al.* 1998; SERGEEV *et al.* 2001; STEIN *et al.* 1991) . Pipe encodes 10 different sulfotransferase isoforms but they have not been shown to act on HSPG substrates. Mutation of PG synthesis enzymes has no effect on production of a *pipe* sulfated product in the salivary gland (ZHU *et al.* 2005). Pipe therefore is a sulfotransferase but is not the *Drosophila* Hs2st ortholog. The Hs2st ortholog has been identified but mutations in Hs2st have not been characterized.

There are two major classes of HSPGs, the glypicans, which are GPI-anchored, and syndecans, which are transmembrane proteins. The *Drosphila* genome encodes two glypicans and only one syndecan, making functional studies easier than in vertebrates where the family has expanded. The two glypicans in Drosophila are known as *dally* and *dally-like* (*dlp*). *dally* is known to be involved in growth factor signaling including Dpp, BMP, Wg, and Hh signaling (HACKER *et al.* 2005; SELLECK 2001). *dlp* is partially redundant with dally in Wg, Hh, and Dpp signaling. The phenotypes observed in early embryos when enzymes in the PG biosynthetic pathways are mutated is likely due to loss of modified Dally and Dlp as the same pathways are affected when the glypicans are mutated. Dlp and the fly syndecan (Sdc) have been shown to mediate Slit-Robo signaling in the CNS of *Drosophila*

(JOHNSON *et al.* 2004) as well other axon guidance events in both *Drosophila* embryos and larvae (FOX and ZINN 2005; JOHNSON *et al.* 2004).

Chondroitin and CS have not been studied in *Drosophila*. The genes responsible for elongation (GalNAcT-II and CS GlcAT-II) and sulfation of CS side chains have been identified by sequence homology, but no mutations currently exist. Study of this type of post-translational modification in *Drosophila* could be very informative as there are likely to be fewer CS modified proteins than in vertebrates.

Results and Discussion

Mummy Encodes a Protein Responsible for BP102 Epitope Production

We have used deficiency (Df) screening to search for ligands for the receptor protein phosphatases (RPTPs) in *Drosophila* using human placental alkaline phosphatase (AP) fused to the extracellular domains of the RPTPs. These fusion proteins bind in very specific patterns when applied to dissected late stage *Drosophila* embryos. All of the fusion proteins bind along the ventral nerve cord. In order to assess if a Df developed well enough to have axons in the ventral nerve cord, all Dfs were also stained with mAb BP102. BP102 labels the axon scaffold in the CNS including the commissures and longitudinal connectives (Figure 1A, C).

The epitope recognized by BP102 has never been identified. It is expressed on all CNS axons but only on the most proximal segments of those axons both *in vivo* and in cell culture (KATSUKI *et al.* 2009; SEEGER *et al.* 1993). The antibody has been thought to bind a carbohydrate epitope because it sensitive to periodate which modifies saccharide rings. While conducting our RPTP ligand screen we found two Dfs on the second chromosome, Df(2L)BSC6 and Df(2R)cn9, that failed to stain with BP102. We set out to define the epitope for BP102 by further mapping these Dfs. Df(2L)BSC6, which is molecularly mapped, deletes cytological segments 26D3 to 26F7. Df(2R)cn9 is not molecularly mapped and deletes cytological segments 42E to 44C1. Our attempts to further map these two regions using other molecularly mapped Dfs resulted in narrowing down of the Df(2L)BSC6 region while the lack of

BP102 staining in Df(2R)cn9 could not be mapped. We became suspicious that Df(2R)cn9 might actually harbor a deletion of the same region as Df(2L)BSC6. The two Dfs were crossed together and failed to complement one another. We believe that the region responsible for the lack of BP102 staining therefore resides in cytological segments 26D3 to 26F7. We were able to further map the region by staining Df(2L)BSC7 and Df(2L)ED384 which both show wildtype levels of BP102 staining. These results further narrowed the region to 26D7-26D10.

We next assessed Df(2L)BSC354. This deficiency deletes about 15 genes and fails to stain with BP102. We ordered available mutations for the genes in this region and began testing them for BP102 staining. Mutation of one gene, *mummy* (*mmy*), results in the failure of BP102 binding (Figure 1D, F). There is a very small amount of residual staining in *mmy* mutants that can be found if the gain is increased during confocal imaging. In order confirm this result, mmy^{1} was crossed to Df(2L)BSC296. This Df deletes extends just to the right of *mmy* and does not greatly overlap with Df(2L)BSC354. The embryos resulting from the cross fail to stain with BP102 confirming the result in the *mmy* homozygote (Figure 1 J, L). *mmy* was originally identified in a screen for mutations that affect cuticle differentiation (NUSSLEIN-VOLHARD and WIESCHAUS 1980). *mmy* encodes a UDP-N-acetylglucosamine diphosphorylase and it catalyzes the following reaction:

UTP + N-acetyl-α-D-glucosamine-1-phosphate

↓

diphosphate +UDP-N-acetyl-α-D-glucosamine (UDP-GlcNAc).

A mammalian ortholog of *mmy* has been isolated from pig liver and was found to have dual specificity for N-acetyl-α-D-glucosamine-1-phosphate and N-acetyl-α-D-galactosamine-1-phosphate. It was subsequently found that the isolated protein actually consisted of two homodimers, known as AGX1 and AGX2. AGX2 differs from AGX1 by a 17 amino acid insertion that changes the specificity from a UDP-GalNAc to UDP-GlcNac pyrophosphorylase (WANG-GILLAM *et al.* 1998). It has also been shown that AGX1 and AGX2 are produced as a result of alternative splicing from the same locus (DIEKMAN and GOLDBERG 1994). It is therefore likely that *mmy* catalyzes the following reaction in addition to the reaction above:

UTP + N-acetyl-galactosamine-1-phosphate

diphosphate + UDP-N-acetyl-galactosamine (UDP-GalNAc).

In some organisms UDP-GlcNAc and UDP-GalNAc can be interconverted by the action of epimerases. So far these epimerases have not been identified in *Drosophila* and therefore it is believed that *mmy* is the major source for UDP-GlcNAc and UDP-GalNAc (ARAUJO *et al.* 2005). UDP-GlcNAc and UDP-GalNAc are major building blocks for most types of protein glycosylation, including N-linked, O-linked, and proteoglycan (PG) synthesis, as well as GPI anchor formation and chitin synthesis.

In addition to affecting cuticle differentiation, *mmy* mutants also have defects in trachea formation, dorsal closure, as well as axonal patterning (ARAUJO *et al.* 2005;

DEVINE *et al.* 2005; SCHIMMELPFENG *et al.* 2006; TONNING *et al.* 2006). The defects in cuticle and tracheal formation have been attributed to a lack of chitin synthesis in *mmy* mutants. Similar defects are found when chitin synthase, encoded by *krotzkopf verkehrt* (*kkv*), is mutated (DEVINE *et al.* 2005) but these phenotypes were not found to be as severe as in loss of *mmy* (ARAUJO *et al.* 2005). *mmy* acts upstream of *kkv* and is involved in the formation of many other saccharide chains in addition to chitin. The CNS phenotype of *mmy* is not found in *kkv* mutants suggesting carbohydrate moieties other than chitin are required for proper formation of the nervous system.

The failure of *mmy* to stain with BP102 was very surprising to us because two papers have been published with BP102 staining in *mmy* mutants. Two alleles, $mmy^{KG08617}$ and mmy^{J1201}, which are both thought to be null alleles, have been shown to stain with BP102 (ARAUJO *et al.* 2005; SCHIMMELPFENG *et al.* 2006). In order to address this discrepancy, we tested these two alleles. The published staining patterns were both achieved using an antibody conjugated to horseradish peroxidase (HRP) instead of the fluorescent method we use for staining. When we tested these alleles using the fluorescent method they failed to stain with BP102 (Figure 2 G, M). We think this can best be explained by the fact that the HRP reaction leads to formation of a precipitate and more of this precipitate forms as the reaction is allowed to proceed. In fact when we increase the gain on the confocal microscope, we have been able to detect a very small amount of residual BP102 staining in the ventral nerve cord of *mmy* embryos.

One explanation for the published results on staining of *mmy* embryos with BP102 is that there is enough residual binding of BP102 to create the published patterns and that this level is not easily detected by the fluorescent method. Another possibility is that the method for collecting the embryos used for our experiments is different from the previous work. In the previous work, embryos are collected overnight at 25 ^{0}C. In our method embryos are collected at room temperature and then shifted to 18 ^{0}C for 24 hours. It could be that *mmy* mutants have enough residual function to synthesize the BP102 epitope at higher temperature possibly due to maternal expression, or that the function of a partially redundant pathway is increased at 25 ^{0}C and compensates for loss of *mmy*.

In order to address the published staining patterns, we stained $mmy^{KG08617}$ and mmy^{J1201} as well as two other alleles with BP102 using a secondary antibody conjugated to HRP and find that both at room temperature and 18 ^{0}C, all *mmy* alleles tested stain with BP102 (Figure 3B-E, G-J). It appears there is a smaller amount of the BP102 epitope at 18 ^{0}C than at room temperature. These data suggest that the HRP staining method allows residual BP102 epitope to be detected while the fluorescent method is not sensitive enough. We next stained room temperature reared embryos using immunofluorescence and find that all alleles stain with BP102 but the levels are greatly reduced as compared to wildtype (Figure 2D', G', J', M'). These data taken together suggest that both staining method and temperature are important for detection of BP102. Residual *mmy* enzymatic function must be greater at higher temperature leading to production of more BP102 epitope. There is precedent for

this temperature dependence. It has been reported that mutations in *neurally altered carbohydrate* (*nac*) are viable and normal when raised at room temperature but have wing and eye defects when raised at 18 degrees (KATZ *et al.* 1988). *nac* mutations interfere with expression of a carbohydrate epitope that an antibody against horseradish peroxidase crossreacts to within the *Drosophila* nervous system (SNOW *et al.* 1987). Therefore we have been able to uncover a role for mmy in BP102 epitope production only by using an immunofluorescence protocol at 18 ^{0}C and this explains why other groups did not report this finding.

Mmy should be absolutely required for GPI-anchor formation as these modifications require UDP-GlcNAc. When GPI-GFP is expressed in wildtype embryos, the expected band of 40 kDa is found on a Western blot. In a *mmy* sample composed of both *mmy* and heterozygous embryos, two distinct bands corresponding to the GPI-linked GFP (40 kDa) and a smaller band of GFP alone (30 kDa) are found (SCHIMMELPFENG *et al.* 2006). These data suggest a loss of GPI-anchor formation in *mmy*. When the epidermis of *mmy* embryos expressing GPI-GFP are examined however, GFP is found on the cell surface. Another GPI-anchored protein, Wrapper, was found to be mislocalized in *mmy* embryos (SCHIMMELPFENG *et al.* 2006). These data suggest that some GPI anchor formation may occur in *mmy* mutants.

Mmy is predicted to be involved in N-linked and O-linked glycosylation. In order to test the effect of *mmy* on N and O-linked glycosylation as well as GPI-anchor formation, Tonning *et al*. (2006) tested the migration of the Knickkopf (Knk) protein on a Western blot. Knk is predicted to be N-glycosylated at 3 positions, O-

glycosylated at 2 positions, and GPI-anchored. In *mmy* loss-of-function mutants, no Knk of wildtype size is found. Another N-glycosylated protein, Tout-velu (Ttv) is also smaller in extracts from *mmy* mutants. When wildtype protein extracts are treated with EndoH, an enzyme which removes N-glycosylation, both Knk and Ttv run even faster, suggesting that mutation of *mmy* does not completely abolish glycosylation. The remaining glycosylation in *mmy* mutants could be due to maternal RNA contribution which has been noted by many groups.

We reasoned that BP102 could not be recognizing a motif on N-glycosylated, O-glycosylated or GPI-anchored proteins because these would be expressed in every cell type. The BP102 epitope is restricted to the proximal segments of CNS axons and in the absence of detergent BP102 can still bind. These data suggested to us that the epitope is almost all extracellular. Other data (see below) suggested that the epitope might be a component of a PG. We decided that the best place to begin dissecting the biosynthesis pathway involved in production of the BP102 epitope was by looking at PG synthesis.

sgl and *sfl* homozygous embryos from heterozygous mothers receive maternal transcript and therefore mutation of either gene does not have visible effects on embryonic growth or viability unless isolated from maternal nulls. Zygotic mutants die during larval life. The composition of GAGs has been determined in both *sgl* and *sfl* mutant larvae. *sgl* second instar larvae are found to have no chondroitin/CS side chains as well as only trace amounts of HS. *sfl* mutants should retain CSPG biosyntheis and affect only the HSPG pathway. This is in fact what was observed. *sfl*

mutant larvae have normal levels of chondroitin/CS but all 5 different forms of sulfated heparan are absent and a nonsulfated precursor of heparin, N-acetyl heparosan, accumulates instead (TOYODA *et al.* 2000).

We examined BP102 staining in first instar larval brain of *sgl* and *sfl*. BP102 stains the larval CNS in a pattern very similar to rhodamine-conjugated phalloidin which we use to visualize the axon scaffold (Figure 4A, B, C). *sgl* mutants do have reduced BP102 staining as compared to the control (Figure 4D) while *sfl* mutants have no change in BP102 or phalloidin staining in larval brain as compared to control (Figure 4G, H, I). Neither mutant would be expected to completely abolish BP102 staining due to maternal contribution. Since *sfl*, an enzyme specific to the HSPG biosynthetic pathway, has no effect on BP102 staining, while *sgl*, an enzyme common to both HSPG and CSPG pathways does reduce BP102 staining, we believe this suggests BP102 is binding to a CSPG not a HSPG.

Matrix Metalloproteinase 1 Regulates BP102 Epitope Expression

One other piece of intriguing data came while conducting our ligand screen for the RPTPs. We found a Df that alters the BP102 epitope expression pattern. One Df on the second chromosome was found to have a very strange BP102 pattern where cells in the periphery express the BP102 epitope. BP102 normally only labels proximal segments of axons within the CNS and does not extend into the periphery (Figure 5A). One gene deleted by this Df is *matrix metalloproteinase 1* (*mmp1*). Mmps, enzymes that are secreted or anchored to the plasma membrane, are capable of cleaving all proteins in the extracellular matrix (ECM) and require the presence of

zinc at the active site (LO *et al.* 2002; YONG 2005). They are known to play roles in restructuring the ECM, cell signaling, cell proliferation, cell survival and differentiation, inflammation, and metastasis as well as many other processes (PAGE-MCCAW 2008; PAGE-MCCAW *et al.* 2007). There are two mmps in Drosophila known as *mmp1* and *mmp2* (LLANO *et al.* 2002; LLANO *et al.* 2000). Mmp1 is a secreted molecule while Mmp2 is GPI-anchored.

mmp1 and *mmp2* were both found in a misexpression screen to affect motor axon guidance when overexpressed in the nervous system in embryos (MILLER *et al.* 2008). Both mmps are expressed in the embryonic CNS with *mmp2* displaying broader expression than *mmp1*. When mutated, both mmps affect motor axon guidance. *mmp1* mutants also have defects in the maintenance of tracheal structure while *mmp2* mutants have defects during the pupal stage. Mutations in both mmps are lethal during larval stages (PAGE-MCCAW *et al.* 2003). For other reasons, we were already studying *mmp1* and *mmp2*, in the lab and tested BP102 staining in the mmp mutants. We found that mutation of *mmp1* but not *mmp2* leads to a shift in BP102 antigen expression (Figure 5D, G). Deletion of both *mmp1* and *mmp2* also leads to a shift in BP102 expression (Figure 5J).

In order to determine the identity of these cells now expressing BP102, we conducted double labeling experiments with an antibody that labels all neurons, anti-futsch (mAb 22c10), and BP102. As both of the antibodies are mouse monoclonals, we directly conjugated 22c10 to a fluorophore to allow visualization of both in the same embryo. We were able to determine that these cells are likely peripheral

sensory neurons and not motor neurons as evidenced by the overlap with anti-futsch. Based on these data we hypothesize that either the BP102 epitope is being produced by sensory axons and then must be constantly cleaved by *mmp1*, or *mmp1* cleaves another protein that is required for production of the BP102 epitope, and thus prevents this epitope from accumulating on any cell that expresses mmp1. We cannot currently distinguish between these two possibilities.

There is one genetically encoded inhibitor of mmp activity in Drosophila. This class of molecules, known as tissue inhibitor of mmps (TIMPs), are secreted molecules which have been shown in many systems to inhibit the activity of mmps by binding to the active site of the proteinase (GOMIS-RUTH *et al.* 1997). Drosophila *Timp* inhibits both *mmp1* and *mmp2* (PAGE-MCCAW *et al.* 2003). It has been shown that *Timp* is better at inhibiting *mmp1* than *mmp2* in Drosophila embryos. When Timp is expressed in the nervous system, the phenotypes recovered phenocopy loss of *mmp1* but not *mmp2* (PAGE-MCCAW *et al.* 2003). Using the Gal4/UAS system, we expressed Timp under the control of pan-neuronal Gal4 line and found that when mmp activity is inhibited in the nervous system, we see the BP102 epitope expressed on the peripheral cells (data not shown). These data suggest that catalytic activity of *mmp1* is required to restrict the expression of the BP102 epitope to the CNS of *Drosophila* embryos.

Since loss of Mmp1 protein or catalytic activity leads to an increase in BP102 epitope expression on peripheral neurons, we reasoned that overexpression of Mmp1 within the nervous system should result in a loss of BP102 antibody staining. We

drove expression of Mmp1 pan-neuronally using a specific Gal4 line, C155-Gal4, and we do in fact find that BP102 staining is absent in these embryos (Figure 6D). When the same experiment is conducted using UAS-mmp2 there is no difference in BP102 antigen expression. Therefore we conclude that Mmp1 is capable of either cleaving the BP102 epitope from CNS axons when overexpressed within the nervous system or cleaving another protein required for production of the BP102 epitope.

Since Mmp1 overexpression results in a loss of the BP102 antigen we can use these embryos to assess whether known HSPGs are the BP102 epitope. Of the two major classes of HSPGs, glypicans and syndecans, *Drosophila* have two glypicans (*dally* and *dally-like*), and one syndecan (*syndecan*). Dlp but not Dally is known to be expressed in the CNS as is the only syndecan molecule (Figure 6G, H) (FOX and ZINN 2005; JOHNSON *et al.* 2004; SPRING *et al.* 1994). If an HSPG is the BP102 epitope we hypothesized that mmp1 should cleave the HSPG and result in an absence of antibody staining at the midline. We find that in embryos overexpressing Mmp1 in the nervous system, both Sdc and Dlp are expressed at normal levels even though BP102 is absent under these conditions (Figure 6J, K). The Sdc antibody is directed against the core protein of Sdc not the side chains and it is not clear if cleavage by mmp1 would cause loss of the antibody binding site. The epitope for the Dlp antibody is not known. While we cannot rule out the possibility that the antibody epitope could still be present, these data suggest that BP102 is not binding to an HSPG but could be binding a CSPG instead.

MMPs are Known to Cleave CSPGs in the Nervous System

There is a strong link in the literature between CSPGs and MMPs. CSPGs are known to be strong inhibitors of axonal regeneration after spinal cord injury. Axons of the CNS possess the ability to regenerate after injury, but cannot physically cross the lesion site. Many inhibitors of growth are found at lesion sites including the myelin-associated proteins Nogo and myelin-associated glycoprotein (MAG) as well as others. A glial "scar" also forms at lesion sites and these glial cells upregulate CSPGs. Many CSPGs have been shown to inhibit growth of axons both *in vivo* and *in vitro* (PIZZI and CROWE 2007). Treatment of mouse sciatic nerve with chondroitinase ABC, an enzyme that cleaves chondroitin side chains from the core protein, prior to injury results in a greater number of axons crossing the injury site (CRESPO *et al.* 2007). In vivo, mmps have been shown to cleave many members of the CSPG family including neurocan, versican, tenascin-C, brevican, NG2, and phosphacan. MMP-2 (not the ortholog of *mmp-2* in *Drosophila*) mutant mice have been shown to have higher levels of CSPGs and after spinal cord injury these mice have reduced motor recovery (PIZZI and CROWE 2007). Mouse MMP-2 has also been shown to cleave an inhibitory CSPG known as NIF and loss of NIF leads to increases in neurite formation and growth in culture assays where dorsal root ganglion neurons are grown on nerve sections (ZUO *et al.* 1998). We believe that taken together our data suggest that the BP102 epitope could be a CSPG or CS side chain that is expressed within the nervous system.

In order to determine if the BP102 epitope is a CSPG, we are planning to knock down the function of many of the components of the CS biosynthetic pathway using an RNAi approach. We also plan to knock down components of the HSPG pathway and enzymes common to both pathways. These RNAi lines have been crossed to a ubiquitous Gal4 line and many of the lines are lethal as would be expected for such important enzymes. These RNAi lines will be crossed to tissue specific Gal4 lines and screened for BP102 staining.

There are many unanswered questions about the BP102 epitope. We are very interested to determine the consequences of BP102 antigen expression on peripheral sensory neurons in the *mmp1* mutant or Timp overexpressing embryos. The cell bodies of these neurons are in the periphery and their axons migrate into the CNS. Does expression of this epitope alter guidance of these axons into the CNS? We would like to know if loss of the BP102 antigen in the CNS results in alterations of axon guidance or integrity of the CNS. We plan to stain Mmp-1 overexpressing embryos with a variety of tissue specific antibodies in order to assess the effect loss of the BP102 eptiope has on the structures where it is normally expressed. If we can determine that the epitope of BP102 is a CSPG or CS moiety, we will not know the identity of the protein or proteins that carry the CS side chains. There are no clear orthologs of known CSPGs in Drosophila and our analysis represents the first study of CSPG function in Drosophila. It may be possible to use the RNAi lines for the CS pathway to study the roles CSPGs play in development, axon guidance, and possibly regeneration within the nervous system.

MATERIAL AND METHODS

Genetics

Deficiency strains and *mmy* [1], *mmy*^{KG04349}, *mmy*^{KG08617}, *sgl*, *sfl*, *mmp1*^{K4809}, *mmp2*^{2353} and *mmp2*^{w307*}, *mmp1*^{Q112*} mutants were obtained from the Bloomington Stock Center. *mmy*^{J1201} and *mmy*^{G131} were obtained from Christian Klambt. UAS-*mmp1*, UAS-*mmp2*, and UAS-*Timp* lines were obtained from Andrea Page-McCaw. All lines were balanced over P(UAS-GFP.S65T)DC5, sn-, CyOarmGFP, TM3armGFP (Bloomington).

Immunohistochemistry

Homozygous deficiency embryos were identified by the absence of GFP fluorescence from the GFP gene on the balancer chromosome using an Olympus GFP dissecting microscope. See (FOX and ZINN 2005; LEE *et al.* 2009) for dissection and staining protocols. Samples are mounted in 70% glycerol in PBS. Immunohistochemistry was performed on live-dissected samples using a goat anti-mouse secondary antibody fused to horseradish peroxidase (Jackson Immunoresearch). HRP immunohistochemistry was carried out as described (PATEL 1994).

The following antibodies were used mAb bp102 1:30, rabbit anti-Syndecan 1:100, mouse anti-Dally-like 1:5 AlexaFluor anti-mouse 488, AlexaFluor anti-mouse 568, AlexaFluor anti-rabbit 568, and AlexaFluor anti-rabbit 488 (Invitrogen) 1:1000. Fluorescein-phalloidin (Invitrogen) was used at 1:2000 to CNS structure.

Confocal imaging was performed using a Zeiss LSM inverted microscope using 20X, 40X, and 63X Zeiss oil-immersion objectives. Stacks were projected using Image J software maximum intensity projections.

Figure Legends

Figure 1. BP102 staining is absent in *mummy* mutants.

All Panels are confocal maximum intensity projections of live-dissected late stage 16 embryos stained with BP102 (magenta) and fluorescein-conjugated phalloidin (green). Anterior is up.

(A-C) Control embryo where BP102 labels the proximal segments of axons in the commissures and longitudinal connectives in the CNS revealing a ladder-like structure. Phalloidin labels the axon scaffold as well as muscles.

(D-F) mmy^{1}/mmy^{1} embryo where BP102 staining is absent while phalloidin staining reveals the presence of the axon ladder.

(G-I) mmy^{1}/CyO has normal BP102 staining.

(J-L) mmy^{1}/Df(2L)BSC354 lacks BP102 staining but phalloidin staining is present.

Figure2. BP102 staining in *mmy* mutants is dependent on temperature.

Panels are maximum intensity confocal projections of live-dissected late stage 16 embryos stained with BP102 (magenta) and fluorescein-conjugated phalloidin (green). Anterior is up. Panels with letter only (i.e., A) are embryos raised at 18 ^{0}C. Panels with letter and ‘ (i.e., A’) are embryos raised at room temperature.

(A-C and A’-C’) Control embryos where BP102 stains the axon ladder at both temperatures.

(D-F and D’-F’) $mmy^{KG04349}$ embryos where BP102 staining is visible at both temperatures. This allele is a hypomorph and does not effect glycosylation.

(G-I and G'-I') *mmy*^{KG08617} embryos where BP102 staining is not apparent at 18 ^{0}C. BP102 is visible at room temperature but at much lower levels than control embryos in panel A'.

(J-L and J'-L') *mmy*^{G131} embryos where BP102 is faintly visible at room temperature but at much lower levels than control in A'.

(M-O and M'-O') *mm*^{yJ1201} embryos where BP102 is barely visible at room temperature but at much lower levels than A'.

Note that the CNS phenotype of mmyKG08617, mmyG131 and mmyJ1201 is more severe at 18 ^{0}C than at room temperature

Figure 3. BP102 staining is present in *mmy* mutants when visualized by HRP immunohistochemistry.

Panels are live-dissected late stage 16 embryos stained with BP102 and visualized with a secondary antibody conjugated to horseradish peroxidase (20X objective and DIC optics). Anterior is up. Panels A-E are embryos raised at 18 ^{0}C. Panels F-J are embryos raised at room temperature.

(A and F) Control where BP102 staining is visualized by a precipitate formed by the peroxidase reaction.

(B and G) *mmy*^{KG04349}

(C and H) *mmy*^{KG08617}

(D and I) *mmy*^{G131}

(E and J) *mmy*^{J1201}

All embryos stain with BP102 at both 18 ^{0}C and room temperature. Note the phenotype of *mmy*^{KG08617} is more severe at 18 ^{0}C than at room temperature.

Figure 4. BP102 staining in *sugarless* and *sulfateless* mutants.

Panels are confocal maximum intensity projections of 1st instar larval brain stained with BP102 (magenta) and fluorescein-conjugated phalloidin (green). Anterior is up.

(A-C) *sgl*/TM3 1st instar larval brain stains with both BP102 and phalloidin which have overlapping staining patterns that fill most of the ventral nerve cord.

(D-F) *sgl*/*sgl* shows reduced BP102 staining while phalloidin levels remain the same.

(G-I) *sfl*/*sfl* has no change in BP102 or phalloidin staining.

Figure 5. Matrix Metalloproteinase 1 regulates expression of the BP102 epitope.

Panels are confocal maximum intensity projections of late stage 16 live-dissected embryos stained with BP102 (magenta) and Syndecan (green). Anterior is up.

(A-C) Control embryo where BP102 is restricted to the proximal segments within the CNS and does not extend into the periphery. Syndecan stains the ventral nerve cord as well as the muscle attachment sites.

(D-F) *mmp1*^{K4809} embryo where BP102 epitope is now expressed on cells in the periphery. We believe these cells to be sensory neurons. Note that BP102 staining appears to be brighter within the CNS than in Panel A.

(G-I) *mmp2*^{2353} BP102 epitope is expressed in the wildtype pattern.

(J-L) *mmp2*^{W307*}*, mmp1*^{Q112*} BP102 epitope is found on peripheral cells and expression within the CNS is stronger.

Figure 6. Mmp-1 cleaves the BP102 epitope when overexpressed but does not alter Syndecan or Dally-like staining.

Panels are confocal maximum intensity projections of live-dissected late stage embryos. Anterior is up.

Panels A-F are embryos stained with BP102 (magenta) and Syndecan (green). Panels G-L are embryos stained with Syndecan (magenta) and Dally-like (green).

(A-C) Control BP102 epitope is expressed within the CNS.

(D-F) Neuronal overexpression of Mmp1 results in loss of BP102 epitope from the CNS.

(G-I) Control stained with Syndecan and Dally-like antibodies.

(J-L) Neuronal overexpression of Mmp1 does result in alteration of Syndecan or Dally-like antibody staining.

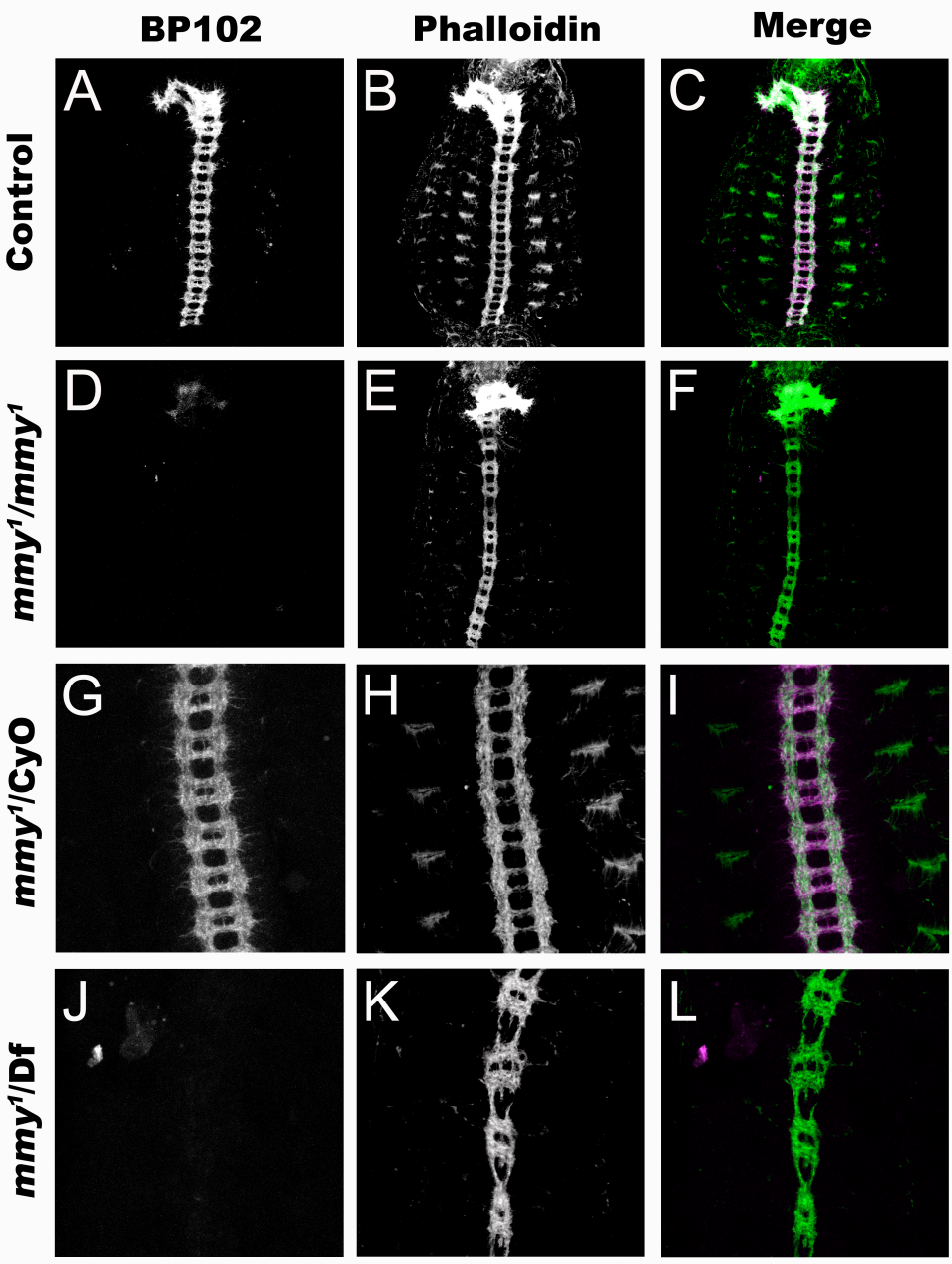
BP102
Phalloidin
Merge
Control
mmy1/mmy1
mmy1/CyO
mmy1/Df
A
B
C
D
E
F
G
H
I
J
K
L

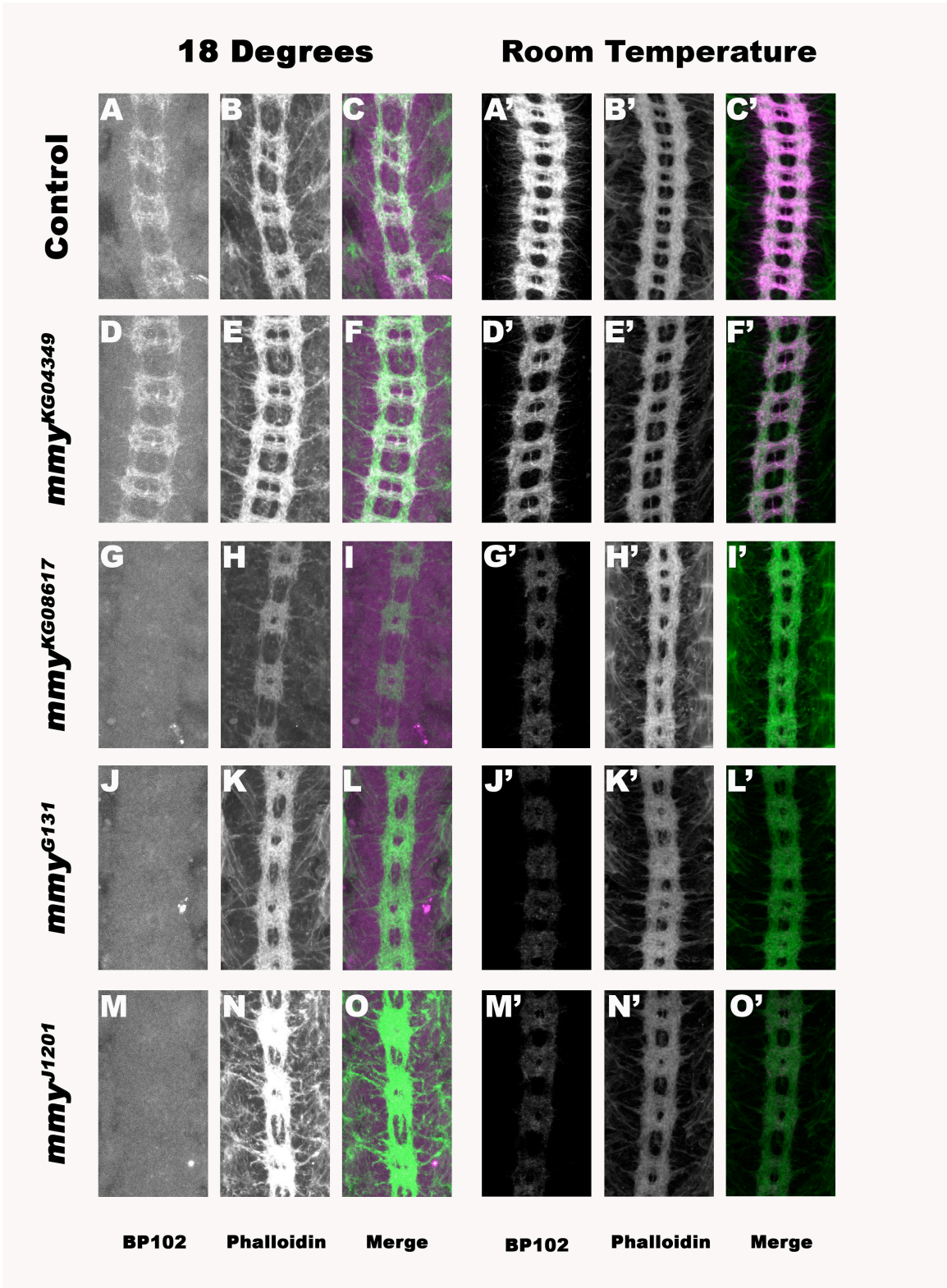
18 Degrees
Room Temperature
Control
mmyKG04349
mmyKG08617
mmyG131
mmyJ1201
A
B
C
A'
B'
C'
D
E
F
D'
E'
F'
G
H
I
G'
H'
I'
J
K
L
J'
K'
L'
M
N
O
M'
N'
O'
BP102
Phalloidin
Merge
BP102
Phalloidin
Merge

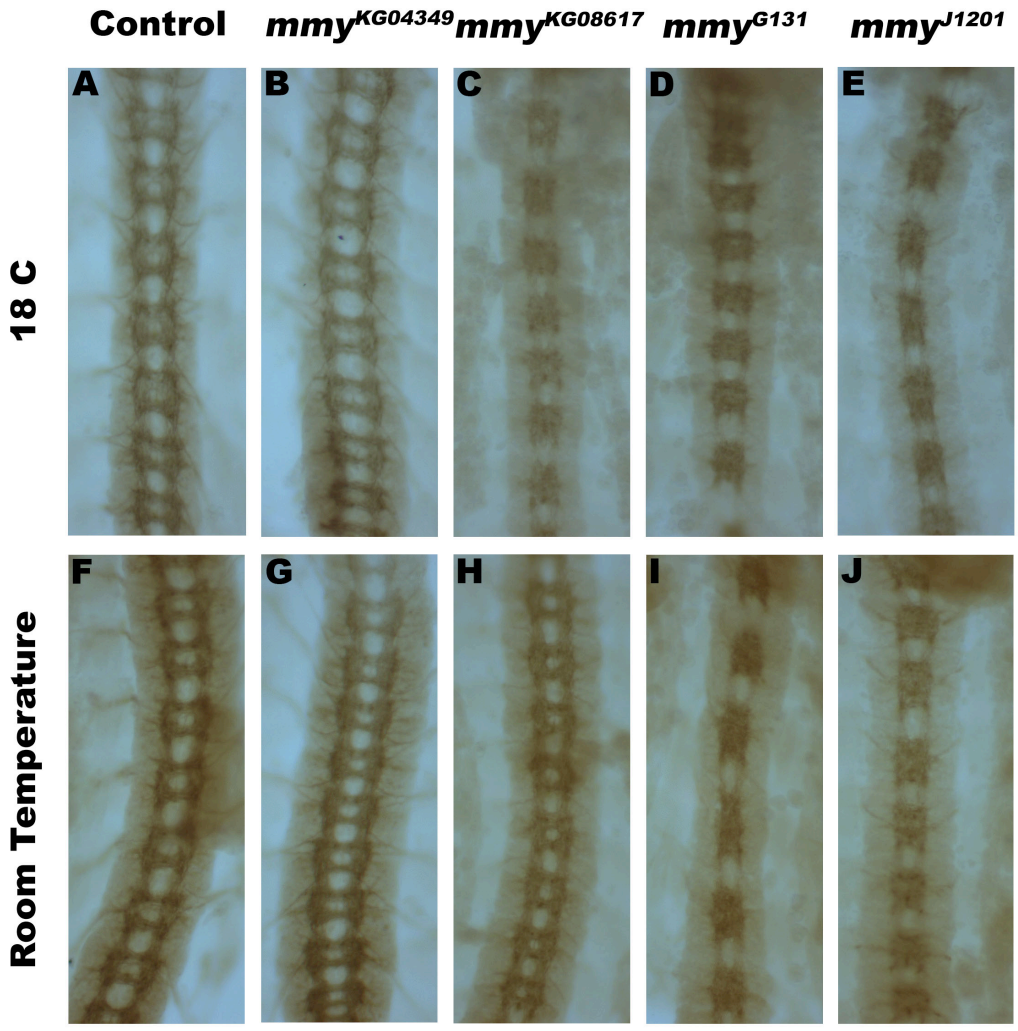
Control
mmy^KG04349
mmy^KG08617
mmy^G131
mmy^J1201
18 C
Room Temperature
A
B
C
D
E
F
G
H
I
J

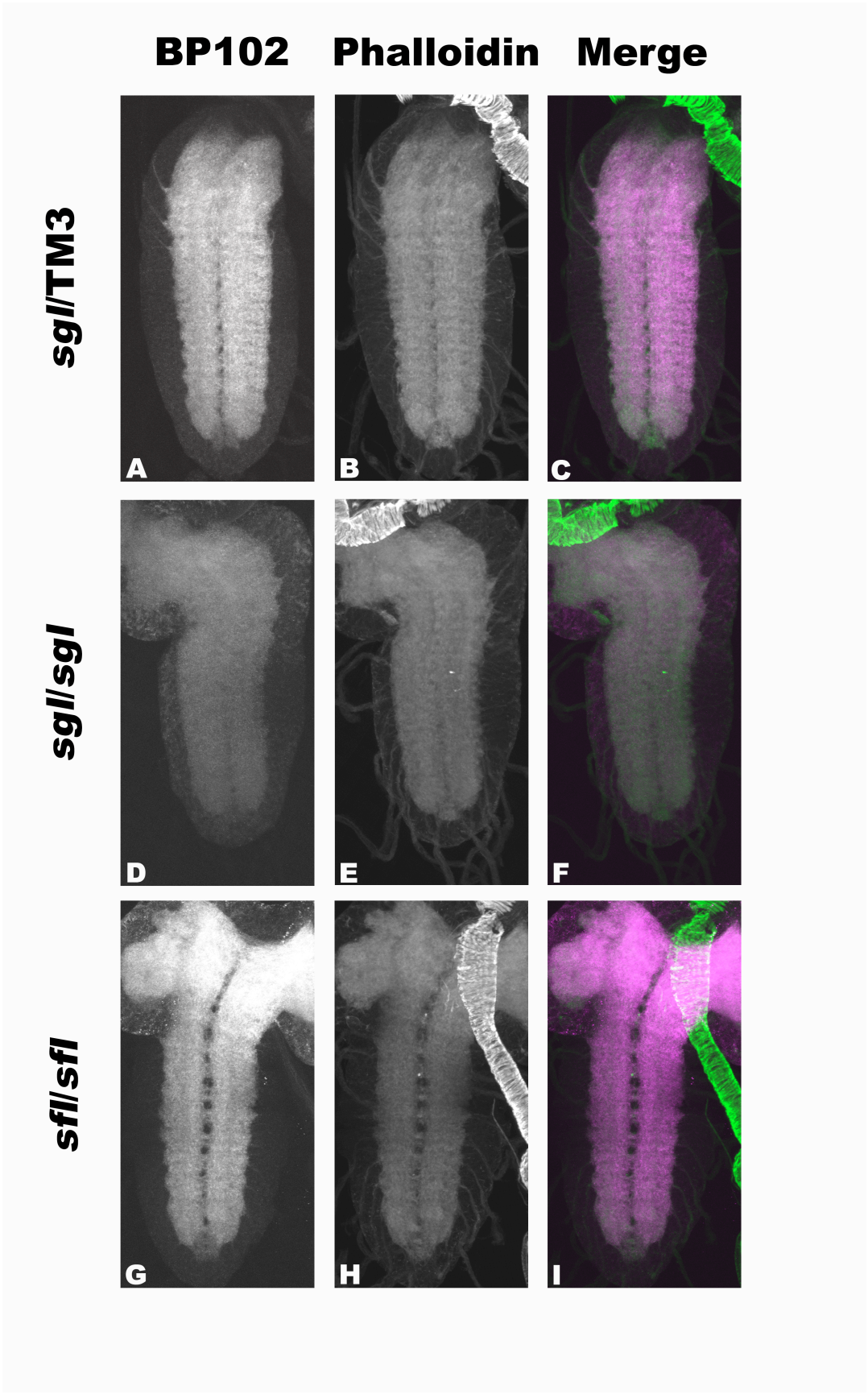
BP102
Phalloidin
Merge
sgl/TM3
sgl/sgl
sfl/sfl
A
B
C
D
E
F
G
H
I

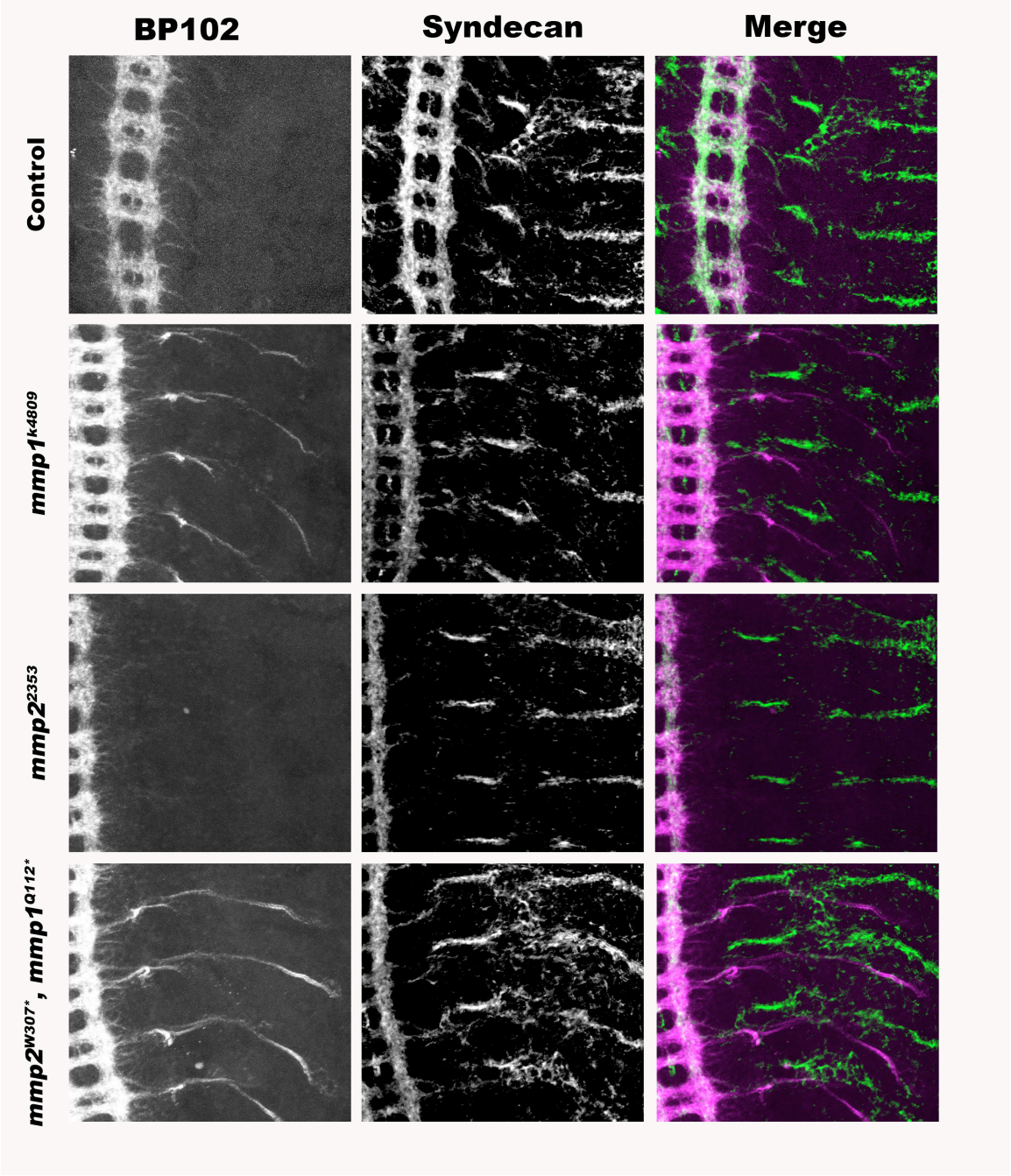
BP102
Syndecan
Merge
Control
mmp1k4809
mmp2W307*, mmp1Q112*
mmp22353

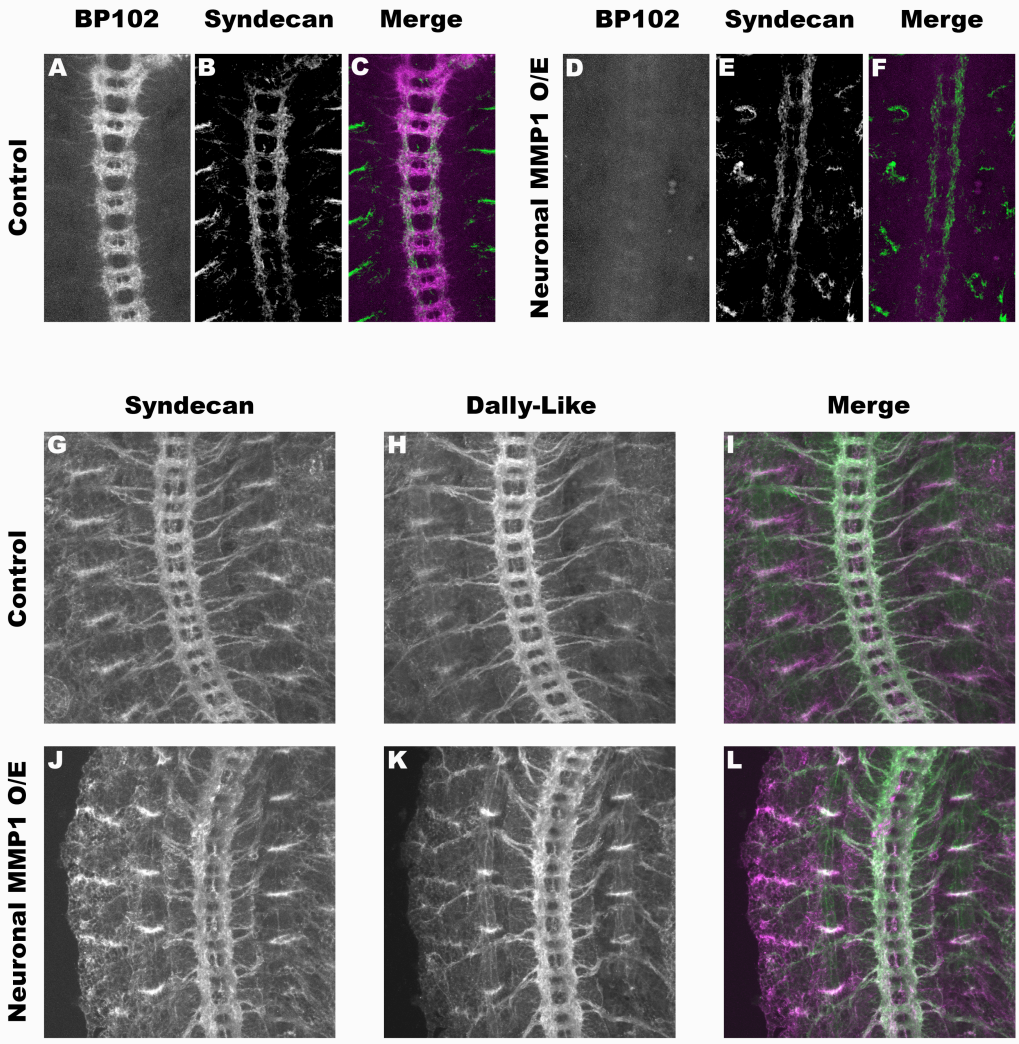
BP102
Syndecan
Merge
BP102
Syndecan
Merge
Control
Neuronal MMP1 O/E
A
B
C
D
E
F
Syndecan
Dally-Like
Merge
Control
Neuronal MMP1 O/E
G
H
I
J
K
L

Chapter 2 References

Araujo, S. J., H. Aslam, et al. (2005). "mummy/cystic encodes an enzyme required for chitin and glycan synthesis, involved in trachea, embryonic cuticle and CNS development--analysis of its role in Drosophila tracheal morphogenesis." Dev Biol **288**(1): 179-93.

Bellaiche, Y., I. The, et al. (1998). "Tout-velu is a Drosophila homologue of the putative tumour suppressor EXT-1 and is needed for Hh diffusion." Nature **394**(6688): 85-8.

Binari, R. C., B. E. Staveley, et al. (1997). "Genetic evidence that heparin-like glycosaminoglycans are involved in wingless signaling." Development **124**(13): 2623-32.

Crespo, D., R. A. Asher, et al. (2007). "How does chondroitinase promote functional recovery in the damaged CNS?" Exp Neurol **206**(2): 159-71.

Devine, W. P., B. Lubarsky, et al. (2005). "Requirement for chitin biosynthesis in epithelial tube morphogenesis." Proc Natl Acad Sci U S A **102**(47): 17014-9.

Diekman, A. B. and E. Goldberg (1994). "Characterization of a human antigen with sera from infertile patients." Biol Reprod **50**(5): 1087-93.

Fox, A. N. and K. Zinn (2005). "The heparan sulfate proteoglycan syndecan is an in vivo ligand for the Drosophila LAR receptor tyrosine phosphatase." Curr Biol **15**(19): 1701-11.

Gomis-Ruth, F. X., K. Maskos, et al. (1997). "Mechanism of inhibition of the human matrix metalloproteinase stromelysin-1 by TIMP-1." Nature **389**(6646): 77-81.

Hacker, U., X. Lin, et al. (1997). "The Drosophila sugarless gene modulates Wingless signaling and encodes an enzyme involved in polysaccharide biosynthesis." Development **124**(18): 3565-73.

Hacker, U., K. Nybakken, et al. (2005). "Heparan sulphate proteoglycans: the sweet side of development." Nat Rev Mol Cell Biol **6**(7): 530-41.

Haerry, T. E., T. R. Heslip, et al. (1997). "Defects in glucuronate biosynthesis disrupt Wingless signaling in Drosophila." Development **124**(16): 3055-64.

Han, C., T. Y. Belenkaya, et al. (2004). "Distinct and collaborative roles of Drosophila EXT family proteins in morphogen signalling and gradient formation." Development **131**(7): 1563-75.

Johnson, K. G., A. Ghose, et al. (2004). "Axonal heparan sulfate proteoglycans regulate the distribution and efficiency of the repellent slit during midline axon guidance." Curr Biol **14**(6): 499-504.

Katsuki, T., D. Ailani, et al. (2009). "Intra-axonal patterning: intrinsic compartmentalization of the axonal membrane in Drosophila neurons." Neuron **64**(2): 188-99.

Katz, F., W. Moats, et al. (1988). "A carbohydrate epitope expressed uniquely on the cell surface of Drosophila neurons is altered in the mutant nac (neurally altered carbohydrate)." EMBO J **7**(11): 3471-7.

Koles, K., J. M. Lim, et al. (2007). "Identification of N-glycosylated proteins from the central nervous system of Drosophila melanogaster." Glycobiology **17**(12): 1388-403.

Lin, X., E. M. Buff, et al. (1999). "Heparan sulfate proteoglycans are essential for FGF receptor signaling during Drosophila embryonic development." Development **126**(17): 3715-23.

Llano, E., G. Adam, et al. (2002). "Structural and enzymatic characterization of Drosophila Dm2-MMP, a membrane-bound matrix metalloproteinase with tissue-specific expression." J Biol Chem **277**(26): 23321-9.

Llano, E., A. M. Pendas, et al. (2000). "Dm1-MMP, a matrix metalloproteinase from Drosophila with a potential role in extracellular matrix remodeling during neural development." J Biol Chem **275**(46): 35978-85.

Lo, E. H., X. Wang, et al. (2002). "Extracellular proteolysis in brain injury and inflammation: role for plasminogen activators and matrix metalloproteinases." J Neurosci Res **69**(1): 1-9.

Miller, C. M., A. Page-McCaw, et al. (2008). "Matrix metalloproteinases promote motor axon fasciculation in the Drosophila embryo." Development **135**(1): 95-109.

Page-McCaw, A. (2008). "Remodeling the model organism: matrix metalloproteinase functions in invertebrates." Semin Cell Dev Biol **19**(1): 14-23.

Page-McCaw, A., A. J. Ewald, et al. (2007). "Matrix metalloproteinases and the regulation of tissue remodelling." Nat Rev Mol Cell Biol **8**(3): 221-33.

Page-McCaw, A., J. Serano, et al. (2003). "Drosophila matrix metalloproteinases are required for tissue remodeling, but not embryonic development." Dev Cell **4**(1): 95-106.

PATEL, N. H., (1994) "Imaging neuronal subsets and other cell types in whole-mount Drosophila embryos and larvae using antibody probes." Methods Cell Biol **44:** 445-487.

Perrimon, N., A. Lanjuin, et al. (1996). "Zygotic lethal mutations with maternal effect phenotypes in Drosophila melanogaster. II. Loci on the second and third chromosomes identified by P-element-induced mutations." Genetics **144**(4): 1681-92.

Pizzi, M. A. and M. J. Crowe (2007). "Matrix metalloproteinases and proteoglycans in axonal regeneration." Exp Neurol **204**(2): 496-511.

Schimmelpfeng, K., M. Strunk, et al. (2006). "Mummy encodes an UDP-N-acetylglucosamine-dipohosphorylase and is required during Drosophila dorsal closure and nervous system development." Mech Dev **123**(6): 487-99.

Seeger, M., G. Tear, et al. (1993). "Mutations affecting growth cone guidance in Drosophila: genes necessary for guidance toward or away from the midline." Neuron **10**(3): 409-26.

Selleck, S. B. (2001). "Genetic dissection of proteoglycan function in Drosophila and C. elegans." Semin Cell Dev Biol **12**(2): 127-34.

Sen, J., J. S. Goltz, et al. (1998). "Spatially restricted expression of pipe in the Drosophila egg chamber defines embryonic dorsal-ventral polarity." Cell **95**(4): 471-81.

Sergeev, P., A. Streit, et al. (2001). "The Drosophila dorsoventral determinant PIPE contains ten copies of a variable domain homologous to mammalian heparan sulfate 2-sulfotransferase." Dev Dyn **220**(2): 122-32.

Snow, P. M., N. H. Patel, et al. (1987). "Neural-specific carbohydrate moiety shared by many surface glycoproteins in Drosophila and grasshopper embryos." J Neurosci **7**(12): 4137-44.

Spring, J., S. E. Paine-Saunders, et al. (1994). "Drosophila syndecan: conservation of a cell-surface heparan sulfate proteoglycan." Proc Natl Acad Sci U S A **91**(8): 3334-8.

Stein, D., S. Roth, et al. (1991). "The polarity of the dorsoventral axis in the Drosophila embryo is defined by an extracellular signal." Cell **65**(5): 725-35.

Takei, Y., Y. Ozawa, et al. (2004). "Three Drosophila EXT genes shape morphogen gradients through synthesis of heparan sulfate proteoglycans." Development **131**(1): 73-82.

The, I., Y. Bellaiche, et al. (1999). "Hedgehog movement is regulated through tout velu-dependent synthesis of a heparan sulfate proteoglycan." Mol Cell **4**(4): 633-9.

Tonning, A., S. Helms, et al. (2006). "Hormonal regulation of mummy is needed for apical extracellular matrix formation and epithelial morphogenesis in Drosophila." Development **133**(2): 331-41.

Toyoda, H., A. Kinoshita-Toyoda, et al. (2000). "Structural analysis of glycosaminoglycans in animals bearing mutations in sugarless, sulfateless, and tout-velu. Drosophila homologues of vertebrate genes encoding glycosaminoglycan biosynthetic enzymes." J Biol Chem **275**(29): 21856-61.

Wang-Gillam, A., I. Pastuszak, et al. (1998). "A 17-amino acid insert changes UDP-N-acetylhexosamine pyrophosphorylase specificity from UDP-GalNAc to UDP-GlcNAc." J Biol Chem **273**(42): 27055-7.

Yong, V. W. (2005). "Metalloproteinases: mediators of pathology and regeneration in the CNS." Nat Rev Neurosci **6**(12): 931-44.

Zhu, X., J. Sen, et al. (2005). "Drosophila pipe protein activity in the ovary and the embryonic salivary gland does not require heparan sulfate glycosaminoglycans." Development **132**(17): 3813-22.

Zuo, J., T. A. Ferguson, et al. (1998). "Neuronal matrix metalloproteinase-2 degrades and inactivates a neurite-inhibiting chondroitin sulfate proteoglycan." J Neurosci **18**(14): 5203-11.